AN ABSTRACT OF THE THESIS OF

David Selkowitz for the degree of Master of Science in Geography presented on November 11, 2005.
Title: Measurement, Modeling, and Remote Sensing of Snow Cover in Areas of Heterogeneous Vegetation

Abstract approved:

Anne W. Nolin

Numerous studies have demonstrated that vegetation canopies affect snow accumulation and ablation processes. In addition, estimates of remotely sensed snow covered area can be biased by the presence of an overlying vegetation canopy. Consequently, any attempts to measure, model, or map the distribution of snow in a region with heterogeneous vegetation cover would benefit from a more complete understanding of both the relationship between vegetation density and snow cover on the ground as well as the relationship between remotely sensed snow covered area and actual snow covered area under various vegetation densities. The research presented here explores both of these relationships.

Chapter 2 describes, qualitatively and quantitatively, the relationship between canopy gap fraction (the inverse of canopy density) and snow accumulation at fine spatial scales in Glacier National Park, Montana. Gap fraction and snow cover data from two winters were compared along eight vegetation-snow transects representing a range of landscape types, including dense forest, variable density forests with openings, forest-grassland mosaics, and burned-unburned forest mosaics. The data suggest that the relationship between gap fraction and snow accumulation depends

on the range of gap fraction values considered. For gap fraction values less than ~ 40%, a significant positive linear relationship exists between gap fraction and snow accumulation. For gap fraction values between ~ 40% and ~ 90%, the relationship is poorly defined, most likely due to the influence of the spatial patterning of vegetation on wind scouring/deposition of snow which cannot be captured by a simple metric such as gap fraction. When gap fraction exceeds ~ 90%, snow cover is almost always shallow or nonexistent due to wind scouring and high solar radiation loads. The poorly defined relationship between gap fraction and snow accumulation in the range of 40-90% gap fraction is not highly problematic because this gap fraction range represents only 24% of the landscape, and the 60-90% range of gap fraction where the gap fraction-snow accumulation relationship is least pronounced represents only 5% of the landscape. The results from these vegetation-snow surveys indicate that at fine spatial scales where topographic variability is minimal, canopy density can explain a substantial portion of the variability in snow accumulation that would otherwise remain unexplained. The high variance in snow accumulation in the 60-90% gap fraction range and the relatively small sample size presented here make it unrealistic, however, to infer an optimum gap fraction for snow accumulation in Glacier National Park or anywhere else.

Chapter 3 provides an assessment of methods for modeling and mapping spatiotemporal variability in snow cover in Glacier National Park. SnowModel, a relatively new physically-based snow evolution model that accounts for the influence of vegetation on snow processes, was used to simulate the spatial distribution of snow water equivalent at hourly time steps for an 850 km^2 model domain in eastern

Glacier National Park. The standard implementation of SnowModel uses an image of land cover type to adjust snow accumulation and ablation for the effects of vegetation. In this non-standard implementation, the model was parameterized using a weighting scheme that allowed the model to utilize a Landsat-derived image of gap fraction to adjust snow accumulation and ablation in a more precise manner than would have been possible if only land cover type information was available. In situ measurements suggest the model did a reasonable job simulating snow evolution patterns and the differences in snow evolution associated with different vegetation densities. Weaknesses in this implementation of SnowModel appear to be its tendency to overestimate snow in the easternmost portion of the model domain (where a significant rain shadow effect exists) and overestimate snow in exposed areas. Due to a lack of in situ measurements at the scale of the model output, it was not possible to conclusively determine if the incorporation of fine scale (28.5 m pixel) information on forest canopy density improved model accuracy.

MODIS-derived images of binary and fractional snow covered area were also evaluated. The binary product consistently mapped a higher percentage of the study area as snow covered than the fractional product. Spatial patterns of snow covered area were similar for the MODIS-derived products and the results from the implementation of SnowModel. Unfortunately, the remotely sensed snow covered area products could not be used to evaluate the model's treatment of snow evolution under different vegetation conditions because gap fraction influences the mapping of snow covered area for the remotely sensed products. Understanding how remotely sensed estimates of snow covered area are influenced by gap fraction density will

hopefully allow for these products to be used as a validation tool for spatially distributed model results in areas of heterogeneous vegetation in the future.

Measurement, Modeling, and Remote Sensing of Snow Cover in Areas of Heterogeneous Vegetation

by
David Selkowitz

A THESIS

submitted to

Oregon State University

in partial fulfillment of
the requirements for the
degree of

Master of Science

Presented November 11, 2005
Commencement June 2006

Master of Science thesis of David Selkowitz presented on November 11, 2005.

APPROVED:

Major Professor, representing Geography

Chair of the Department of Geosciences

Dean of the Graduate School

I understand that my thesis will become part of the permanent collection of Oregon State University libraries. My signature below authorizes release of my thesis to any reader upon request.

David Selkowitz, Author

ACKNOWLEDGEMENTS

The author expresses his appreciation to Dr. Anne Nolin and Dr. Daniel Fagre for extensive assistance in crafting the research questions, study design, and analysis methodology presented in this thesis. The author wishes to thank Dr. Glen Liston for assistance with snow evolution modeling and Dr. Tom Painter for processing MODIS images to create maps of fractional snow covered area. The author also wishes to thank primary field assistants Bill Baum, Sarah Thoma, and Ali White for extraordinary performance under difficult and occasionally dangerous conditions in the field. Additional field assistance came from Daniel Fagre, Karen Holzer, Lisa McKeon, and Blase Reardon of the USGS Glacier Field Station, Glacier National Park backcountry rangers, and numerous volunteers including Michelle Arsenault, Robert Friedel, Jeff Schmalenberg, and members of the University of Illinois Outdoor Adventure Club.

CONTRIBUTION OF AUTHORS

Dr. Daniel Fagre of the USGS Northern Rocky Mountain Science Center, Glacier Field Station, helped formulate the research questions, construct the study design, and interpret the results of the snow survey and vegetation data that forms the basis for Chapter 2 and part of Chapter 3. Dr. Glen Liston of Colorado State University, Department of Atmospheric Science, provided the code for, as well as extensive assistance with running the snow evolution model used in Chapter 3. Dr. Tom Painter of the University of Colorado, National Snow and Ice Data Center processed MODIS reflectance images to produce images of fractional snow covered area used in Chapter 3.

TABLE OF CONTENTS

TABLE OF CONTENTS (Continued)

LIST OF FIGURES

LIST OF FIGURES (Continued)

LIST OF FIGURES (Continued)

LIST OF FIGURES (Continued)

LIST OF TABLES

LIST OF TABLES (Continued)

Measurement, Modeling, and Remote Sensing of Snow Cover in Areas of Heterogeneous Vegetation

CHAPTER 1: INTRODUCTION

The presence or absence of a vegetation canopy, as well as the density and structure of that canopy have a significant impact on snow accumulation and ablation (often referred to together as snow evolution). The vegetation canopy can also affect remotely sensed estimates of snow covered area (SCA). In recent years, researchers have attempted to combine modeling and remote sensing approaches to map the distribution of snow depth or snow water equivalent (SWE) over space. Successful application of this integrated approach requires an in-depth understanding of both the relationship between vegetation and the processes affecting snow evolution on the ground and the effect of the vegetation canopy on remotely sensed estimates of SCA.

Vegetation canopies can affect the snow cover evolution through a variety of mechanisms. These include interception and sublimation of snowfall by the vegetation canopy, modification of the solar and thermal radiation regimes at the snow surface, and modification of local wind characteristics. Reduced seasonal snow accumulation below forest canopies due to interception and subsequent sublimation of snowfall has been documented by numerous researchers in a variety of snow regimes (Satterlund and Haupt 1967, Satterlund and Haupt 1970, Storck et al 2002, Gary and Troendle 1982, Golding and Swanson 1986, Hedstrom and Pomeroy 1998, Lundberg et al 2004). Reduction in seasonal snow accumulation has been found to be most significant in colder, drier environments because conditions are more conducive to sublimation of intercepted snow from the canopy (Hedstrom and Pomeroy 1998, Storck et al 2002). Vegetation canopies also attenuate incoming

solar (shortwave) radiation (Davis et al 1997, Berry and Rothwell 1992, Hardy et al 2004, Link et al 2004) and enhance the amount of thermal (longwave) radiation received at the snow surface (Link et al. 2004). Finally, vegetation canopies reduce wind speed below the forest canopy (Marks et al 1998, Link and Marks 1999, Marks and Winstral 2001) or on the lee side of individual trees where vegetation is sparse (Hiemstra et al 2002). Reduced wind speeds result in reduced turbulent fluxes (often a cause of significant snow ablation) (Marks et al 1998), as well as decreased wind scouring and increased wind deposition (Hiemstra et al 2002), resulting in a net increase in snow accumulation. The effects of vegetation canopies on the evolution of seasonal snow cover are discussed in more detail in Chapter 2.

Although physically based snow evolution models have been available for nearly three decades (Marks 1988), only recently have these models begun to incorporate the effects of vegetation canopies on snow accumulation and ablation processes. Researchers have employed various algorithms for adjusting solar radiation, thermal radiation, and wind speed measurements to more accurately reflect sub-canopy conditions (Hardy et al 1997, Link and Marks 1999, Koivusalo and Kokkonen 2002). Models have also been developed to simulate the amount of snow intercepted and sublimated from vegetation canopies (Hedstrom and Pomeroy 1998), as well as the spatial distribution of snow evolution in sparsely forested environments (Hiemstra et al 2002). Attempts to incorporate the effects of vegetation canopies on snow accumulation and ablation processes are described in more detail in Chapter 3.

Mapping SCA in areas with significant vegetation canopies can be difficult because the fraction of a pixel actually covered by snow at the ground surface may not correspond with the fraction of the pixel that appears to be snow covered when viewed from above. Remotely sensed estimates of SCA have been available since 1966 (Hall et al 2002). Until relatively recently, only binary maps identifying individual pixels as snow covered or snow free were available. The multiple scales of spatial heterogeneity of snow cover (particularly in windy environments and near the end of the season) necessitated the development of improved mapping techniques capable of mapping the fraction of each pixel covered by snow. These improved techniques (e.g. Nolin et al 1993, Painter et al 2003) do not generally account for the effect of a vegetation canopy on the retrieval of remotely sensed SCA. The traditional binary mapping technique used to create the current MODIS-derived SCA product available from NASA does use the Normalized Difference Vegetation Index (NDVI) in conjunction with the Normalized Difference Snow Index (NDSI) to decrease the probability of mapping forested snow covered areas as snow free (Hall et al 2002). It has not yet been determined, however, to what extent this adjustment removes the bias towards mapping forested snow covered areas as snow free.

The research presented in this thesis aims to describe, both qualitatively and quantitatively, the impact of various vegetation canopies on snow evolution processes in the Northern Rocky Mountains. The data collected towards this end is then used to aid in the assessment of modeling and remote sensing techniques for mapping the spatiotemporal distribution of snow cover in areas of heterogeneous

vegetation cover. Data collection, modeling, and remote sensing focuses on Glacier National Park, Montana, where a wide range of climate and vegetation regimes are represented. This thesis includes an introduction (this chapter), two manuscripts (Chapter 2 and Chapter 3), and a conclusion tying the results of the two manuscripts together. Chapter 2 presents the methodology, results, error analysis, discussion and conclusions regarding relationships between snow cover and vegetation canopies. Chapter 3 presents the methodology, results, error analysis, discussion and conclusions regarding modeling and remote sensing of snow cover in areas of heterogeneous vegetation. Chapter 4 summarizes the conclusions from chapters 2 and 3 and further explains their significance.

VARIABLE SNOW COVER ACCUMULATION ASSOCIATED WITH VEGETATION TYPE AND DENSITY IN GLACIER NATIONAL PARK, MONTANA, USA

David Selkowitz
Anne W. Nolin
Daniel Fagre

To be submitted to *Hydrological Processes*

Abstract

Numerous studies have demonstrated relationships between vegetation cover type or density and snow accumulation. This study describes, qualitatively and quantitatively, the relationship between canopy gap fraction (the inverse of canopy density) and snow accumulation at fine spatial scales in the Northern Rocky Mountains of Montana. Gap fraction and snow cover data from two winters are compared along eight vegetation-snow transects representing a range of landscape types, including dense forest, variable density forests with openings, forest-grassland mosaics, and burned-unburned forest mosaics. The data suggest that the relationship between gap fraction and snow accumulation depends on the range of gap fraction values considered. For gap fraction values less than ~ 40%, a significant positive linear relationship exists between gap fraction and snow accumulation. For gap fraction values between ~ 40% and ~ 90%, variance in snow accumulation is high and the relationship between gap fraction and snow accumulation is poorly defined, most likely due to the influence of the spatial patterning of vegetation on wind scouring/deposition of snow which cannot be captured by a simple metric such as gap fraction. When gap fraction exceeds ~ 90%, snow cover is almost always shallow or nonexistent due to wind scouring and high solar radiation loads. The poorly defined relationship between gap fraction and snow accumulation in the range of 40-90% gap fraction is not as problematic as it initially appears, as this range of gap fraction values occupies a relatively small portion of the landscape. The high variance in snow accumulation in the range of 40-90% gap fraction and the relatively

small sample size presented here, however, make it unrealistic to infer an optimum gap fraction for snow accumulation in Glacier National Park or anywhere else. Additional research efforts should focus on examining relationships between gap fraction and snow accumulation at multiple scales and across a wider range of climate conditions.

1. Introduction

In mountain and northern environments, the spatiotemporal distribution of snow cover exerts a dominant influence on many hydrological and ecological processes. These processes include streamflow, soil moisture dynamics, animal movement and mortality, and vegetation phenology. Understanding the inter-annual and intra-annual variability in any of these processes requires an understanding of seasonal snowpack dynamics. The distribution of snow depth or snow water equivalent (SWE), however, are almost never uniform over space. While a significant portion of the spatial variability in snow depth and SWE can often be explained by topographic structure (i.e. slope, aspect, and curvature), in vegetated environments, much of the remaining unexplained variability is due to heterogeneous vegetation distributions. While terrain remains relatively constant over time, landscape vegetation patterns can change significantly due to factors such as fire, climatic variability, and changes in human land use. Consequently, attempts to model both the current and future spatiotemporal distributions of seasonal snow cover require a solid understanding of snow accumulation and ablation dynamics under different vegetation conditions.

Many researchers have examined the effect of vegetation, particularly forest cover, on the accumulation and ablation dynamics of seasonal snowpacks. The literature suggests three primary mechanisms by which forest cover can affect the evolution of a seasonal snow cover: 1) via interception and subsequent sublimation of snowfall by the forest canopy, 2) via modification of the solar and thermal

radiation characteristics at the snow surface, below the canopy, and 3) via modification of local wind characteristics (figure 1).

Canopy interception of snowfall leading to increased sublimation (and consequently a reduced snow accumulation under the forest canopy) has been well documented by a number of studies (Satterlund and Haupt 1967, Satterlund and Haupt 1970, Storck et al 2002, Gary and Troendle 1982, Golding and Swanson 1986, Hedstrom and Pomeroy 1998, Lundberg et al 2004). The amount of snow intercepted by the forest canopy is highly variable and depends on both canopy density and weather conditions (Hedstrom and Pomeroy 1998, Lundberg and Koivusalo 2003). Snow intercepted by the forest canopy can be released by mass unloading of branches, deposited on the ground as liquid water via meltwater drip, or sublimated into the atmosphere. Sublimation of intercepted snow represents a net loss of water to the soil-water system, while mass unloading and meltwater drip do not (Storck et al 2002). The fraction of intercepted snow lost to the atmosphere via sublimation depends on local climate conditions. Sublimation rates are typically high during cold, dry conditions and much lower during warmer, moister conditions. Seasonal sublimation losses range from approximately 5-15% for coastal snow regimes (Satterlund and Haupt 1970, Storck et al 2002) to greater than 30% in continental mountain and boreal forest snow regimes (Lundberg and Koivusalo 2003).

Forest canopies also affect the net radiation budget at the snow surface. Forest canopies attenuate solar (shortwave) radiation, resulting in significant

radiation extinction at the snow surface (Davis et al 1997, Berry and Rothwell 1992, Hardy et al 2004, Link et al 2004). The deposition of litter from the forest canopy onto the snow surface below the canopy, however, typically lowers the snow cover albedo, increasing the amount of shortwave radiation absorbed by the snow cover (Melloh et al 2002, Hardy et al 2000). Canopies also tend to enhance the amount of thermal radiation incident upon the snow surface, reducing the effective decrease in net allwave radiation (the sum of shortwave and longwave radiation) (Link et al. 2004). Under certain conditions, this can even lead to greater net allwave radiation below the canopy than in small openings (Price 1988, Berry and Rothwell 1992).

The presence of forest cover can substantially alter local wind characteristics. Consequently, this can affect both the snow surface mass and energy balances at a point as well as the spatial patterning of precipitation, snow scouring, and snow deposition. Wind speeds are consistently lower in areas where forest cover is present compared to wind speeds in the open (Marks et al 1998, Link and Marks 1999, Marks and Winstral 2001). Given that the magnitude of turbulent fluxes (sensible heat and latent heat) are dependent on wind speed, higher wind speeds in open areas or low density forests can result in both higher snow sublimation rates under dry conditions and higher condensation rates under moist conditions (Marks et al. 1998). Sublimation is a process that inherently reduces the mass of the snow cover. Condensation, essentially the inverse of sublimation, often results indirectly in snow cover mass reduction during warm moist conditions (e.g. rain-on-snow events) by

increasing the snow cover's energy balance and consequently providing energy for snowmelt (Marks et al 1998).

While increased wind speed does not likely 'cause' more or less precipitation at a given point, the amount of frozen precipitation received at the snow or ground surface appears to vary inversely with wind speed. Marks and Winstral (2001) demonstrated dramatic differences in winter precipitation measured at a sheltered site and a nearby open site in a semiarid mountain basin in Idaho. In windy environments where low density snowfall events are common, significant redistribution of snow by wind can also occur in between snowfall events. High wind speeds in open areas result in wind scouring of snow, while reduced wind speeds in the lee of forest patches or below the forest canopy result in deposition of snow immediately downwind of forest patches and along forest edge environments. In their examination of an alpine treeline environment in Wyoming, Hiemstra et al (2002) found substantial snow drifts immediately downwind of conifer tree islands and minimal snow cover across the remainder of their study area..

Relatively few studies to date have explored fine scale relationships between vegetation and snow cover. The majority of research examining vegetation effects on snow accumulation and ablation has focused on differences in snow cover development (or related processes) at the stand scale (note that in this context a clearing is also a type of stand). Most studies have either analyzed stand-averaged differences between the measurements of interest or simply chosen representative points within each stand for comparison (e.g. Gary and Troendle 1982, Pomeroy et al

2002, Hardy et al 1997, Link et al 2004, Link 1999, Marks et al 1998, Koivusalo and Kokkonen 2002). The size of the stands being compared is rarely reported. Consequently, the 'stands' being analyzed and compared take on a more abstract meaning. This does not typically represent a problem when the research objective is to demonstrate or model differences in snow processes for different land cover types. For spatially distributed models, however, it is necessary to explicitly define the spatial scale of the model grid element. At this point it becomes useful, if not essential, to know the spatial scale over which a process can be assumed homogeneous. Even for modeling efforts focusing on relatively coarse scale variability in snow cover, it is important to recognize any finer scale variability (i.e. sub-grid variability), as this finer scale variability can introduce bias into the model results (Bloschl 1999). Accounting for this fine scale variability is likely to be most crucial in environments where fine scale spatial variability in snow cover has been demonstrated to be substantial and non-random (e.g. discontinuously forested landscapes subject to consistently high winds). In addition, despite a recent increase in interest in the scaling properties of snow covers (Bloschl 1999, Shook and Gray 1996), few if any studies have investigated how the scaling properties of a snow cover (e.g. the correlation length) might change depending on local vegetation conditions.

The primary objective of the research presented in this paper is to describe, qualitatively and quantitatively, how fine scale (i.e. 10-100 m scale) snow accumulation patterns relate to fine scale forest cover patterns such as the presence-

absence of forest and differences in forest canopy density. This research objective will be guided by the hypothesis that during the accumulation phase of the snow season (i.e. the part of the season prior to peak snow accumulation when snow depth is generally increasing), fine scale forest vegetation patterns have a substantial, quantifiable impact on patterns of snow water equivalent or snow depth.

2. Study Area and Methods

a. Study area description

Montana's Glacier National Park (GNP) is an ideal study area for examining the effects of forest cover on snow accumulation. GNP, which constitutes the southern section of Waterton-Glacier International Peace Park, straddles the Continental Divide just south of the United States-Canada border in northwestern Montana (figure 2) and encompasses 4082 km^2 of mountainous terrain. Elevations range from 967 m along west side valley bottoms to over 3000 m along and near the Continental Divide. The mountains are composed primarily of sedimentary rock up to 1.3 billion years old and have been extensively reshaped by alpine glaciers. Many basins in the park remain glacierized, though glaciers have retreated considerably since the end of the Little Ice Age (ca 1850) and active glaciers occupy only a small fraction of the landscape. Vegetation exhibits substantial variation from west to east as well as along an elevational gradient. The landscape composition ranges from mixed-species old growth larch, hemlock, and Douglas fir forests along west side valley bottoms to subalpine and alpine grasses and shrubs at the higher elevations to

a more xeric mosaic of coniferous forest, aspen, and grassland along the eastern boundary of the park. The majority of this diverse vegetation matrix has not been significantly impacted by human activity in the past century. Climate also differs considerably between the east and west sides of the Continental Divide, with consistently colder, drier, and windier conditions prevalent east of the Divide. The wide range of vegetation and climate regimes represented in GNP make this area an ideal natural laboratory for examining the effects of vegetation on snow accumulation.

b. Vegetation snow transects

Eight vegetation-snow transects were established in Glacier National Park in the late summer and fall of 2003. Transects were located on both sides of the Continental Divide and ranged in mean elevation from 970 m along a west side valley bottom to 1960 m near the alpine treeline east of the Continental Divide (figure 3). Each transect consisted of 30 points spaced at approximately 30 m intervals along an azimuth (figure 4), with the exception of the Mount Brown transect, which consisted of 15 points spaced at 30 m intervals along two separate azimuths. Transects were designed to maximize within-transect variability in vegetation type and forest density while simultaneously minimizing within-transect variability in all other factors expected to influence snow accumulation and ablation patterns. Transects were typically flat or paralleled the contours of the local terrain. In addition, all transects were located in areas that could be visited by field crews on

skis or snowshoes in a single day. All transects were located in areas where the avalanche hazard to field crews was considered minimal or nonexistent.

Start and end points (separated by 870 m) for transects were chosen with the aid of conventional topographic maps, high resolution digital orthophoto quadrangles (DOQs), and preliminary site visits. The other 28 points for each transect were then located in a geographic information system (GIS) at 30 m intervals along the line connecting the start and end points. All 30 points were then loaded onto a Precision Lightweight GPS Receiver (PLGR), which was used in the field to locate each point. PLGR's have a stated locational accuracy of ±5-10 m, and consequently, points along the transect were typically offset slightly from the line between the start and end points, and were also not always exactly 30 m apart. The PLGR's locational imprecision added a desired element of random variation into the exact placement of points along each transect. At each point, two 1.5 m sections of 0.95 cm diameter (3/8 inch) rebar were connected with hose clamps and inserted 10-30 cm into the ground (depending on soil hardness) to mark the survey point location. A flag identifying the survey point was placed on the top section of rebar at each point. Additional brightly colored flagging was placed in areas where trees or tall shrubs were located near the survey point. During the summer of 2004, high precision differentially corrected point locations were obtained for most survey points using a Trimble GeoXT GPS receiver and the Trimble Pathfinder Office software package.

In order to estimate the winter forest canopy gap fraction at each point along each transect, hemispherical photographs were collected at each point following the

protocol outlined in Frazer et al. (2001). A total of 240 hemispherical photographs (30 photographs along eight transects) were acquired with a Nikon Coolpix 880 digital camera equipped with a Nikon FC-E8 fisheye converter. The camera was mounted and horizontally leveled on a tripod approximately 1 m above the ground surface, facing toward the sky. Although attempts were made to acquire images only during ideal lighting conditions (uniform overcast skies or twilight), some images were acquired during sunny or partly sunny conditions due to the limited field season and consideration for the safety of field crews. The hemispherical photographs were acquired during October 2003 and August, September, October and December 2004. At points where deciduous vegetation was present, photographs were acquired after the majority of leaves or deciduous needles were shed for the season to ensure gap fraction estimates derived from the photographs would be representative of winter conditions. Each photograph was analyzed using the Gap Light Analyzer 2.0 (GLA) (Frazer et al. 1999), a freely distributed image processing software package designed to quantify gap fraction and sub-canopy solar radiation from hemispherical photographs. For each image, GLA was used to register the image, threshold the image so that black pixels corresponded to canopy vegetation and white pixels corresponded to sky, and then calculate the gap fraction (also known as the sky view fraction) for the image. Canopy gap fraction estimates were produced for field of view cones of ~ 70° and 150° (figure 5) because a prior study indicated point snow accumulation patterns correlated better with gap fraction measurements from reduced field of view cones than with gap fraction measurements from the full

hemisphere (Teti 2003). Gap fraction estimates were not produced for the full hemisphere because topographic features commonly present in sky view cones larger than 150° could not be easily discriminated from the forest canopy.

Snow surveys were repeated along each vegetation-snow transect during the winters of 2003-2004 and 2004-2005 (hereafter referred to as water years 2004 and 2005) as snow conditions and logistical considerations allowed (tables 1, 2). A total of 960 snow depth measurements were collected over the course of the two winters. Snow depth was measured to the nearest centimeter at a point 1 m in the up-transect direction from each survey point location as indicated by the rebar stake. SWE measurements were also collected when snow water equivalent was sufficient for accurate measurement with a Federal sampler. During some surveys during water year 2005, 10 depth measurements (including the original measurement acquired 1 meter in the up-transect direction) were collected in line with the transect, ranging from 4 meters down-transect to 5 meters up transect (see figure 4).

Time series of snow water equivalent, precipitation, and temperature data for four SNOTEL sites in the greater Glacier National Park area were acquired from the Natural Resources Conservation Service's National Water and Climate Center (http://www.wcc.nrcs.usda.gov). These data were used to establish a detailed picture of the evolution of seasonal snowpacks across the region for water years 2004 and 2005, as well as to compare the two water years to historical averages. PRISM spatial datasets of temperature and precipitation acquired from the Spatial Climate Analysis Service of Oregon State University (http://www.ocs.oregonstate.edu/prism/,

see Daly et al. 2002) were used to compare precipitation and temperature for water years 2004 and 2005 to 30 year climate normals for Glacier National Park east and west of the Continental Divide.

3. Results

Analysis of daily precipitation, temperature, and snow water equivalent data from the Flattop Mountain, Emery Creek, Pike Creek, and Many Glacier SNOTEL stations (see figure 3) indicated that water years 2004 and 2005 were characterized by below average precipitation and above average temperatures across the region. These precipitation and temperature anomalies resulted in below average snowpacks for both water years (figures 6, 7). The SWE/PRE ratio for November-March is the ratio of the change in cumulative SWE to cumulative precipitation between November 1 and March 31 and provides an additional simplified indication of snow cover conditions for the period (Serreze et al 1999). While SWE/PRE ratios were near average for water year 2004 at all area SNOTEL stations, SWE/PRE ratios were significantly lower than average at all area SNOTEL stations for water year 2005 (figure 7).

Heavy snowfall during November, December, and January of water year 2004 resulted in average or above average snow cover west of the Continental Divide, while below average snowpacks developed over this period east of the Continental Divide (figures 6, 7). Above average temperatures and below average precipitation across the entire region during March and April led to rapid snowmelt

and early meltout dates (figures 6, 7). Below average precipitation and above average temperatures between November 2004 and early March 2005 resulted in significantly below average snowpacks. Storms during the second half of March and first half of April brought snowpacks closer to normal later in the year, though meltout dates were still earlier than normal (figures 6, 7). Analysis of the PRISM datasets indicated similar temporal patterns in precipitation and temperature. November-May precipitation was near the 30 year average for both sides of the Continental Divide for water year 2004 (94.5% west of the Divide and 95.5% east of the Divide) and significantly below average for water year 2005 (74.6% west of the Divide and 72.1% east of the Divide) (figure 8). November-May temperatures were slightly above the 30 year average for water year 2004 (+0.62 °C west of the Divide and +0.69 °C east of the Divide) and significantly above average for water year 2005 (+1.16 °C west of the Divide and +1.30 °C east of the Divide) (figure 8).

In order to facilitate the discussion of relationships between vegetation and snow cover, the eight vegetation-snow transects were placed into one of four categories based on their vegetation characteristics: 1) dense forests 2) variable density forests with shrub and meadow openings, 3) forest-grassland mosaics, and 4) burned-unburned forest mosaics.

a. Dense forests

The Divide and West Entrance Flats vegetation-snow transects consisted entirely of dense coniferous or dense mixed forest. The Divide vegetation-snow

transect (mean elevation 1830 m) was located along the lower northwestern slopes of Divide Peak just west of the boundary between Glacier National Park and the Blackfeet Indian Reservation, approximately 7.5 km south of Saint Mary. The transect traversed dense subalpine forest comprised of lodgepole pine (*Pinus contorta*), subalpine fir (*Abies lasiocarpa*), and Engelmann spruce (*Picea engelmannii*). Canopy gap fraction at points along this transect ranged from 14 to 25 percent for the 150° field of view cone (figure 9a). Gap fraction values along this transect exhibited minor spatial autocorrelation, (figure 10a). The West Entrance Flats vegetation-snow transect was located in a flat area (mean elevation ~ 970 m) of mixed coniferous-deciduous forest just to the north of the west entrance station to Glacier National Park. The forest is composed primarily of a mixture of western larch (*Larix occidentalis*), lodgepole pine (*Pinus contorta*), Engelmann spruce (*Picea engelmannii*), subalpine fir (*Abies lasiocarpa*), black cottonwood (*Populus trichocarpa*), and paper birch (*Betula papyrifera*). Canopy gap fraction values along this transect ranged from 22 to 33 percent for the 150° field of view cone (figure 9b). Gap fraction percentages along this transect did not appear to exhibit any significant spatial autocorrelation (figure 10b).

Snow depth was significantly correlated with gap fraction along both transects on all survey dates (tables 3 and 4, figures 11 and 12). Snow depth at the two points along the West Entrance Flats transect where gap fraction exceeds 30% suggest that this relationship may become nonlinear when gap fraction exceeds ~ 30% (figures 11 and 12). The relationship between gap fraction and snow depth

along these two transects is also visible in plots of gap fraction and snow depth versus distance (figure 9), where high gap fraction values (small openings) often correspond to deeper snow measurements in March 2004. While snow depth showed minimal spatial autocorrelation along the West Entrance Flats transect, significant spatial autocorrelation was evident along the Divide transect (figure 10). The similarity between correlograms of gap fraction and snow depth for each transect provide additional evidence of the relationship between gap fraction and snow depth.

b. Variable density forests with shrub and meadow openings

The Calf Robe Mountain, Fielding, and Mount Brown transects traversed variable density, primarily coniferous forests with small openings where shrub or grassy vegetation was present. The Calf Robe Mountain vegetation-snow transect (mean elevation 1700 m) was located along the lower southeast slopes of Calf Robe Mountain, just east of the junction between the Firebrand Pass and Autumn Creek trails, approximately 2.5 km west of Marias Pass. The transect traversed areas of dense coniferous forest, small pockets of deciduous forest, as well as small meadows and forest openings with significant shrubs. The forested areas of this transect were composed of lodgepole pine (*Pinus contorta),* Engelmann spruce (*Picea engelmannii*), and subalpine fir (*Abies lasiocarpa*), with small patches of black cottonwood (*Populus trichocarpa*) and trembling aspen (*Populus tremuloides).* Canopy gap fraction along this transect ranged from 12 to 81 percent for the 150° field of view cone (figure 13). Gap fraction measurements along this transect

exhibited slight spatial autocorrelation. The Fielding vegetation-snow transect was located along the gently sloping lower south slopes (mean elevation 1450 m) of Elk Mountain, just north of the Glacier National Park boundary and the Burlington Northern-Santa Fe Railroad line, approximately 8 km southwest of Marias Pass. The Fielding transect included areas of dense coniferous forest as well as small meadows and forest openings with significant shrubs. The forested areas of the transect were dominated by lodgepole pine (*Pinus contorta*), with minor contributions from subalpine fir *(Abies lasiocarpa)*, Engelmann spruce *(Picea engelmannii)*, and Douglas fir *(Pseudotsuga menziesii)*. Canopy gap fraction along this transect ranged from 26 to 54 percent for the 150° field of view cone (figure 13). Gap fraction percentages along this transect exhibited spatial autocorrelation. The Mount Brown vegetation-snow transect (mean elevation approximately 1850 m) was located on the middle southwestern slopes of Mount Brown, to the east and south of the Mount Brown Lookout trail. Areas of potentially high avalanche hazard prevented this transect from being extended for a full 870 m in a single direction. The transect followed a bearing of 110° from point 1 to point 13, cut north and upslope to where points 14 and 15 were located in small clearings, and then extended along a bearing of 250° from point 16 to point 30 (figure 13). The transect traversed areas of medium and high density coniferous forest and included two small meadow clearings (points 14 and 15). The forest was composed primarily of lodgepole pine (*Pinus contorta*), subalpine fir (*Abies lasiocarpa*), and Douglas fir (*Pseudotsuga menziesii)*.

Canopy gap fraction along this transect ranged from 16 to 52 percent for the 150° field of view cone (figure 13).

SWE or snow depth were significantly correlated with gap fraction for all surveys along the Fielding transect and all but one survey along the Calf Robe Mountain transect. SWE was significantly correlated with gap fraction along the Calf Robe Mountain transect in March 2004, but not in February 2004 or December 2005 (tables 5, 6 and 7, figures 15 and 16). The relationship between gap fraction and snow depth/SWE appeared to be more pronounced along the Fielding transect than along the Calf Robe Mountain and Mount Brown transects. Along the Calf Robe Mountain transect, the gap fraction-SWE relationship appeared to be fairly linear for the range of gap fraction values below ~ 40%. For the more open survey point locations where gap fraction exceeded 40%, however, snow accumulation did not appear to be closely related to gap fraction, particularly for water year 2005. Gap fraction was only loosely correlated with SWE along the Mount Brown transect for all three survey dates. SWE measurements exhibited minimal spatial autocorrelation along both the Calf Robe Mountain and Fielding transects (figure 16). Given the spatial arrangement of the Mount Brown vegetation-snow transect (figure 15), correlograms were not created for this transect.

c. Forest-grassland mosaics

The White Calf Mountain vegetation-snow transect (mean elevation 1960 m) was located along the lower eastern slopes of White Calf Mountain just west of the

boundary between Glacier National Park and the Blackfeet Indian Reservation, about 5.5 km west of U.S. Highway 89. The transect included areas of low density coniferous forest, high density coniferous forest, a large meadow, and pockets of shrubs and deciduous forest. The forested areas of this transect were composed of lodgepole pine (*Pinus contorta*), limber pine (*Pinus flexilis*), subalpine fir (*Abies lasiocarpa*), Engelmann spruce (*Picea engelmannii*), and trembling aspen (*Populus tremuloides*). Canopy gap fraction along this transect ranged from 24 to 96 percent for the 150° field of view cone (figure 17a). Gap fraction measurements along this transect exhibited significant spatial autocorrelation, primarily due to the large meadow that spanned the central portion of the transect (figure 18a). The Two Dog Flats vegetation-snow transect (mean elevation 1470 m) was located along the lower southeastern slopes of Singleshot Mountain just above the Two Dog Flats area adjacent to the Going to the Sun Road. The transect included areas of low density coniferous forest, high density coniferous forest, areas of shrubs and deciduous trees, and a meadow. The forested areas of this transect consisted primarily of lodgepole pine (*Pinus contorta*), subalpine fir (*Abies lasiocarpa*), Douglas fir (*Pseudotsuga menziesii)*, and trembling aspen (*Populus tremuloides).* Canopy gap fraction along this transect ranged from 20 to 97 percent for the 150° field of view cone (figure 17b). Gap fraction measurements along this transect exhibited significant spatial autocorrelation, primarily due to the meadow that spans the northeastern third of the transect (figure 18b).

Due to the nonlinear relationships between gap fraction and SWE along the White Calf Mountain and Two Dog Flats transects, no correlation statistics were calculated for these transects. For these transects, snow depth appeared to increase linearly as a function of gap fraction up to ~ 50% gap fraction. The range of gap fraction values between 50-90% appeared to be a transition zone, where SWE values varied widely (figures 19 and 20). Above ~ 90% gap fraction, SWE was consistently shallow or absent altogether. For these two transects, the plots of gap fraction and SWE versus distance (figure 17) are particularly useful for illustrating the spatial patterning of snow cover and its relationship to gap fraction. For both transects, the large meadows (where gap fraction values are near 100% for several points in a row) have very shallow (or nonexistent) snow cover. The gap fraction and SWE versus distance plots also illustrate that while open areas (with gap fraction near 100%) typically have very shallow snow covers, very small decreases in gap fraction (typically indicative of small tree islands or the edge of a forest) can result in dramatic increases in snow cover. Both gap fraction and SWE/snow depth showed a high level of spatial autocorrelation along these two transects (figure 18).

d. Burned-unburned forest mosaics

The Camas/Moose Burn vegetation-snow transect was located in a flat area (mean elevation ~ 1090 m) to the north of the Camas Road approximately three kilometers east of the Outside North Fork Road. The western half of this transect (points 1-15) consisted primarily of standing burnt young lodgepole pine (*Pinus*

contorta) forest, while the eastern half of the transect (points 15-30) consisted of a mixture of conifers that sustained varying degrees of damage during the Moose Fire of 2001. Species along the eastern half of the transect include lodgepole pine (*Pinus contorta*), Engelmann spruce (*Picea engalmannii*), and subalpine fir (*Abies lasiocarpa*). Canopy gap fraction along this transect ranged from 23 to 85 percent for the 150° field of view (figure 21). Gap fraction percentages exhibited significant spatial autocorrelation related to the burn severity which decreased from west to east (figure 22).

Gap fraction and snow depth were not significantly correlated along this transect for either of the two survey dates (table 8, figure 23). Gap fraction and snow depth did, however, appear to be linearly related up to ~ 50% gap fraction in December 2003 (figure 23). Snow depth exhibited minimal spatial autocorrelation along this transect (figure 22).

4. Analysis of potential errors

Before proceeding to the discussion of relationships between vegetation and snow cover along the vegetation-snow transects, it is worth discussing potential measurement and analysis errors and the effects they may have had on the reported results. Potential errors were divided into the following categories: (1) errors in measuring gap fraction, (2) errors in measuring snow depth and snow water equivalent, and (3) errors resulting from within-transect topographic variability. A list of potential errors and their estimated impact on the results is provided in table 9.

a. Errors in estimating gap fraction

In order to obtain a precise measurement of winter gap fraction, hemispherical photographs must be acquired under uniform sky illumination conditions, the vegetation canopy in the photograph must be identical to the canopy present during the winter, the camera lens must be perfectly level (normal to the force of gravity), and surrounding topography must be distinguishable from the forest canopy. In practice, not all of these assumptions could be met for every single point along each vegetation-snow transect. Uniform sky illumination conditions exist only shortly before sunrise and shortly after sunset, as well as on some cloudy days. While the majority of hemispherical photographs used in this study were obtained under twilight or uniform overcast conditions, nonuniform illumination conditions did exist in some hemispherical photographs. We attempted to account for the nonuniform illumination in these photographs by adjusting the thresholding level in the GLA software. This was, however, a subjective process where the introduction of additional error was possible. A threshold value of 128 was used to discriminate between sky and canopy for the vast majority of hemispherical photographs. It is difficult to estimate the magnitude or bias of errors associated with non-uniform illumination conditions, but we believe this may have been a significant source of error in determining the relationship between gap fraction and snow cover along transects with a small range of gap fraction values.

Though we were interested in determining the winter canopy gap fraction for each survey point, hemispherical photographs were acquired during the summer and fall. We chose not to acquire hemispherical photographs in the winter because this would have resulted in substantial disturbance to the snow cover at each survey point. For the majority of survey points (> 80%) where no deciduous vegetation canopy was present above 1 m, seasonal changes in canopy gap fraction were not an issue. For the minority of survey points where deciduous vegetation exceeded 1 m in height, photographs were taken later in the fall after the majority of deciduous leaves were down for the season. In some cases, a small percentage (< 20%) of leaves remained on the branches of deciduous vegetation. This probably resulted in a slight underestimation (up to ~ 5%) of gap fraction at a small number of survey points.

For each hemispherical photograph, the camera lens was leveled using two bubble levels. Leveling errors of less than 5° may have been somewhat common, given the difficulty in leveling the camera and the need to obtain a significant number of photos in quick succession when ideal lighting conditions existed. While very significant errors in leveling would have resulted in a bias towards lower gap fraction values (because the camera lens would be viewing a lower fraction of sky and a higher fraction of the adjacent vegetation), we believe this was not a significant source of error in the measurement of gap fraction.

Given the steep, mountainous topography present throughout the study area, topographic features were visible in most hemispherical photographs along the outer edge of each photo. Manually discriminating between topographic features and

canopy vegetation for hundreds of hemispherical photographs would have been extremely difficult and somewhat subjective for most cases. Calculating gap fraction for the 150° field of view cone (rather than the entire 180° field of view cone) minimized the extent to which topographic features influenced gap fraction values. We believe that the presence of topographic features in hemispherical photographs likely resulted in a slight underestimation of gap fraction at many survey points.

b. Errors in measuring snow depth and snow water equivalent

Successfully determining relationships between vegetation cover and snow accumulation required the ability to measure subtle differences between snow cover. The Federal snow sampler used for measuring snow water equivalent was not sensitive enough to measure the subtle (differences < 2.5 cm or 1 inch) in SWE that existed in shallow snow covers (< 20 cm) along certain transects during certain periods. While SWE was generally measured for each snow survey, snow depth was used as a substitute for SWE when snow cover was shallow. All cases where snow depth is compared to gap fraction (rather than SWE) are clearly identified in the results section.

Another source of error was the potential scale mismatch between the single snow depth or SWE measurement taken at each survey point (integrating about 0.01 m^2 for depth and 0.1 m^2 for SWE) and the 150° field of view cone gap fraction measurements (which would theoretically integrate a 3543 m^2 area of canopy, assuming trees extended 9 m above the camera lens, for a total height of 10 m).

While we explored using field of view cones smaller than 150° to calculate gap fraction, we ultimately decided to use the 150° field of view cone because it allowed for discrimination between sheltered open sites (such as a small forest clearing) and exposed open sites (such as a large meadow). In order to evaluate the impact of this scale mismatch on our results, we compared sets of single point snow depth measurements with the mean depth values for sets of 10 snow depth measurements from several surveys taken around the time of peak accumulation for water year 2005 (table 10). These data indicate correlations were typically high ($r = 0.78$ or higher) between single point snow depths and the mean snow depths for ten points. The lone exception is the West Entrance Flats survey conducted on February 9, 2005. In this case, much of the variability in this shallow snow cover (mean depth 13 cm) was likely related to microtopographic features on the forest floor, rather than variability in the forest canopy.

c. Errors resulting from within-transect topographic variability

While each vegetation-snow transect was designed to minimize the effect of factors such as aspect, slope, and elevation on snow cover, all transects exhibited some level of topographic variability. While the small range of elevation within each transect likely had little effect of snow accumulation, microclimatic differences associated with different slopes and aspects, as well as local topographic hollows, probably had a more significant effect on snow accumulation for a minority of snow survey points (up to 20%). In a single instance, a data point was removed from

analysis on the Divide transect because its slope and aspect differed dramatically from all other points. In all other cases, however, we believe that the benefit of a larger sample size outweighed any benefits that could be realized by eliminating substantial portions of the dataset to reduce slope and aspect variability.

4. Discussion

The snow depth, snow water equivalent, and gap fraction data collected along these eight vegetation-snow transects indicate that gap fraction has a significant effect on snow depth/SWE. This is reflected not only by the scatter plots and correlation (r) and significance (p) values for these two variables, but also by the covariance of spatial autocorrelation for gap fraction and snow depth/SWE. Data from these snow surveys do confirm the influence of gap fraction on snow depth/SWE. It is difficult, however, to generalize this relationship across climate regimes (i.e. wet and mild vs colder, drier, and windier) and landscape types because not all vegetation-snow transects included the full range of gap fraction values.

Our analysis indicates the relationship between gap fraction and SWE or depth varies across the range of gap fraction values. For gap fraction values less than ~ 40%, variance in peak season SWE was usually low (between 7 and 55 cm for surveys including a full range of gap fraction values) and closely related to gap fraction. This relationship is most likely due to the substantial snowfall interception by the forest canopy and subsequent sublimation of intercepted snow from the canopy. Between ~ 40% and 90% gap fraction, variance in peak season SWE was

usually much higher (between 25 and 269 cm for surveys including a full range of gap fraction values), and only loosely related to gap fraction. In this 'transition zone', the increased solar radiation associated with increasing gap fractions likely results in a significant reduction in snow cover, partially counteracting the decrease in canopy interception and sublimation associated with higher gap fractions. Wind also becomes an important factor as gap fraction increases above 40%, with increased sublimation from the snow surface and wind scouring resulting in snow cover losses. The poorly defined relationship between gap fraction and snow accumulation in the range of 40-90% gap fraction can also be attributed to the importance of spatial patterning characteristics of the vegetation canopy that are not captured by a simple metric such as gap fraction. Where solar radiation and wind are concerned, the spatial organization of canopy gaps (or individual trees in sparsely forested environments) becomes extremely important (see, for example, Golding and Swanson 1986, Hiemstra, Liston, and Reiners 2002). Locations with identical gap fractions may have very different levels of exposure to wind and solar radiation, depending on the orientation of the canopy. The data suggest that the highest variance in snow accumulation existed in the range of 60-90% gap fraction, (34 to 464 cm for peak season SWE for surveys including a full range of gap fraction values) where canopy gaps are most likely to be asymmetric.

Above 90% gap fraction, snow cover was almost always shallow or nonexistent, with low variance in peak season SWE (0 to 10 cm for surveys including the full range of gap fraction values). This is presumed to be due primarily

to the substantial wind scouring that occurs in open environments east of the Continental Divide in Glacier National Park. The high levels of exposure to solar radiation and sublimation from the snow surface are also likely factors for the shallow or nonexistent snow cover found in areas with gap fraction exceeding 90%.

Although it may initially appear highly problematic that gap fraction has a limited ability to explain snow accumulation for half of the entire range of gap fraction values, it is important to consider this range of gap fraction values in terms of the fraction of the landscape it represents. A landscape analysis of gap fraction for Glacier National Park based on remotely sensed imagery and hemispherical photos (see Selkowitz et al., submitted) indicates that only 24% of the landscape is likely to be in the gap fraction range of 40-90%. Only 5% of the landscape falls into the gap fraction range of 60-90%, where the gap fraction-snow accumulation relationship is least pronounced. The spatial distribution of gap fraction values between 40 and 90% indicates that pixels with gap fraction values in this range are located primarily at high elevations, near the alpine treeline. This range of gap fraction values is also common in areas of standing burnt forest and on south facing slopes with extensive deciduous (primarily shrub) vegetation.

The substantial variability in snow accumulation in the range of 40-90% gap fraction makes it difficult to determine an optimal gap fraction percent for seasonal snow accumulation. More importantly, the optimal gap fraction for snow accumulation is determined by climate conditions and is therefore not likely to be the same for different years and locations. For continental climate regimes where high

winds and dry snowfall events are common (e.g. Glacier National Park east of the Continental Divide), the optimal gap fraction for snow accumulation appears to be in the range of 40-60% gap fraction. Although some of the deepest snow measurements in this study were collected at locations where gap fraction exceeded 60%, these were typically isolated pockets of deep snow surrounded by shallower snow (or in some cases, bare ground). Mean seasonal snow accumulation above 60% gap fraction in this study was consistently lower than mean snow accumulation in the range of 40-60% gap fraction. It is beyond the scope of this study to identify the specific causes of increased or decreased snow accumulation in certain gap fraction ranges. It is likely, however, that below 40% gap fraction, interception and sublimation of snowfall by the forest canopy significantly reduced the snow cover. It is also likely that, above 60% gap fraction, increased exposure to wind scouring, sublimation from the snow surface, as well as high solar radiation loads resulted in lower mean snow accumulation in this range of gap fraction values. For less continental climate regimes where high winds are less common, higher density snowfall events are more common, and winter days are usually cloudy (e.g. Glacier National Park below treeline west of the Continental Divide), the optimum gap fraction for snow accumulation may be greater than 60%. The data from this study, however, cannot be used to examine this hypothesis because transects west of the Continental Divide did not include the full range of gap fraction values.

It is important to note that the data presented here were representative of average and below average snow years, and the relationships between gap fraction

and snow accumulation demonstrated in this study may not hold for a heavy snow year. Though it is difficult to predict how relationships between gap fraction and snow accumulation would look during a heavy snow year, a number of factors suggest that gap fraction-snow accumulation relationships would be less pronounced. During major storm events, snowfall could potentially exceed the maximum interception capacity of the forest canopy. At this point, additional snow cover would slough off of the canopy and would no longer be exposed to sublimation. In addition, consistently stormy conditions would mean a decrease in sublimation of snow intercepted by the canopy, which occurs primarily under cold dry conditions between storms. In open environments where wind scouring, sublimation from the snow surface, and exposure to solar radiation consistently result in minimal seasonal snow accumulation, snow accumulation would likely be much higher during a heavy snow year, though still less than most forested environments. Though wind scouring would still occur consistently during a heavy snow year, individual layers of snowfall would be converted relatively quickly to the denser lower layers of the snowpack (due to the weight of fresh snowfall deposited above), protecting that snowfall layer from wind scouring. Once a layer of snowfall was covered by fresh snowfall, it would also be protected from sublimation. Stormy conditions typical of a heavy snow year would also mean a decrease in solar radiation, another cause of snow ablation in open environments.

It is not clear what effect changing the measurement scales for gap fraction and snow depth/SWE would have on the relationship between these two variables.

Given that many modeling and remote sensing efforts use grid cells that are substantially larger than 30 m, this is an important research question that should be considered. The data presented here suggest that, particularly in windy environments, simply knowing the mean gap fraction for a large (e.g. 500 m x 500 m) grid cell may be insufficient to improve model results or snow covered area retrievals. An example that illustrates this concept is a hypothetical 500 m x 500 m grid cell, 3/4 of which is covered by dense forest with a gap fraction of 20%, and 1/4 of which is an open meadow, with a gap fraction of 100%. The mean gap fraction for this grid cell would be 36.3%, a value that would normally suggest high snow accumulation. In actuality, however, snow accumulation in this hypothetical grid cell would be quite low.

5. Conclusions

Numerous studies have established the influence of vegetation canopies on seasonal snow accumulation. This research quantified the relationship between canopy density and snow accumulation at fine spatial scales (10-100 m). Further research is necessary to examine how the relationship between vegetation density and snow accumulation changes across spatial scales. In addition, more work is needed to establish how vegetation-snow accumulation relationships vary in different climate regimes (e.g. coastal vs continental). Understanding the influence of vegetation canopies on seasonal snow accumulation at multiple scales and under a wide range of climate conditions will allow for improved representation of seasonal

snow evolution processes in land surface models, particularly in areas of heterogeneous vegetation cover. This will be a critical step toward accurately simulating potential future snow cover distributions where vegetation type and density are expected to change due to forest succession, fire or other natural disturbances, human manipulation, or climatic fluctuation.

Acknowledgements

This work was supported primarily by NASA Grant NNG04GC52A. The authors wish to thank Bill Baum, Sarah Thoma, and Ali White for assistance with collection of field data under difficult and occasionally dangerous conditions. Additional field assistance came from Karen Holzer, Lisa McKeon, and Blase Reardon of the USGS Glacier Field Station, Glacier National Park backcountry rangers, and numerous volunteers including Michelle Arsenault, Robert Friedel, Jeff Schmalenberg, and the University of Illinois Outdoor Adventure Club.

References

Berry, G.J. and Rothwell, R.L. 1992. Snow ablation in small forest openings in southwest Alberta. *Canadian Journal of Forest Research* **22**: 1326-1331.

Bloschl, G. 1999. Scaling issues in snow hydrology. *Hydrological Processes* **13**: 2149-2175.

Daly, C., W. P. Gibson, G.H. Taylor, G. L. Johnson, P. Pasteris. 2002. A knowledge-based approach to the statistical mapping of climate. Climate Research, 22: 99-113.

Davis, R.E., Hardy, J.P., Ni, W., Woodcock, C., McKenzie, J.C., Jordan, R., and Li, X. 1997. Variation of snow cover ablation in the boreal forest: a sensitivity study on the effects of conifer canopy. *Journal of Geophysical Research* **102**(D24): 29,389-29,395.

Frazer, G.W., Canham, C.D., and Lertzman, K.P. 1999. Gap Light Analyzer (GLA), Version 2.0: Imaging software to extract canopy structure and gap light transmission indices from true-colour fisheye photographs, users manual and program documentation. Copyright 1999: Simon Fraser University, Burnaby British Columbia, and the Institute of Ecosystem Studies, Millbrook, New York.

Frazer, G.W., Fournier, R.A., Trofymow, J.A., Hall, R.J. 2001. A comparison of digital and film fisheye photography for analysis of forest canopy structure and gap light transmission. *Agricultural and Forest Meteorology* **109**: 249-263.

Gary, H.L., Troendle, C. 1982. Snow accumulation and melt under various stand densities in lodgepole pine in Wyoming and Colorado. USDA Forest Service Rocky Mountain Forest and Range Experiment Station, Research Note RM-417.

Golding, D.L., Swanson, R.H. 1986. Snow distribution patterns in clearings and adjacent forest. *Water Resources Research* **22**: 1931-1940.

Hardy, J.P., Davis, R.E., Jordan, R., Li, X., Woodcokc, C., Ni, W., McKenzie, J.C. 1997. Snow ablation modeling at the stand scale in a boreal jack pine forest. *Journal of Geophysical Research* **102**: 29,397-29,405.

Hardy, J.P., Melloh, R., Robinson, P., Jordan, R. 2000. Incorporating effects of forest litter in a snow process model. *Hydrological Processes* **14**: 3227-3237.

Hardy, J.P., Melloh, R., Koenig, G., Marks, D., Winstral, A., Pomeroy, J.W., Link, T. 2004. Solar radiation transmission through conifer canopies. *Agricultural and Forest Meteorology* **126**: 257-270.

Hedstrom, N.R. and Pomeroy, J.W. 1998. Measurements and modelling of snow interception in the boreal forest. *Hydrological Processes* **12**: 1611-1625.

Hiemstra, C.A., Liston G.E., Reiners, W.A. 2002. Snow redistribution by wind and interactions with vegetation at upper treeline in the Medicine Bow Mountains, Wyoming, U.S.A. *Arctic, Antarctic, and Alpine Research* **34**: 262-273.

Koivusalo, H., Kokkonen, T. 2002. Snow processes in a forest clearing and in a coniferous forest. *Journal of Hydrology* **262**: 145-164.

Link, T.E., Marks., D. 1999. Point simulation of seasonal snow cover dynamics beneath boreal forest canopies. *Journal of Geophysical Research* **104**: 27,841-27,857.

Link, T.E., Marks, D., Hardy, J.P. 2004. A deterministic method to characterize canopy radiative transfer properties. *Hydrological Processes* **18**:3583-3594.

Lundberg, A., and Koivusalo, H. 2003. Estimating winter evaporation in boreal forests with operational snow course data. *Hydrological Processes* **17**: 1479-1493.

Lundberg, A., Yuichiro, N., Thunehed, H., Halldin, S. 2004. Snow accumulation in forests from ground and remote-sensing data. *Hydrological Processes* **18**:1941-1955.

Marks, D., Kimball, J., Tingey, D., Link, T. 1998. The sensitivity of snowmelt processes to climate conditions and forest cover during rain-on-snow: a case study of the 1996 Pacific Northwest flood. *Hydrological Processes* **12**: 1569-1587.

Marks, D., Winstral, T. 2001. Comparison of snow deposition, the snow cover energy balance, and snowmelt at two sites in a semiarid mountain basin. *Journal of Hydrometeorology* **2**(3): 213-227.

Melloh, R., Hardy, J.P., Bailey, R.N., Hall, T.J. 2002. An efficient snow albedo model for the open and sub-canopy. *Hydrological Processes* **16**: 3571-3584.

Pomeroy, J. W., Gray, D.M., Hedstrom, N.R., Janowicz, J.R., 2002. Prediction of seasonal snow accumulation in cold climate forests. *Hydrological Processes*, **16:** 3543-3558.

Price, A.G. 1988. Prediction of snowmelt rates in a deciduous forest. Journal of Hydrology **101:** 145-157.

Satterlund, D.R., Haupt, H.F. 1967. Snow catch by conifer crowns. *Water Resources Research* **3**(4): 1035-1039.

Satterlund, D.R., Haupt, H.F. 1970. The disposition of snow caught by conifer crowns. *Water Resources Research* **6**(2): 649-652.

Shook, K., Gray, D.M. 1996. Small-scale spatial structure of shallow snow covers. *Hydrological Processes* **10:** 1283-1292.

Storck, P., Lettenmaier, D.P., and Bolton, S.M. 2003. Measurement of snow interception and canopy effects on snow accumulation and melt in a mountainous maritime climate, Oregon, United States. *Water Resources Research* **38**(11): 1223.

Teti, P. 2003. Relations between peak snow accumulation and canopy density. *The Forestry Chronicle* 79(2), 307-312.

List of tables

List of figures

Figure 22. Correlogram of gap fraction and March 2004 snow depth for burned-unburned forest mosaic transect.

Figure 23. Scatter plots of gap fraction vs snow depth for burned-unburned forest mosaic for all water year 2004 surveys.

Table 1. Snow survey dates by transect for water year 2004.

	Nov	Dec	Jan	Feb	Mar
Camas		30			17
West Entrance Flats		14			16
Mount Brown				13	28
Fielding		15			19
Calf Robe Mountain			1	12	22
White Calf Mountain	26		22		25
Divide		26			26
Two Dog Flats				14	20

Table 2. Snow survey dates by transect for water year 2005.

	Nov	Dec	Jan	Feb	Mar
Camas					
West Entrance Flats		31		9	
Mount Brown		22	2		
Fielding				14	
Calf Robe Mountain		24		13	16
White Calf Mountain		28		11	15
Divide		19		10	18
Two Dog Flats					

Table 3. Correlation between gap fraction and snow depth along the Divide vegetation-snow transect for all survey dates.

	Dec 2003	Mar 2004	Dec 2004	Feb 2005	Mar 2005
Correlation (r)	0.64	0.72	0.65	0.56	0.68
Significance (p)	0.00018	0.00001	0.00015	0.00142	0.00005

Table 4. Correlation between gap fraction and snow depth along the West Entrance Flats vegetation-snow transect for all survey dates.

	Dec 2003	Mar 2004	Dec 2004	Feb 2005
Correlation (r)	0.52	0.50	0.40	0.47
Significance (p)	0.00294	0.00475	0.02698	0.00868

Table 5. Correlation between gap fraction and snow water equivalent along the Calf Robe Mountain vegetation-snow transect for all survey dates.

	Jan 2004	Feb 2004	Mar 2004	Dec 2004	Feb 2005	Mar 2005
Correlation (r)	0.39	0.48	0.50	0.28	0.40	0.39
Significance (p)	0.03237	0.00781	0.00506	0.14082	0.03295	0.03215

Table 6. Correlation between gap fraction and snow water equivalent or snow depth along the Fielding vegetation-snow transect for all survey dates.

	Dec 2003	Mar 2004	Feb 2005
Correlation (r)	0.65	0.44	0.56
Significance (p)	0.00011	0.01518	0.00117

Table 7. Correlation between gap fraction and snow water equivalent along the Mount Brown vegetation-snow transect for all survey dates.

	Feb 2004	Mar 2004	Dec 2005
Correlation (r)	0.30	0.46	0.31
Significance (p)	0.11349	0.01115	0.09696

Table 8. Correlation between gap fraction and snow depth along the Camas/Moose Burn vegetation-snow transect for all survey dates.

	Dec 2003	Mar 2004
Correlation (r)	0.29	0.23
Significance (p)	0.14300	0.21991

Table 9. Potential errors and estimated magnitude and direction.

Process Affected	Error	Direction of Effect	Magnitude of Effect	Comments
gap fraction estimation	variable illumination conditions	both	up to 5% gap fraction	more significant for dense forest transects where range of gap fraction values is smaller
gap fraction estimation	deciduous leaves in canopy	negative (gap fraction ↓)	up to 5% gap fraction	less than 5% of measurements affected
gap fraction estimation	leveling errors	negative (gap fraction ↓)	up to 1% gap fraction	
gap fraction estimation	lack of distinction between topographic features and canopy	negative (gap fraction ↓)	up to 5% gap fraction	less significant for dense forests
snow measurement	SWE measurement errors	both	up to 2.5 cm	SWE measurements not used for shallow snow covers (less than 20 cm)
vegetation-snow comparisons	scale mismatch between canopy and snow measurements	both	unknown	see table 10
vegetation-snow comparisons	variability in snow accumulation due to within-transect topographic variability	both	up to 50% of total accumulation (but usually much lower)	minimal effect for most survey points

Table 10. Correlation between single point depth measurements and mean depth for ten points.

Survey	Date	Correlation	Mean Depth	Std Dev Depth
Divide	3/18/2005	0.84	40.6	19.5
West Entrance Flats	2/9/2005	0.55	13.0	6.3
Calf Robe Mountain	3/16/2005	0.90	35.9	29.6
Fielding	2/14/2005	0.84	15.4	4.9
Mount Brown	12/22/2004	0.89	68.7	19.4
White Calf Mountain	3/15/2005	0.78	31.8	21.3

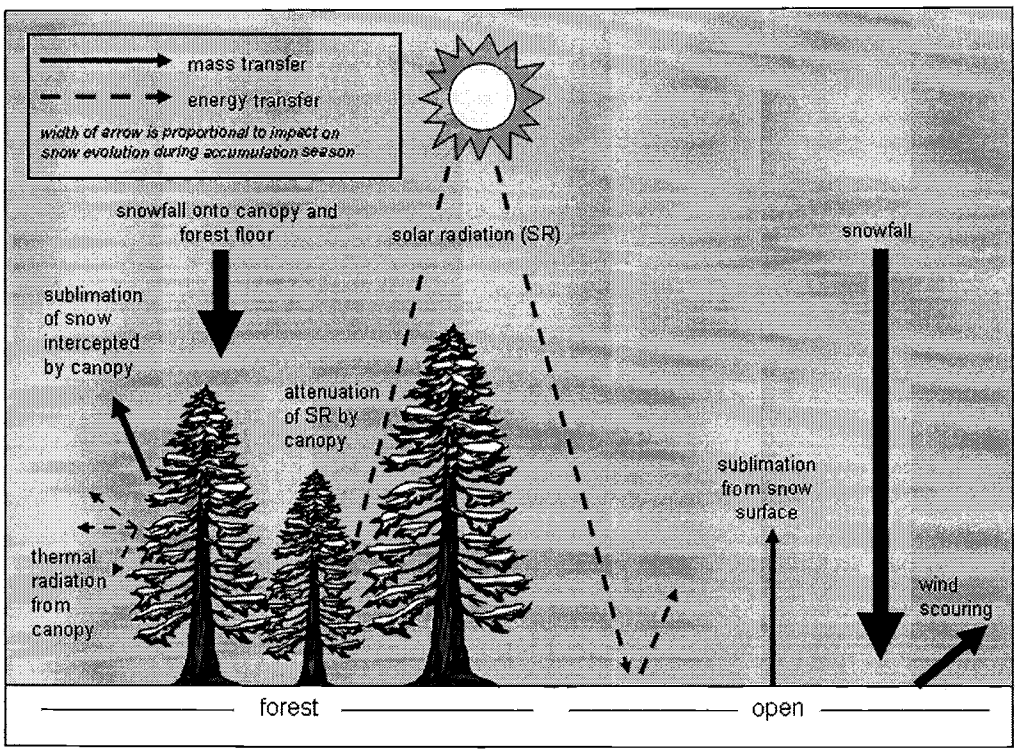

Figure 1. A diagram of the primary physical processes affecting snow evolution during the snow accumulation season in cold climates.

Figure 2. Glacier National Park locator map.

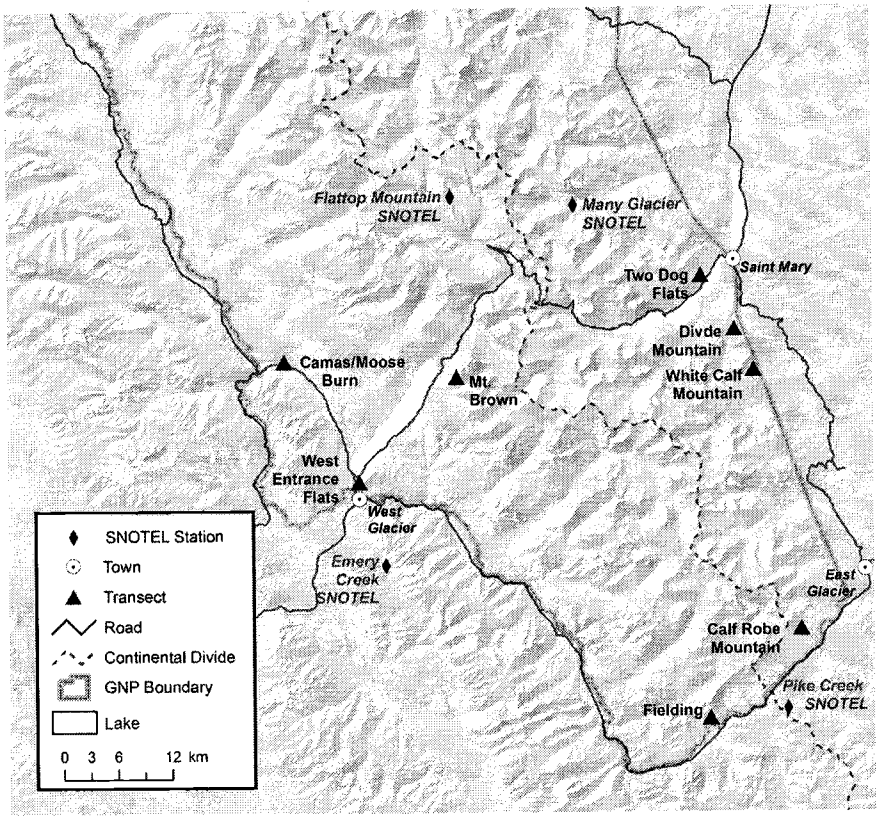

Figure 3. Location of vegetation-snow transects and SNOTEL sites in the greater Glacier National Park area.

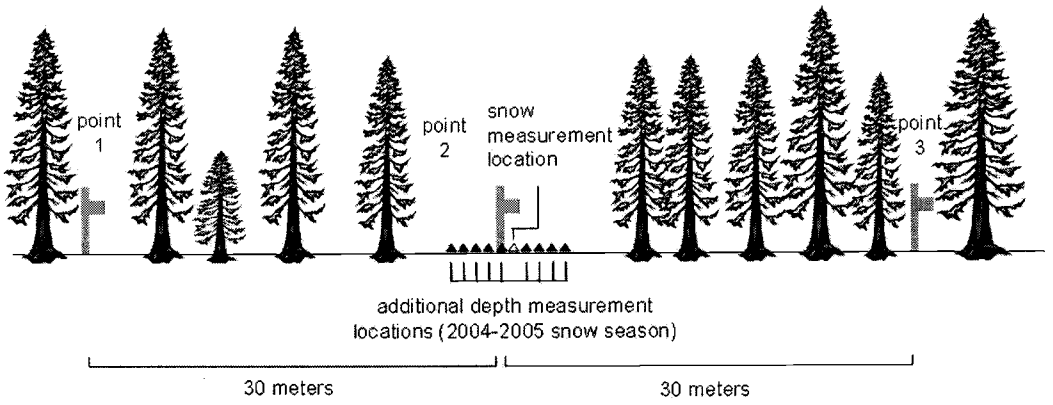

Figure 4. Schematic diagram of typical vegetation-snow transect.

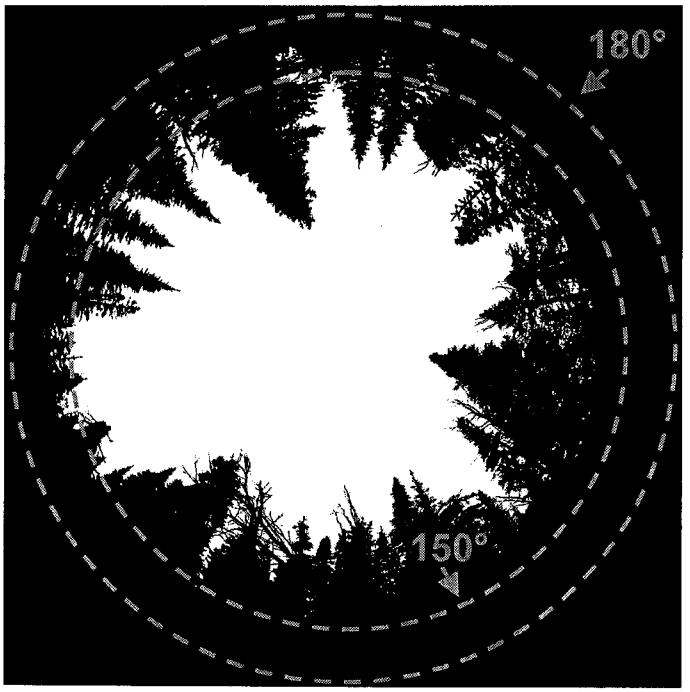

Figure 5. Hemispherical digital photograph labeled with 150° and 180° field of view cones. A threshold has been applied so that the gap area appears white and vegetation is black.

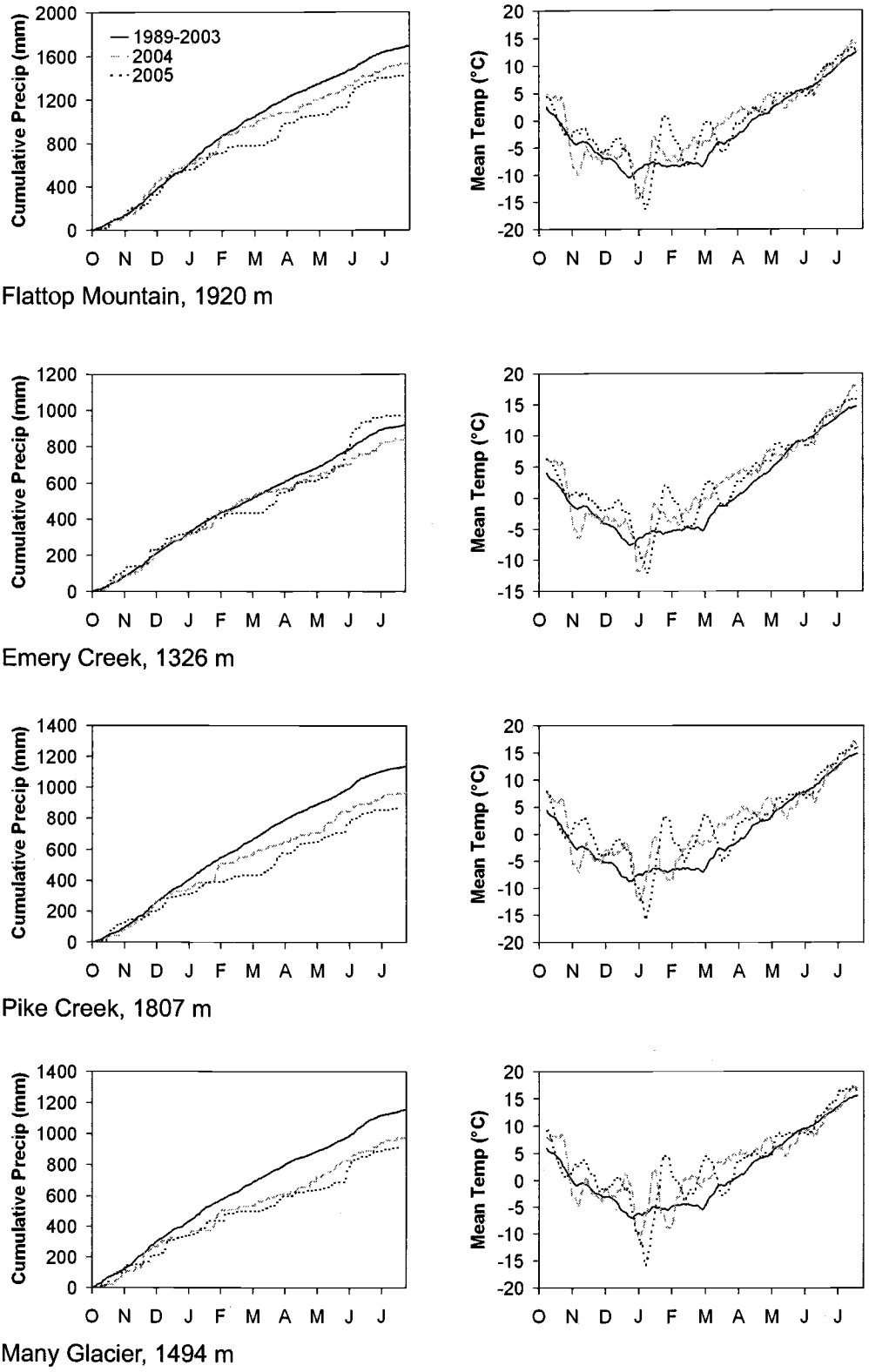

Figure 6. Time series of precipitation and temperature for area SNOTEL stations.

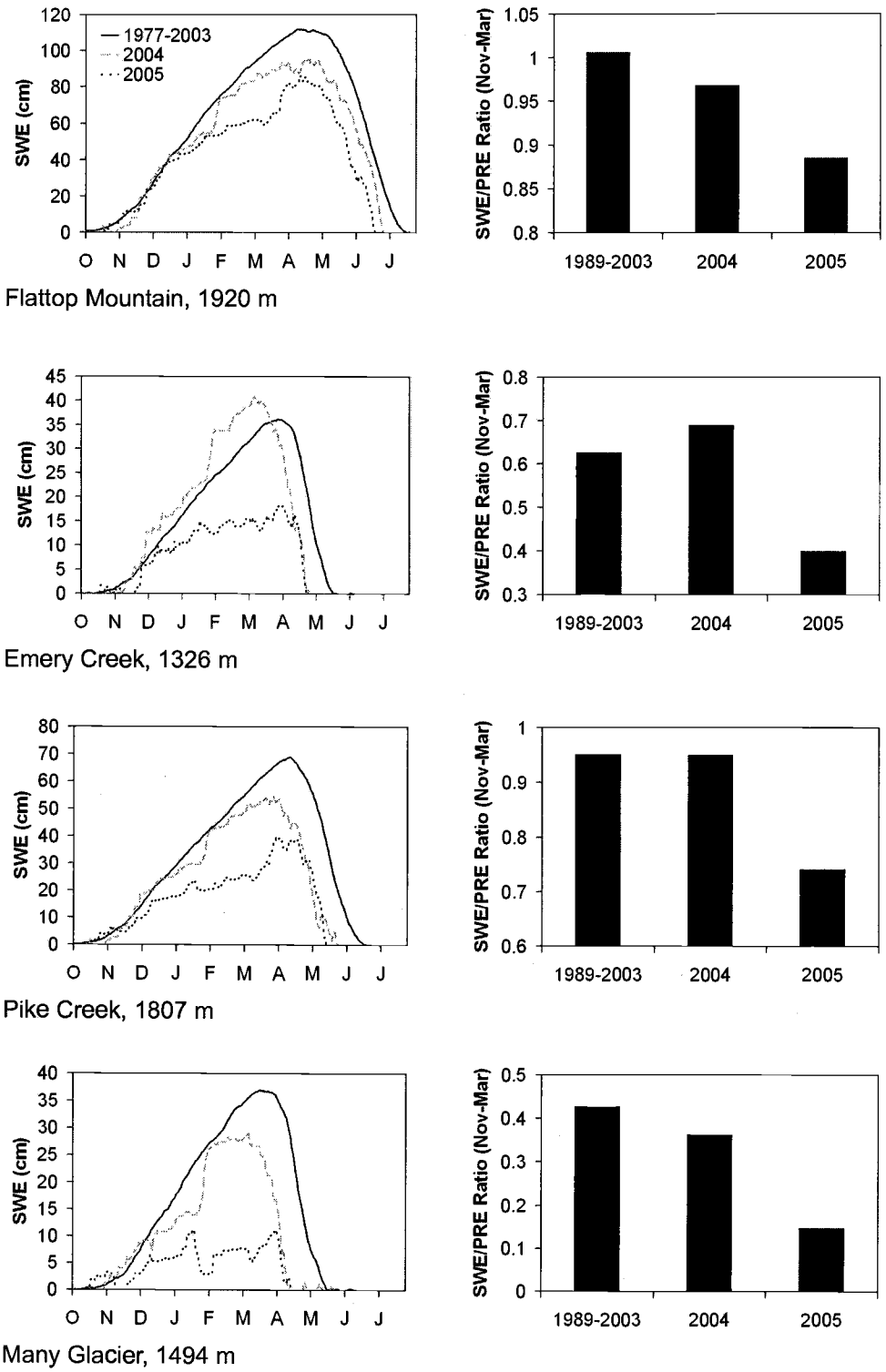

Figure 7. Time series of SWE and November-March SWE/PRE ratios for area SNOTEL stations.

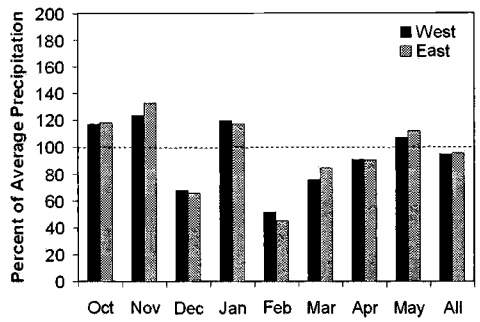

a) 2004 precipitation percent of average

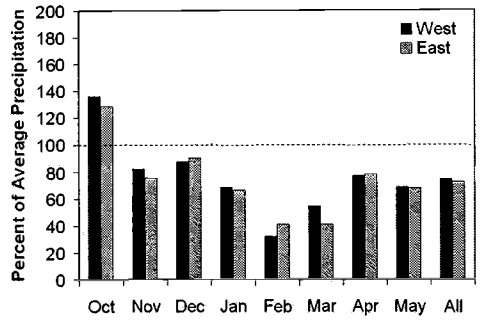

b) 2005 precipitation percent of average

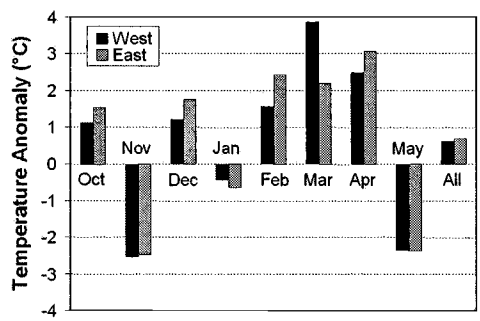

c) 2004 temperature anomalies

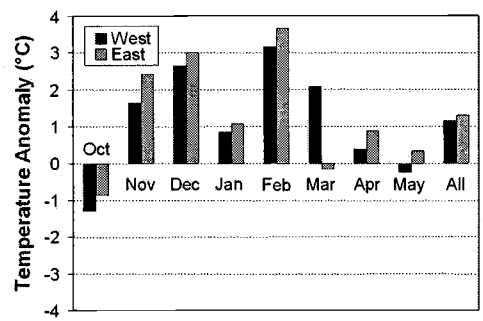

d) 2005 temperature anomalies

Figure 8. Monthly precipitation and temperature compared to 1971-2000 30 year normals for Glacier National Park east and west of the Continental Divide.

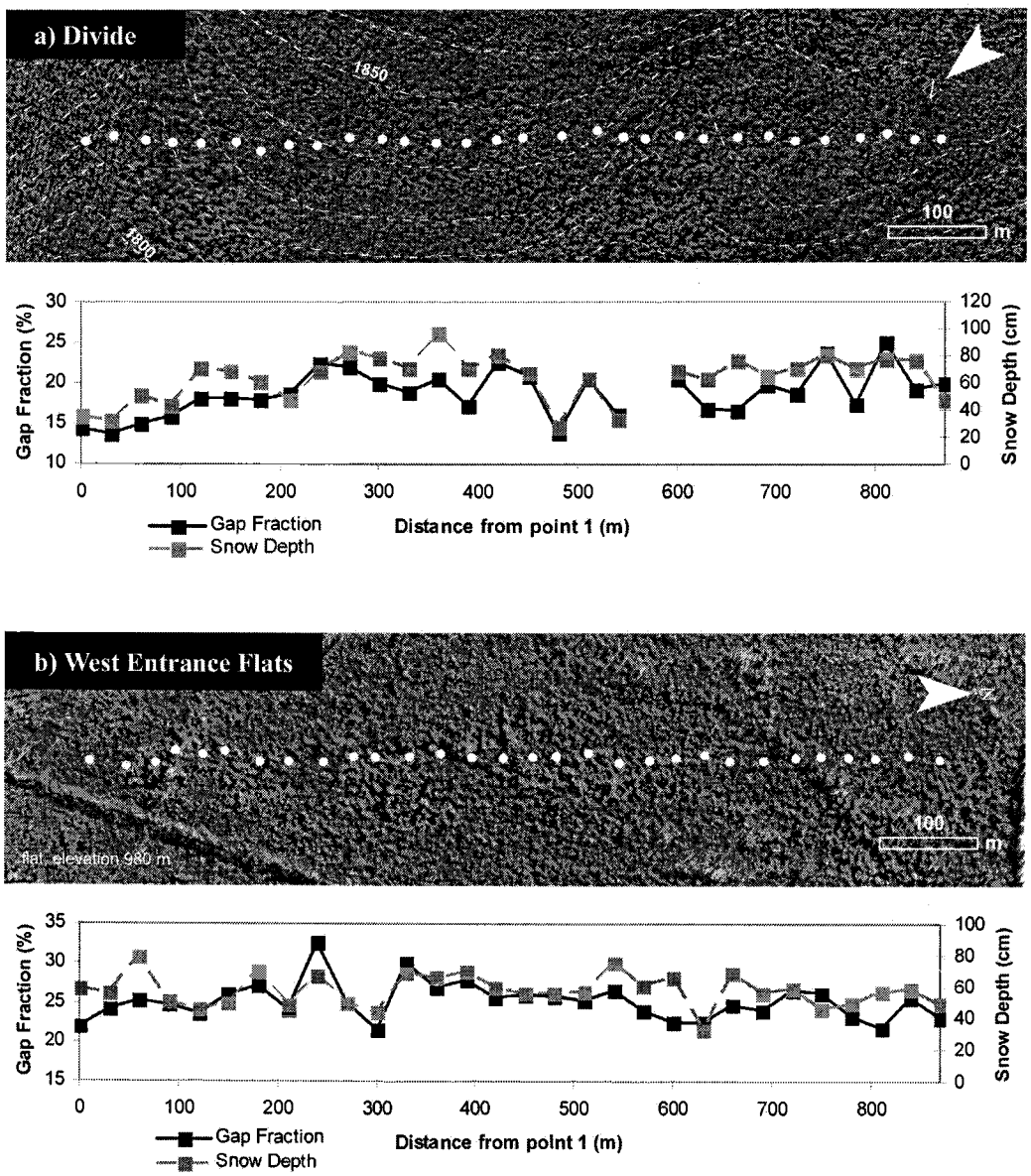

Figure 9. Gap fraction and March 2004 snow depth plots for dense coniferous forest vegetation-snow transects, a) Divide, b) West Entrance Flats.

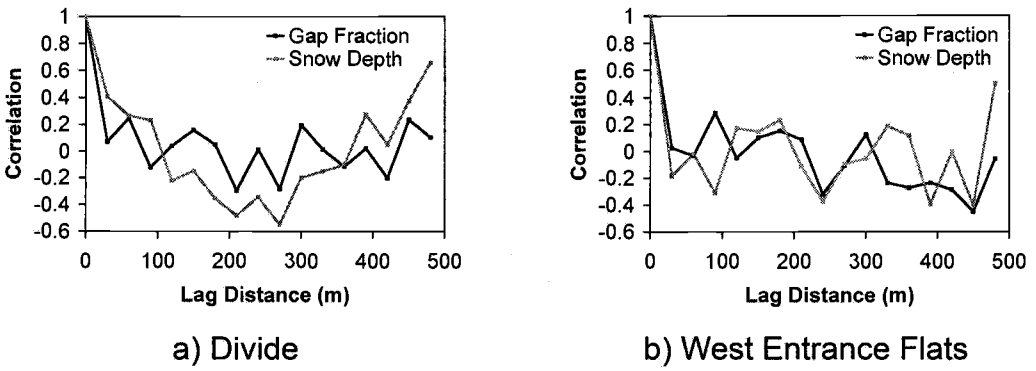

Figure 10. Correlograms of gap fraction and March 2004 snow depth for dense coniferous forest vegetation-snow transects, a) Divide, b) West Entrance Flats.

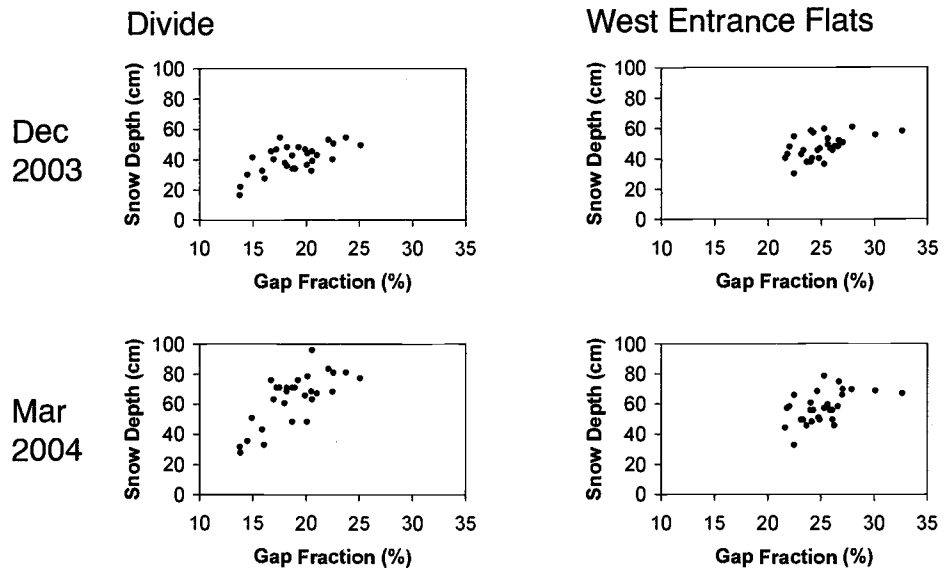

Figure 11. Scatter plots of gap fraction vs snow depth for dense forest vegetation-snow transects for all water year 2004 surveys

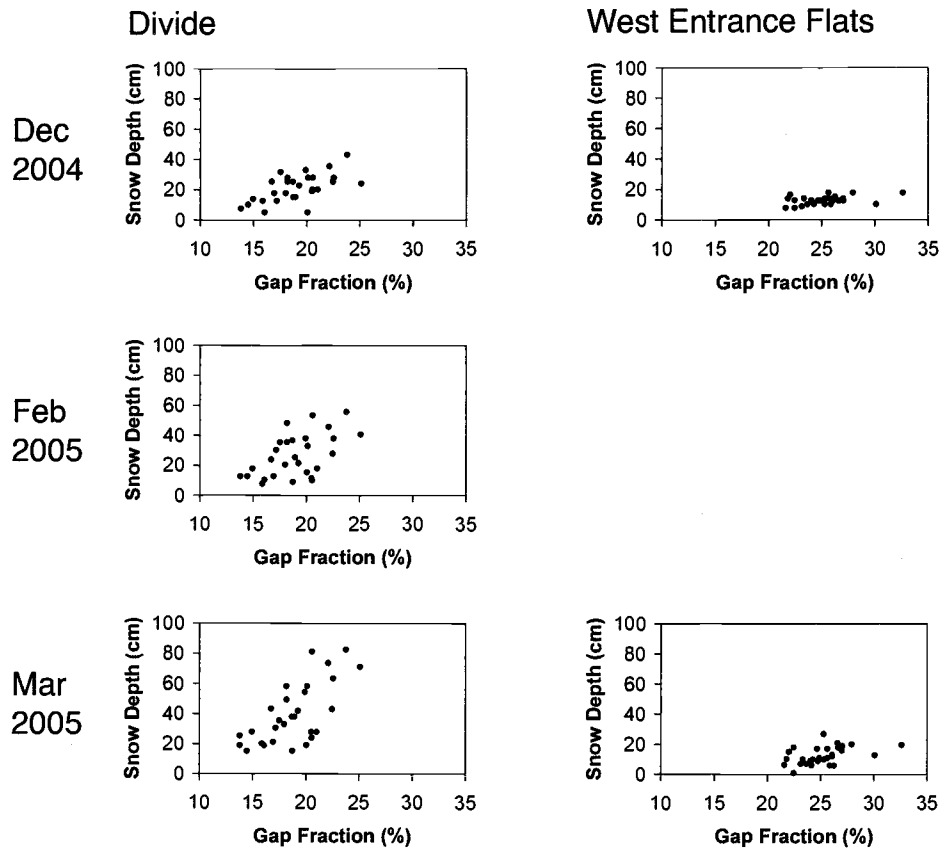

Figure 12. Scatter plots of gap fraction vs snow depth for dense forest vegetation-snow transects for all water year 2005 surveys.

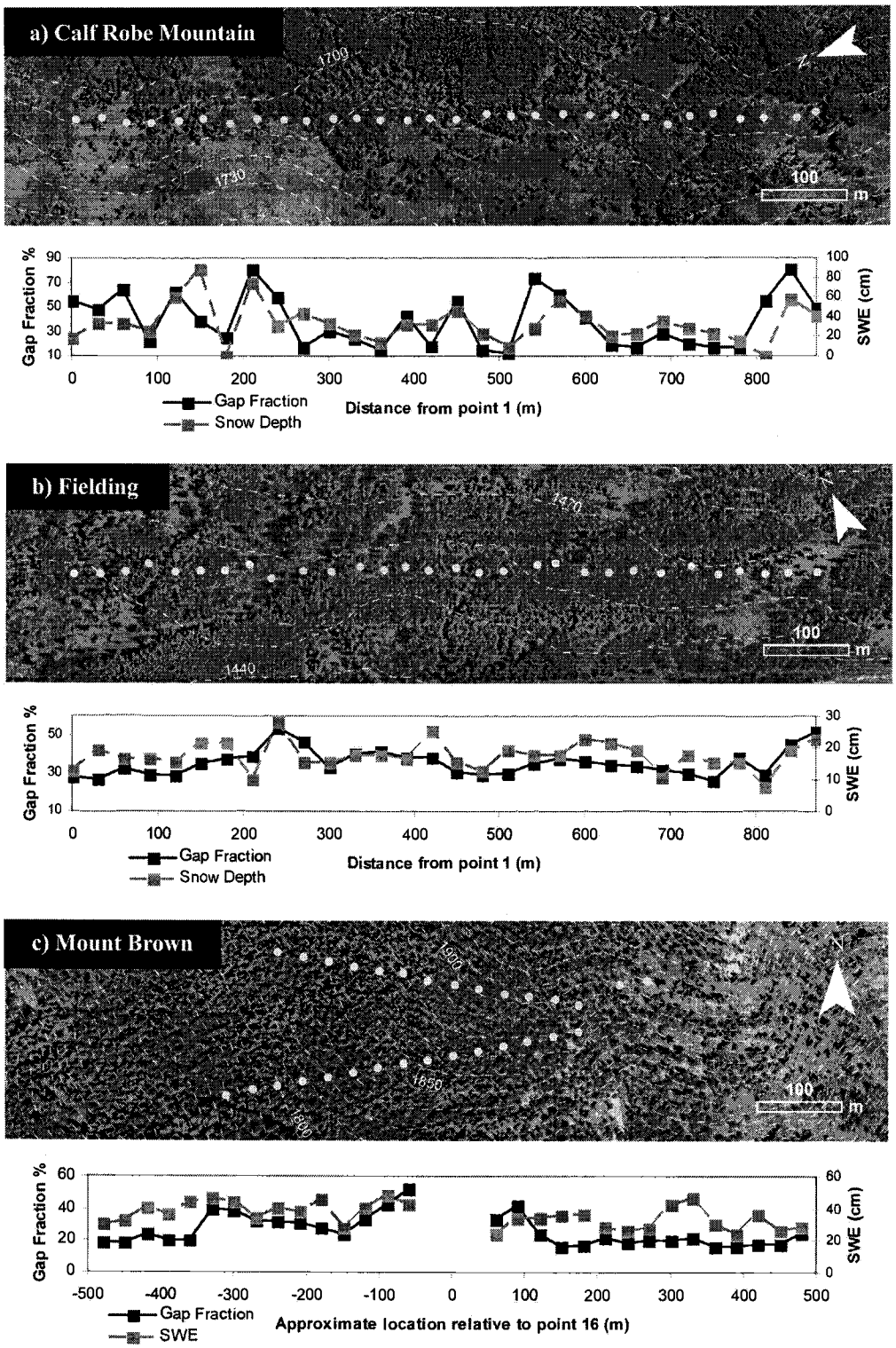

Figure 13. Gap fraction and March 2004 SWE for variable density forest transects, a) Calf Robe Mountain, b) Fielding, and c) Mount Brown.

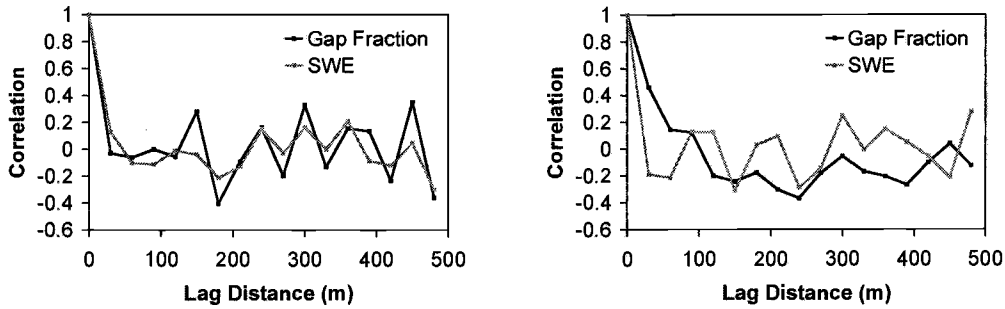

a) Calf Robe Mountain b) Fielding

Figure 14. Correlograms of gap fraction and March 2004 snow water equivalent for variable density forests vegetation-snow transects, a) Calf Robe Mountain, b) Fielding.

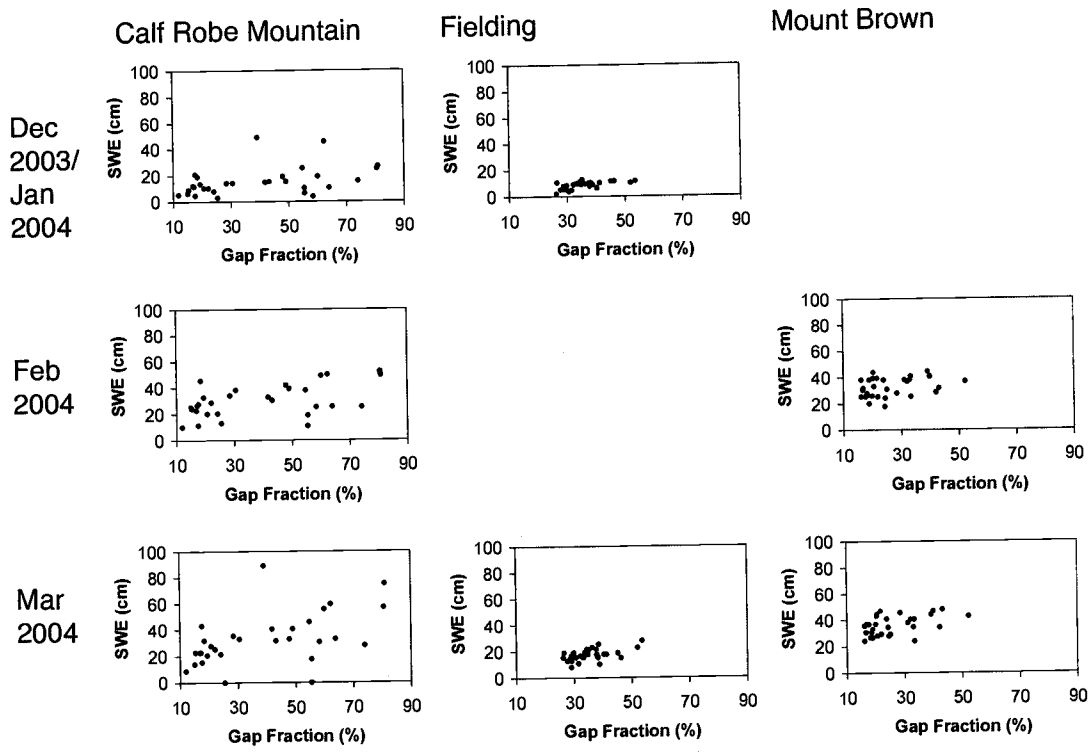

Figure 15. Scatter plots of gap fraction vs SWE for variable density forest transects for all water year 2004 surveys.

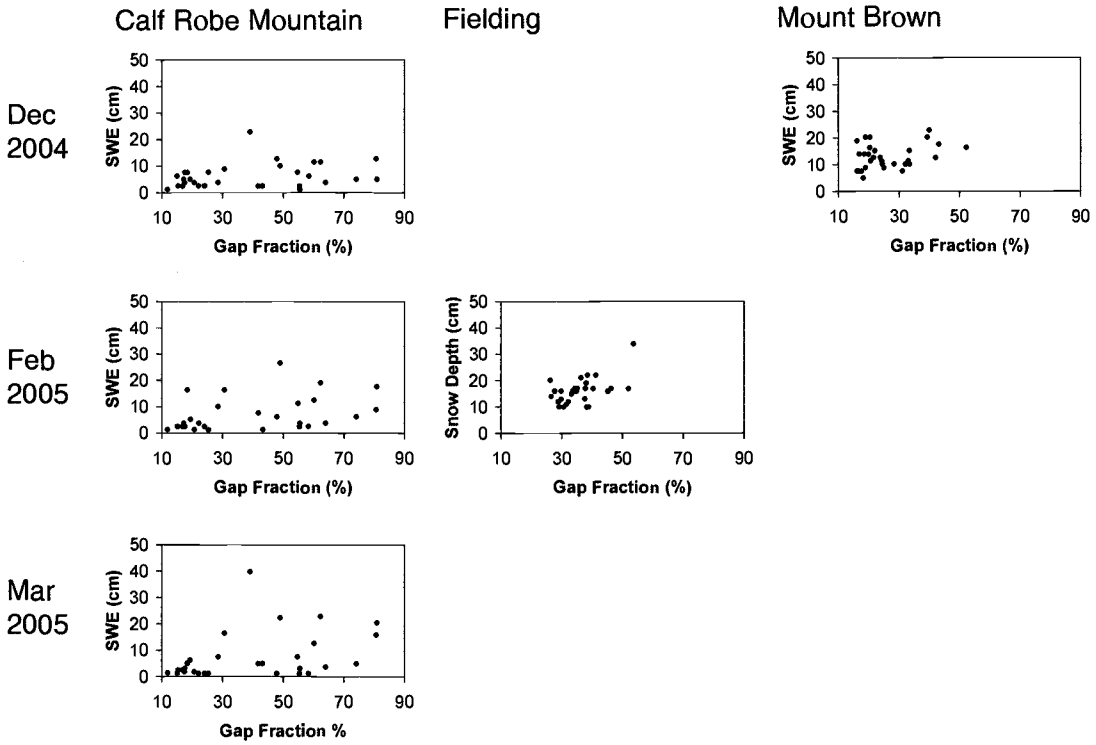

Figure 16. Scatter plots of gap fraction vs snow depth or SWE for variable density forest transects for all water year 2005 surveys.

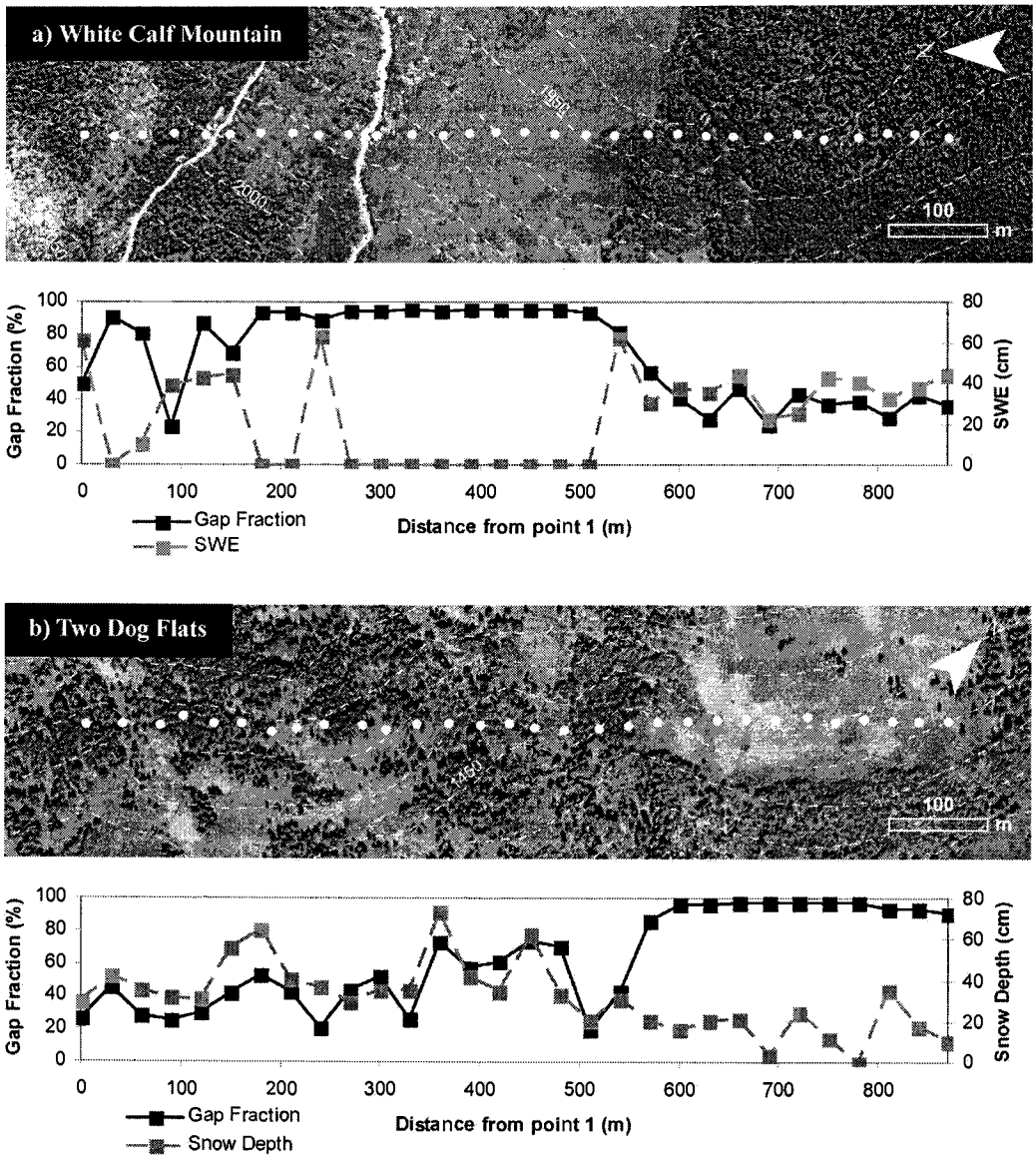

Figure 17. Gap fraction and February/March 2004 SWE for forest-grassland mosaic transects, a) White Calf Mountain, b) Two Dog Flats.

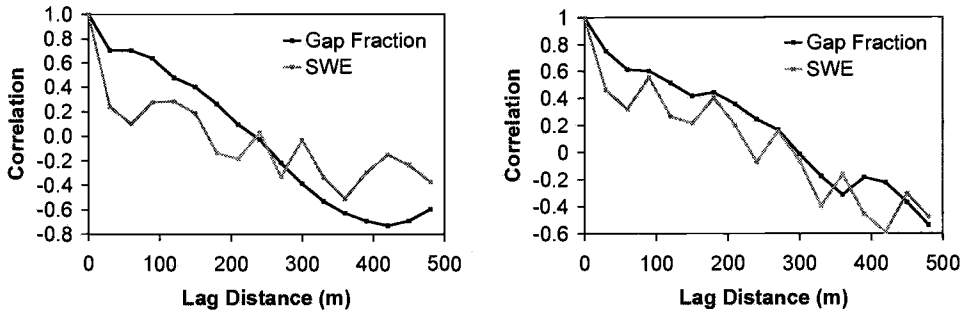

a) White Calf Mountain b) Two Dog Flats

Figure 18. Correlograms of gap fraction and February/March 2004 SWE for forest-grassland mosaic transects, a) White Calf Mountain, b) Two Dog Flats.

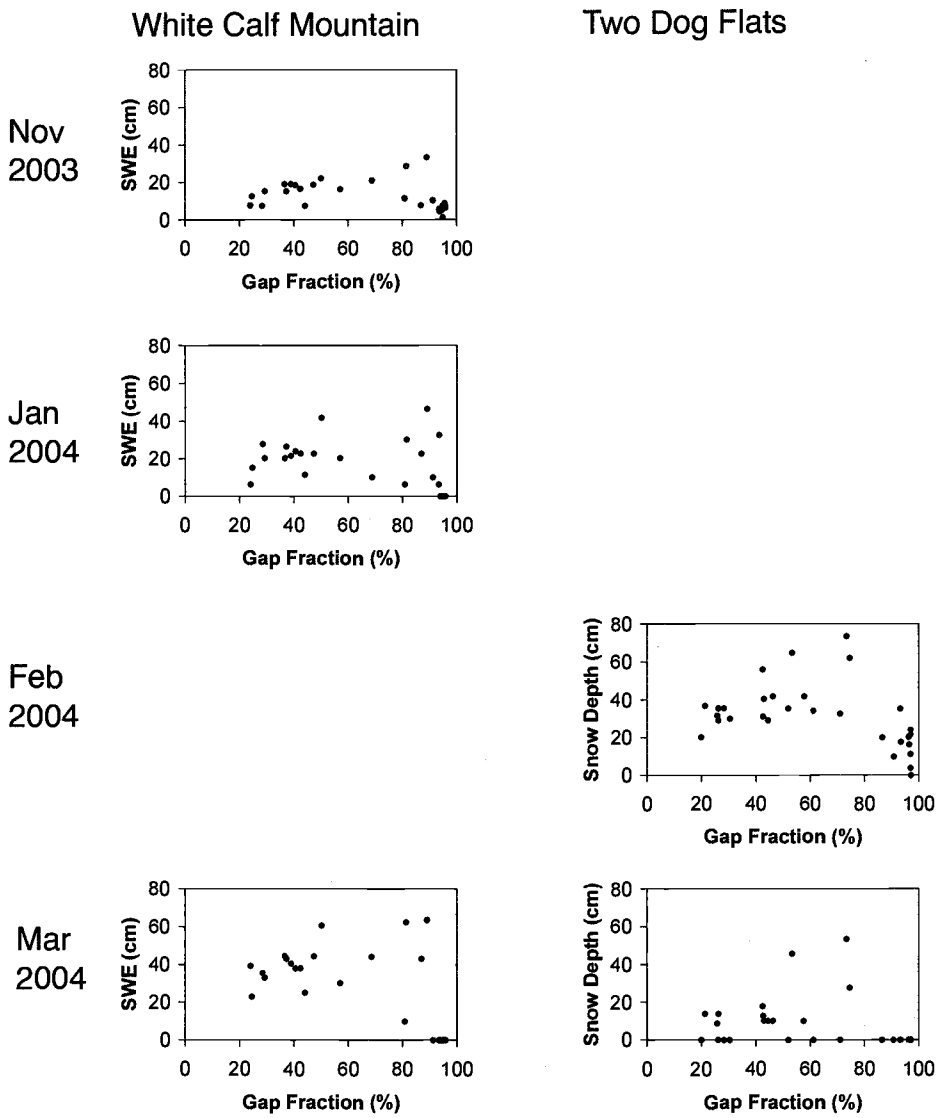

Figure 19. Scatter plots of gap fraction vs SWE for forest-grassland mosaic transects for all water year 2004 surveys

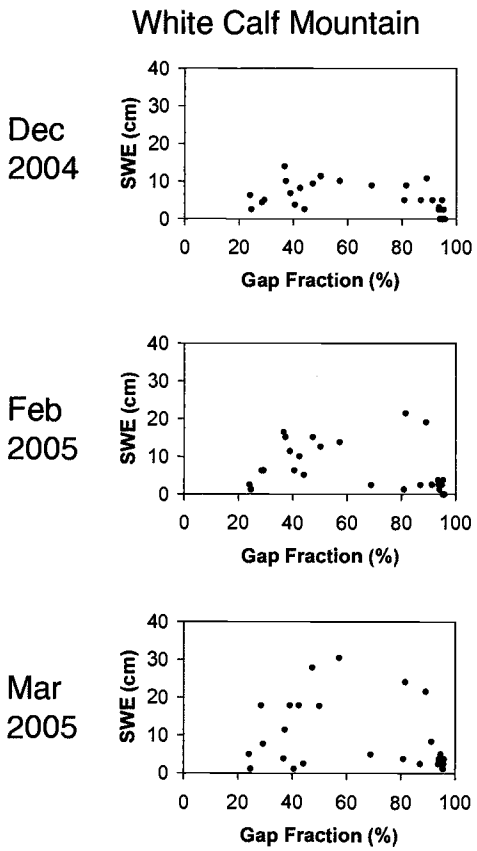

Figure 20. Scatter plots of gap fraction vs SWE for forest-grassland mosaic transects for all water year 2005 surveys.

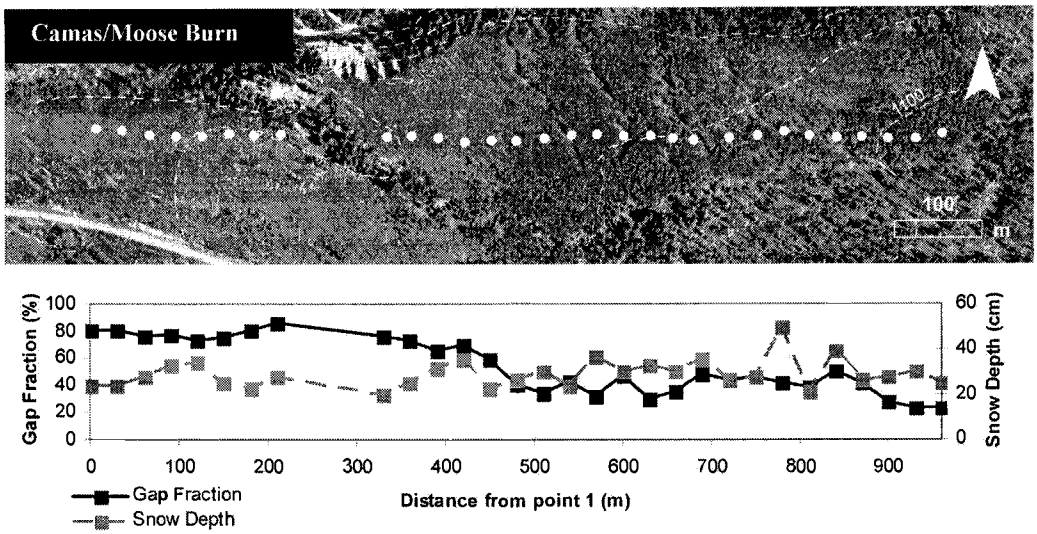

Figure 21. Gap fraction and March 2004 snow depth for burned-unburned forest mosaic transect.

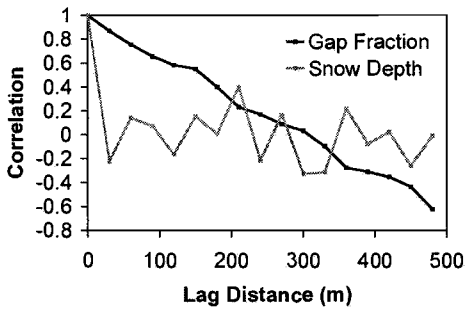

Camas/Moose Burn

Figure 22. Correlogram of gap fraction and March 2004 snow depth for burned-unburned forest mosaic transect.

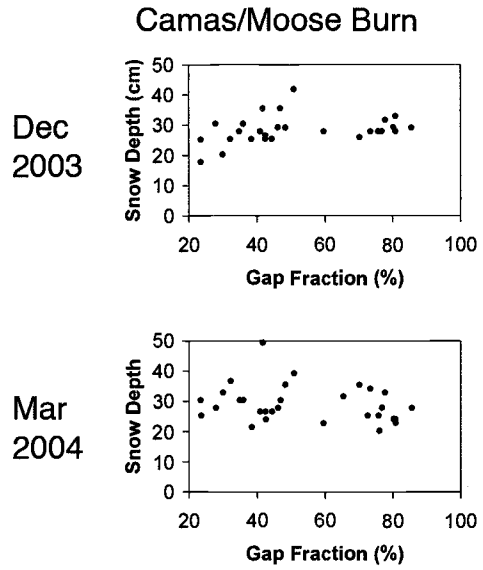

Figure 23. Scatter plots of gap fraction vs snow depth for burned-unburned forest mosaic for all water year 2004 surveys.

ASSESSMENT OF MODELING AND REMOTE SENSING TECHNIQUES FOR MAPPING THE SPATIOTEMPORAL DISTRIBUTION OF SNOW COVER IN AREAS OF HETEROGENEOUS VEGETATION

David Selkowitz
Anne W. Nolin
Daniel Fagre
Glen Liston
Tom Painter

To be submitted to *Journal of Hydrometeorology*

Abstract

Methods for modeling and mapping spatiotemporal variability in snow cover were evaluated for Glacier National Park, Montana, a mountainous region with heterogeneous vegetation distributions including coniferous forests, grassland, and shrub vegetation. SnowModel, a relatively new physically-based snow evolution model that accounts for the influence of vegetation on snow processes, was used to simulate the spatial distribution of snow water equivalent at hourly time steps for an 850 km^2 model domain in eastern Glacier National Park. The standard implementation of SnowModel uses an image of land cover type to adjust snow accumulation and ablation for the effects of vegetation. In this non-standard implementation, the model was parameterized using a weighting scheme that allowed the model to utilize a Landsat-derived image of gap fraction to adjust snow accumulation and ablation in a more precise manner than would have been possible if only land cover type information was available. In situ measurements suggest the model did a reasonable job simulating snow evolution patterns and the differences in snow evolution associated with different vegetation densities. Weaknesses in this implementation of SnowModel appear to be its tendency to overestimate snow in the easternmost portion of the model domain (where a significant rain shadow effect exists) and overestimate snow in exposed areas. MODIS-derived images of binary and fractional snow covered area were also evaluated. The binary product consistently mapped a higher percentage of the study area as snow covered than the fractional product. Both the binary and fractional SCA products underestimated

snow cover in late February, when model results and in situ observations suggested snow cover was near 100%. Spatial patterns of snow covered area were similar for the MODIS-derived products and the results from the implementation of SnowModel. Unfortunately, the remotely sensed snow covered area products could not be used to evaluate the model's treatment of snow evolution under different vegetation conditions because gap fraction influences the mapping of snow covered area for the remotely sensed products. Understanding how remotely sensed estimates of snow covered area are influenced by gap fraction density will hopefully allow for these products to be used as a validation tool for spatially distributed model results in areas of heterogeneous vegetation in the future.

1. Introduction

In cold regions, snow cover variability typically exerts a strong influence on hydrological and ecological processes, including streamflow, soil moisture dynamics, animal movement and mortality, and vegetation phenology. Consequently, understanding snow cover variability over both time and space is key to understanding the hydrology and ecology of these systems. Numerous studies have demonstrated that the type, density, and structure of vegetation influences the accumulation and ablation of a seasonal snow cover (Gary and Troendle 1982, Golding and Swanson 1986, Hedstrom and Pomeroy 1998, Hiemstra et al. 2002, Storck et al. 2003, Lundberg et al. 2004 and many others). In forested environments, interception and subsequent sublimation of snowfall by the forest canopy reduce the seasonal snow accumulation beneath the canopy (Gary and Troendle 1982, Golding and Swanson 1986, Hedstrom and Pomeroy 1998, Storck et al. 2003, Lundberg et al. 2004). Forest canopies also attenuate solar (shortwave) radiation, resulting in reduced ablation rates (Davis et al. 1997, Berry and Rothwell 1992, Hardy et al. 2004, Link et al. 2004). Reduced ablation rates below the forest canopy are often partially offset by enhanced thermal radiation (Price 1988, Link et al. 2004) and enhanced absorption of solar radiation due to decreased snow albedo (Hardy et al. 2000, Melloh et al. 2002). Wind speeds are lower below the forest canopy, as well as in the lee of individual trees in sparsely forested environments. This reduces the magnitude of turbulent fluxes (sublimation and condensation) that often contribute significantly to snow cover ablation (Marks et al. 1998, Link and Marks 1999, Marks

and Winstral 2001). Lower wind speeds below the canopy or in the lee of individual trees also prohibit wind scouring and allow for wind deposition in locations where wind transport of snow is significant (Hiemstra et al. 2002).

A number of researchers have attempted to incorporate the effects of vegetation on snow accumulation and ablation into physically based snow evolution models. Hardy et al. (1997) used a radiative transfer model, a wind speed modification algorithm, and measured sub-canopy air temperature to model snow cover ablation at boreal forest stands in central and northern Canada. Link and Marks (1999) used a number of simple algorithms to adjust solar radiation, thermal radiation, and wind speed measurements from the non-forested environments to reflect sub-canopy conditions for boreal forest stands in central and northern Canada. A physically based snow evolution model driven with these adjusted measurements accurately simulated the snow cover evolution below the forest canopy at a number of sites. Koivusalo and Kokkonen (2002) used a similar approach to simulate the evolution of snow cover in an opening and in a forest stand at a sub-arctic site in Finland. Marks et al. (2002) used data from two weather stations to effectively simulate spatiotemporal patterns of snow cover accumulation and ablation in a semi-arid mountain basin in Idaho. They used data from an exposed weather station to drive the model for exposed pixels and data from a forest-sheltered weather station to drive the same model for sheltered pixels. Their results demonstrated that accounting for differences in snow evolution between exposed and sheltered sites was crucial to the success of a spatially distributed snow modeling effort undertaken in a windy

environment with heterogeneous vegetation cover. Hiemstra et al. (2002) used a wind-transport model and a highly detailed vegetation map to simulate the spatial patterns of snow accumulation in a sparsely forested high elevation environment in Wyoming.

Remotely sensed estimates of snow covered area (SCA) are often used to improve modeled estimates of snow water equivalent (SWE; Elder et al. 1998, Cline et al. 1998). In remote areas that lack meteorological instrumentation, remotely sensed SCA sometimes represents the only information on the spatial and temporal distribution of snow. Remotely sensed SCA products include (i) binary snow cover products that map each pixel as either snow covered or snow free and (ii) fractional SCA products that attempt to map the fraction of each pixel covered by snow. Mapping SCA in forested or partially forested regions presents a challenge because the true fraction of a pixel that is covered by snow does not necessarily correspond to the fraction of snow visible to the remote sensing instrument. The situation becomes even more complex when significant amounts of snow are present in the forest canopy. The algorithm used to produce the binary SCA product available from NASA EOS Data Gateways uses the Normalized Difference Vegetation Index (NDVI) in conjunction with the Normalized Difference Snow Index (NDSI) to decrease the probability of mapping snow covered areas overlain by dense forest as snow free (Hall et al. 2002, Klein et al. 1998). In addition, several techniques for mapping fractional SCA that account for the effect of forest canopies overlying snow cover have been developed (e.g. Vikhamar and Solberg 2003, Metsamaki et al.

2005). Other fractional snow cover mapping approaches that provide additional snow cover information such as grain size (e.g. the Multiple Endmember Snow Covered Area and Grainsize, MEMSCAG, model presented in Painter et al. 2003) do not account for potential biases in the fraction of snow cover mapped underneath forest canopies. Relatively little is known about the effects of the forest canopy on mapping fractional snow covered area. In order to accurately estimate fractional SCA in forested and partially forested regions, algorithms such as MEMSCAG and its MODIS equivalent, the MODIS Snow Covered Area and Grainsize (MODSCAG) algorithm, will require information on the effects of a wide range of forest canopy cover densities on mapped fractional SCA (Painter et al. 2003).

The primary objective of the research presented in this paper is to assess modeling and remote sensing techniques for mapping the spatial distribution of snow cover in areas of heterogeneous vegetation cover. This research will be guided by two hypotheses: (1) incorporating forest density information into a physically based snow evolution model will improve modeled estimates of snow water equivalent, and (2) MODIS derived remotely sensed SCA will increase as gap fraction increases, and this increase will be more pronounced for fractional (subpixel) estimates of SCA than for binary estimates of SCA.

2. Study area and methods

a. Glacier National Park

Glacier National Park (GNP) straddles the Continental Divide in the Rocky Mountains of northwest Montana (figure 1). GNP includes more than 4000 km^2 of mountainous terrain ranging in elevation from 1000 to slightly more than 3000 m. Though only a few active glaciers remain within the park, alpine glaciers have extensively reshaped the terrain throughout GNP. Much of the park below tree line (~ 2200 m elevation) is covered by coniferous forests of variable density interspersed with smaller areas of grassland and shrub vegetation. Large meadows are common along the eastern edges of the park, which is the transition zone between the Rocky Mountains and the high plains. The vast majority of the GNP landscape has not been significantly impacted by human activities for the past 100 years. The climate is colder, drier, and windier east of the Continental Divide, with warmer, wetter, conditions prevalent west of the Divide.

b. Mapping gap fraction

In order to improve spatially distributed snow evolution model results, as well as to assess the effect of vegetation density on remotely sensed estimates of SCA, a moderate resolution (28.5 m per pixel) image of winter canopy gap fraction was created for Glacier National Park and the surrounding area. Winter canopy gap fraction (also known as sky view fraction) is defined as the fraction of sky visible from beneath a forest canopy during the winter months. An map of winter canopy

gap fraction was derived from a July 7, 2001 Landsat ETM+ image processed using the normalized difference vegetation index (NDVI) and linear spectral unmixing and then calibrated with in situ measurements of canopy gap fraction.

The six visible and infrared bands of the Landsat ETM+ image were acquired from the University of Maryland's Global Land Cover Facility (http://glcf.umiacs.umd.edu). A visual examination of this image indicated the entire image was cloud free. All bands were atmospherically corrected using dark pixel subtraction (Chavez 1988, 1989, 1996). The NDVI was then calculated using bands 3 and 4 for each pixel in the image. All pixels with an NDVI value lower than –0.05 were classified as open (100% gap fraction) and removed from the remainder of image processing steps. The threshold of –0.05 was chosen based on examination of high resolution (~ 1 m/pixel) digital orthophotographs from August 2004 provided by the National Park Service. Pixels with values below this NDVI threshold were removed in order to eliminate those pixels composed primarily of rock, snow, ice, water, or man-made substances from the linear spectral unmixing process, therefore minimizing the number of end members necessary to accurately map the fractional abundance of vegetation types within each pixel.

Linear spectral unmixing compares the spectral signature of each pixel with the spectral signatures of known end members. The spectral signature of each pixel in the image is then modeled as a linear combination of the known end member spectra (Adams et al. 1986). Four vegetation type end members were chosen to represent the diversity of vegetation types across the GNP landscape: coniferous

forest, deciduous vegetation (forest or shrub), grassland, and standing burnt forest. Groups of spatially coherent pixels representative of each of these four categories were then selected based on field visits and high resolution digital orthophotos acquired in August 2004. The linear spectral unmixing algorithm was then applied using the spectra from the representative sample pixels as inputs. This resulted in component images indicating the fractional abundance of each of the four end members within each pixel, as well as an additional image indicating the root mean squared error (RMSE) associated with these estimates of abundance. Collections of spatially coherent pixels with fractional abundance scores significantly greater than 1 were then chosen to replace the original end member pixels. The application of the linear spectral unmixing algorithm and the selection of new end member pixels based on abundance scores was repeated several times in order to improve the accuracy of the final fractional abundance images.

Transforming the component vegetation images into a single image of gap fraction required the collection of a dataset of in situ measurements of canopy gap fraction. Forty-three groups of four hemispherical photographs each were acquired near the center of each of four Landsat ETM+ pixels at four field sites (figure 2) during the summer of 2005. Each group of four Landsat pixels/photograph points was separated by a minimum of 85.5 m (three Landsat pixels) in all directions (figure 3). All points where the canopy contained any significant deciduous vegetation above 1 m in height were removed from the calibration dataset. In addition to those groups of hemispherical photographs, an additional 18 clusters photographs were

taken over four Landsat pixels in the calibration data set where the Landsat map indicated that vegetation was present but gap fraction was known to be 100% (e.g. large meadows or low tundra). Gap fraction (defined as the percentage of sky visible from a point 1 m above the ground) was calculated for each hemispherical photograph using the Gap Light Analyzer 2.0 (GLA) (Frazer et al. 1999), a freely distributed image processing software package designed to quantify gap fraction and sub-canopy solar radiation from hemispherical photographs. For each image, GLA was used to register the image, threshold the image so that black pixels corresponded to canopy vegetation and white pixels corresponded to sky, and then calculate the gap fraction for a 150° field of view cone (figure 4). Relationships between the fractional abundances of coniferous and grassland vegetation and in situ gap fraction were used to create an image of gap fraction for the study area (further details are described in the results section).

c. Physically based snow evolution modeling

A physically based, spatially distributed snow evolution modeling system, SnowModel (Liston and Elder, in review), was used to simulate the distribution of snow cover at 60-m grid cell resolution for a 850 km^2 model domain centered on the Saint Mary drainage of Glacier National Park (figure 5). The model was run from October 1, 2003 to August 15, 2004 and from October 1 2004 to June 30 2005. SnowModel requires elevation and vegetation input grids as well as a time series of meteorological inputs (air temperature, relative humidity, wind speed, wind

direction, and precipitation) from one or more weather stations in or near the model domain. SnowModel consists of a series of four sub-models that distribute meteorological data over the model domain, model surface energy exchanges for each grid cell, simulate the evolution of snow cover for each grid cell, and account for wind redistribution of snow between grid cells. Meteorological observations required to run the model were obtained from two weather stations and two SNOTEL stations located within or near the model domain (figure 5). Hourly or daily observations of air temperature, relative humidity, wind speed, wind direction, and precipitation were obtained from these stations (table 1). Hourly mean air temperature, relative humidity, wind speed, or wind direction data were not available from either of the SNOTEL stations. Daily precipitation data were resampled to hourly data by distributing daily precipitation data equally throughout the day in order to allow the model time step to be one hour. High quality precipitation data were not available from the Saint Mary RAWS or Sun Point USGS weather stations, and only the Sun Point USGS station provided high quality wind speed and wind direction data representative of wind patterns across the model domain.

The standard implementation of SnowModel requires an input vegetation grid with each cell classified into one of 23 predefined vegetation types or 7 user defined vegetation types. The vegetation type defined for a given grid cell controls the manner in which vegetation-snow interactions are modeled within that pixel. Each forest class is given a predefined leaf area index (LAI) value. Snow interception and sublimation from the forest canopy are calculated as a function of this LAI value,

and solar and thermal radiation are also adjusted by a function of this LAI value. Wind speed is reduced below forest canopies, resulting in decreased sublimation losses from the snow cover, decreasing potential for wind scouring and increasing potential for deposition of suspended snow. SnowModel predefined vegetation types include only 3 broadly defined coniferous forest classes (only two of which can be found within GNP). Recent data indicate that even small differences in the density of coniferous forest can significantly impact snow accumulation in GNP (Selkowitz et al, submitted). To account for the full range of coniferous forest densities found within GNP (where coniferous forest occupies over two thirds of the landscape), we chose to run SnowModel three times, each with a different vegetation grid and then weight each output grid based on the gap fraction grid described above. Model runs used the following parameters:

1) all pixels in the model domain designated as coniferous forest, no wind redistribution ("conifer model")
2) all pixels in the model domain designated as grassland, no wind redistribution ("grass model")
3) all pixels in the model domain designated as grassland, wind redistribution ("wind model")

The conifer model was intended to simulate snow cover evolution under a dense coniferous forest canopy with a leaf area index of 2.5 (equivalent to a gap fraction of

15%, according to calculations using the Gap Light Analyzer). The grass model was intended to simulate snow cover evolution in a wind-sheltered environment where the forest canopy had no effect on incoming radiation or snowfall. The wind model was intended to simulate snow cover evolution in an open grassland environment where significant wind redistribution of snow could occur when wind and snow conditions allowed. To produce a final model output grid for a given date and time, the original conifer, grass, and wind output grids were resampled to 28.5 m spatial resolution and then a final SWE output grid was created by weighting the conifer, grass, and wind model grids based on gap fraction (figure 6). Equations for the model weighting scheme are presented in table 2.

The increasing weight of the grass model and the decreasing weight of the conifer model between 15 and 60% gap fraction were intended to represent the increasing exposure to solar radiation and decreasing amount of canopy interception of snowfall within this gap fraction range. The increasing weight of the wind model and the decreasing weight of the grass model between 60% and 100% gap fraction were designed to represent a pixel's increasing likelihood of exposure to high winds within this gap fraction range. In the absence of substantial melt during the accumulation season due to solar radiation (generally an uncommon occurrence), the model would simulate maximum seasonal snow accumulation for pixels with a 60% gap fraction value (excluding a small minority of 100% gap fraction pixels sheltered by topography). Given the presence of high winds (virtually guaranteed during the winter months within the model domain), the model would simulate minimal snow

accumulation above 90% gap fraction. Maximum snow accumulation at 60% gap fraction and minimal snow accumulation above 90% gap fraction are similar to results reported by Selkowitz et al. (in review).

Measurements of snow water equivalent were collected periodically during the winters of 2003-2004 and 2004-2005 along several snow survey routes within the model domain (figure 5). The Two Dog Flats, Divide, and White Calf transects were each 870 m in length. These vegetation-snow transects were designed to study differences in snow accumulation associated with variability in vegetation type and forest density (Selkowitz et al, submitted), and in situ gap fraction was measured at each survey point along each transect. The Divide, Preston-low, Preston-mid, and Preston-high transects were part of longer snow surveys that covered a range of topography and vegetation. No in situ gap fraction measurements were made for points along these surveys. These point-based SWE measurements were not designed to validate a model with a spatial resolution of 28.5 m. Thus, to avoid comparing single point SWE measurements with coarser model grid cell SWE values, nearby points separated by 1 km or less from these snow surveys were grouped and averaged for comparison with model results. For the 870 m vegetation-snow transects (where within transect topographic variability was minimal), survey points were grouped by in situ gap fraction measurements. For the other survey points, nearby survey points within 1 km with similar elevation, aspect, slope, and vegetation characteristics were grouped and the mean gap fraction for the group was

obtained from an average of the corresponding pixels from the gap fraction map described above.

A mosaicked high resolution digital orthophotograph acquired between August 10 and 12 2004 was used to assess the model's ability to simulate wind redistribution of snow cover in high elevation alpine areas where no in situ measurements were available. All drifts larger than ~ 40,000 m^2 were visually identified, outlined, and digitized in ArcGIS. The extent and spatial arrangement of observed late lying snowdrifts were then compared quantitatively and qualitatively to the model output grid from August 10, 2004.

d. Remote sensing of snow covered area

Remotely sensed images of binary and fractional snow covered area (SCA) derived from MODIS images were used to assess the modeled results as well as the effect of vegetation density on the SCA products themselves. MODIS binary SCA images were acquired from the NASA EOS Data Gateway for February 22, March 30, and May 01 2004. The MODSCAG product was also used in this study to map the fraction of snow covered area in each MODIS pixel. For areas with incomplete snow cover, this product is expected to provide superior results to the MODIS binary snow cover product because the latter assumes 100% snow cover for pixels with approximately 50% or more snow cover and zero snow cover for pixels with snow cover less than 50%. Hydrologically, a fractional SCA mapping approach is needed because lower elevation snow cover tends to melt earlier than higher elevation snow

cover and the binary classification will generally underestimate the low elevation snow and overestimate the high elevation snow. However, the MODIS binary SCA product incorporates a correction for vegetation cover that allows it to more accurately map snow cover in areas with varying densities of forest canopy. The MODSCAG product does not have such a correction and only maps the projected area of snow cover; it is not able to account for snowcover beneath a forest canopy. To facilitate analysis of the differences between binary SCA, fractional SCA, and modeled SCA, comparative statistics were calculated for snow cover in three elevation zones (< 1500 m, 1500-2000 m, and > 2000 m), two climate zones (eastern GNP and western GNP, defined by location relative to the Continental Divide), and five gap fraction zones (< 20%, 20-40%, 40-60%, 60-80%, and 80-100%). Elevation zones were chosen to correspond with valleys (< 1500 m), mid elevation slopes (1500-200 m), and alpine/subalpine areas (> 2000 m). Climate zones were designated to differentiate between the continental, high wind environment to the east of the Continental Divide and the more moderate, maritime-influenced environment to the west of the Continental Divide. Gap fraction zones were chosen to correspond with high density forest (< 20% gap fraction), medium density forest (20-40% gap fraction), low density forest (40-60% gap fraction), sparse forest or shrub vegetation (60-80% gap fraction), and open or nearly open (80-100% gap fraction).

3. Results

a. Gap fraction mapping

Applying the NDVI mask to the atmospherically corrected 6 band Landsat image removed 16.2% of all pixels from the image (24.8% of pixels within the Glacier National Park boundary, where glaciers, late-lying snow cover, and rocky alpine terrain are more prevalent) (figure 7). The remaining pixels were processed using the linear spectral unmixing algorithm, which produced component images for each end member (figure 8) and an RMSE image (figure 9). A visual examination of the four vegetation component images (figure 8) gives an initial assessment of the accuracy of the application of this combination of NDVI masking and linear spectral unmixing to this image. The numerous lakes that occupy the glacially-carved valleys on both sides of the park are evident, as are the extensive areas of rock, snow, and ice that cover the eastern two-thirds of the park. The grassland vegetation that dominates the high plains to the east of Glacier National Park is evident in the northeastern part of the image. Coniferous forest dominates the landscape in the valleys along the western edge of the park. Large patches of deciduous vegetation are present throughout the landscape, particularly in areas adjacent to the elevated areas of rock and ice shown in black. These patches likely represent the extensive shrub vegetation that occurs in many subalpine areas of the park. The RMSE image is a quantitative measure of the fit of the linear mixture model to the spectral signature of a given pixel. Spatially coherent areas of high RMSE indicate potential problems in the spectral unmixing process, whereas a lack of spatial coherence is

considered a likely indicator of a relatively successful attempt at fractional abundance mapping. Though this RMSE image shows relatively little spatial coherence, areas of high RMSE do cluster around the areas of rock and ice removed by the NDVI mask. This is to be expected, given that these areas likely contain some rock or snow, neither of which were included as end members in the linear spectral unmixing process. The higher areas of RMSE in the southwestern part of the image correspond to the Flathead Valley, a more developed area where urban land use is more common. This is also not surprising, given that no urban land use end members were included in the spectral unmixing process.

Gap fraction measurements derived from hemispherical photographs showed varying degrees of correlation with the vegetation type abundance estimates (table 3, figure 10). Canopy gap fraction was most closely correlated with conifer fraction, which was not surprising, given that coniferous vegetation represents the vast majority of the vegetation canopy exceeding 1 m in height in this region. As the conifer component dropped below approximately 50% and gap fraction exceeded approximately 50% the data showed evidence of a departure from linearity, as well as increasing variance (figure 10). Using all data points where gap fraction was less than 100%, the following linear model was constructed for estimating gap fraction based on remotely sensed conifer fraction:

$$g = -67.5\ c + 77.5$$

where g is equal to gap fraction and c was equal to conifer fraction (r^2 =0.688, p = 0.0000). This model was used to transform the spectrally unmixed conifer fraction image into an image representing gap fraction for each pixel within the study area. Close examination of this image revealed numerous areas where canopy gap fraction was known to be 100% (e.g. large meadows) that were mapped as having a gap fraction of significantly less than 100%. In order to correct these errors, areas with a grass fractional abundance exceeding 0.55 were reclassified as having a gap fraction of 100% in order to create the final gap fraction image for GNP and the surrounding area (figure 11). All in situ gap fraction measurements less than 100% in the calibration dataset were associated with grass fractional abundance scores of 0.53 or lower. A subsequent examination of sample areas of the grass fractional abundance image overlaid with a high resolution digital orthophotograph revealed only three isolated pixels where grass fractional abundance scores exceeded 0.55 and forest appeared to be present.

b. Physically based snow evolution modeling

Results from the implementation of SnowModel indicated that the model accurately simulated the evolution of snow cover at locations near the Continental Divide (figure 12), but significantly overestimated snow cover along the eastern fringe of the model domain (figure 13). Despite the significant underestimation of SWE for locations near the eastern fringe of the model domain, differences in simulated snow cover for different gap fraction densities in most cases reflect

differences in observed snow cover for the same gap fraction densities. Model results and observed SWE both indicate that seasonal snow accumulation was highest in sheltered open areas (gap fraction ~ 50-70%), lower in more densely forested areas (gap fraction less than ~ 30%) and lowest in exposed open areas (gap fraction > 90%) (figure 13 a and d). Though the model does capture the significant reduction in seasonal snow accumulation for exposed open areas, it still significantly overestimates snow accumulation in these areas. Finally, the model underestimates the difference between seasonal snow accumulation under a dense forest canopy (mean gap fraction of 22%) and an extremely dense forest canopy (17%) (figure 13c).

A visual comparison of the digitized snowdrifts and modeled snow covered area for the same date indicates that the model simulates snow cover in the general vicinity of most of the persistent late-lying snowfields (figure 14). Modeled SCA agrees within 0.3% of observed SCA for the model domain on August 10, 2004 (table 4). The distributions of modeled and observed SCA by slope aspect differ slightly, with the model overestimating snow covered area for south, southwest, west and northwest aspects and underestimating snow covered area for northeast and east aspects (figure 15). A prominent difference between modeled and observed SCA is the tendency for the model to place late lying snowdrifts in steep terrain immediately below the crests of ridges, while observed snowdrifts were typically located in flatter terrain downslope of the modeled snowdrifts.

c. Snow covered area mapping

The MODIS binary snow product mapped more land within the GNP boundary as snow covered than the fractional SCA product, though the differences in SCA between the two products decreased as the season progressed (figures 16 and 17). For all dates, the percent of area mapped as snow covered was a function of both elevation and gap fraction for the binary and fractional SCA products (figures 18-20). Both binary and fractional SCA increased as elevation increased for all dates, and this relationship between mapped SCA and elevation became more pronounced later in the season.. In general, for both products, the percentage of mapped SCA increased as gap fraction increased, though in many cases SCA percent dropped off for the highest gap fraction class (80-100%). The increase in mapped SCA with an increase in gap fraction was more pronounced later in the season. The pattern of differences between mapped SCA for gap fraction classes (increasing SCA with increasing gap fraction class) was similar for both the binary and fractional SCA products, except for the March 30 image. On March 30, west of the Continental Divide, the increase in mapped SCA with increasing gap fraction was evident in the fractional SCA product but mostly absent (excluding the 1500-2000 m elevation zone) from the binary SCA product. At low elevations east of the Continental Divide on March 30, SCA increased as gap fraction increased in the fractional SCA product, but decreased as gap fraction increased in the binary SCA product.

d. Comparison of modeled and remotely sensed SCA

Spatial patterns in modeled SCA agreed relatively well with the MODIS-derived SCA products, though the model's overestimation of snow cover in the easternmost portion of the model domain appears to be confirmed by the MODIS SCA products, particularly on March 30 (figure 21). The relationship between modeled SCA and gap fraction indicated by the binary and fractional SCA products is only evident for the 1500-2000 m elevation zone on March 30 (figure 22).

4. Analysis of potential errors

Prior to discussing the results mentioned above, it is worth considering potential errors associated with the measurements and modeling techniques presented in order to understand the effect they could have on the results. A list of potential errors and their estimated impact on the results is provided in table 5.

a. Gap fraction mapping

Errors associated with the in situ measurement of gap fraction are discussed in more detail in Selkowitz et al. (in review). We believe the most significant potential error in measuring gap fraction was the non-uniform illumination in some hemispherical photographs. In order to minimize the potential for errors in gap fraction measurement due to non-uniform illumination, all hemispherical photographs were acquired slightly before or slightly after sunrise or sunset. Attempting to map the distribution of gap fraction for an area the size of Glacier

National Park using remotely sensed imagery introduces several additional potential sources of error. An assumption of the linear spectral unmixing algorithm used to produce the fractional abundance images for each type of vegetation is that all potential end members are included in the model. In order to reduce the number of potential end members, all pixels with an NDVI below -0.05 were removed from the spectral unmixing process. Some pixels that contained a significant enough vegetation component to raise the NDVI above -0.05 likely also contained a significant non-vegetation component. This is most likely why the RMS error image shows higher RMS error values near the upper limits of vegetation growth, where many pixels contain a mixture of rock, bare soil, or snow in addition to vegetation. The impact of this unmet assumption of the linear spectral unmixing model most likely had a significant impact on a small minority of pixels (mostly located at high elevations) and a minimal impact on all other pixels. Another small minority of pixels with a NDVI just below -0.05 likely contained a vegetation component, though this vegetation component was probably grass or short shrubs with a gap fraction of 100%.

An analysis of the relationship between gap fraction and conifer fraction (figure 10) indicates that significant errors in mapping gap fraction may sometimes occur when the coniferous vegetation component for a pixel is below ~ 40%. In situ measurements indicate that instances of 100% gap fraction may correspond with conifer components as high as 40% in rare cases. Mapping all pixels with a grass

component exceeding 55% reduces the number of pixels where gap fraction is underestimated, but some misrepresented pixels may remain.

It is also important to note that the spectral reflectance for each pixel for each band in a remotely sensed image such as the Landsat ETM+ image used in this study is typically a function of not only the material present within the ground instantaneous field of view which the pixel represents, but also (to a lesser extent) the surrounding area. The resulting 'blurring' of features is often referred to as the "point spread function". Consequently, gap fraction mapping in areas where gap fraction varies substantially over short distances on the ground (e.g. a forest meadow-edge) is likely to be inaccurate. In order to minimize the impact of this problem on the calibration of the linear spectral unmixing results with the in-situ gap fraction measurements, we chose to compare clusters of four hemispherical photographs with clusters of four Landsat pixels, rather than compare single hemispherical photographs with single Landsat pixels. In addition, all hemispherical photograph points were selected in areas where gap fraction did not appear to vary significantly (at the 28.5 m spatial scale) over short distances on the ground.

Significant landscape changes occurred across some areas of GNP between July 7, 2001 (the date the Landsat ETM+ image was acquired) and the study period (October 2003-June 2005). The majority of landscape changes in this period resulted from extensive fires during the summers of 2001 and 2003 and one fire during the summer of 2002. Landscape changes between 2001 and 2005 had very little effect on the calibration dataset, and the region of the park chosen for assessment of the

snow evolution model was not significantly impacted by the fires of 2001 or 2003 (though a small portion of the landscape was effected by a stand replacing fire in 2002). Other areas of the park experienced more significant landscape changes due to fire, especially west of the Continental Divide.

b. Physically based snow evolution modeling

SnowModel has been demonstrated to produce reasonably accurate simulations of snow evolution when forced with meteorological observations from nearby locations representative of the landscape type where the snow cover is being modeled (Liston and Elder, in review). The most significant potential source of error in the modeling process was probably the interpolation of meteorological observations over the model domain. The model's significant overestimation of SWE at most locations along the eastern edge of the model domain can be explained by its failure to capture the west-to-east decreasing precipitation gradient. This is, however, a known and accepted limitation of the model that could be solved by using data from meteorological stations representative of the spatial variability in weather conditions across the model domain. An additional potential source of error was the model's inability to account for redistribution of snow via avalanches or sloughing from steeper slopes to gentler slopes. This was probably the reason why modeled late lying snowdrifts were closer to the crests of ridges than observed late lying snow drifts.

c. Snow covered area mapping

The largest potential source of error in mapping snow covered area was most likely the influence of vegetation on mapped SCA. Observed relationships between snow cover and gap fraction in GNP (Selkowitz et al, submitted), as well as the March 30 model results for the 1500-2000 m elevation zone indicate that the pattern of increasing SCA with increasing gap fraction was a real phenomenon. The slight decrease in mapped SCA for the 80-100% gap fraction class observed for some dates, locations, and elevation zones was almost certainly a reflection of decreased snow cover in areas where gap fraction exceeds 80%. The increase in SCA associated with an increase in gap fraction, however, was probably exaggerated by the SCA retrieval algorithms. We expected to see the pattern of increasing SCA associated with increasing gap fraction to be consistently more pronounced for the fractional SCA product, since no adjustments for vegetation cover have been incorporated into this product. In some cases, such as at low elevations east of the Continental Divide on March 30, the relationship between gap fraction and SCA was significantly different for the binary and fractional SCA products. In other cases, the relationship between mapped SCA and gap fraction class were very similar for the binary and fractional products.

The point spread function discussed earlier also affects the MODIS imagery used to produce both the binary and fractional SCA products. Consequently, the patchiness of snow cover is likely to be underrepresented, particularly by the 500 m MODIS binary SCA product. Even isolated patches of snow cover or snow free

ground larger than 500 x 500 m may be obscured due to the point spread function, especially if these patches happen to be spread across the ground instantaneous field of views of multiple pixels.

5. Discussion

Previous studies have demonstrated that vegetation cover in general and canopy gap fraction in particular have a significant impact on the evolution of a seasonal snow cover. Studies have indicated that even small differences in gap fraction can significantly impact snow accumulation (Selkowitz et al, in review). In order to account for the impact of forest canopies of variable density on snow cover accumulation and ablation in a spatially distributed snow evolution model, an image of gap fraction covering the model domain is necessary. The coniferous and grassland vegetation components derived from a Landsat ETM+ image pre-processed with a NDVI mask and processed via linear spectral unmixing can be used to create a reasonably accurate map of gap fraction for relatively large areas when in situ measurements of gap fraction are available. Unfortunately, it appears that a limitation of this technique is the uncertainty in mapping gap fraction in the range of 60-100%. The vast majority of pixels with a gap fraction of 100% are, however, accurately represented because of the NDVI mask applied to the imagery in the first processing step. This means that only the small minority of pixels in the image with a gap fraction between 60 and 99% (less than 5% of the image) are likely to be affected by this problem.

The non-standard implementation of SnowModel described in this paper is a useful technique for simulating the spatiotemporal variability in snow cover at a moderate spatial resolution (28.5 m) over a relatively large area (850 km^2). To accurately simulate snow cover across the entire domain, however, requires input data from meteorological stations representative of the spatial variability in meteorological conditions across the entire domain. A potential alternative when meteorological data do not represent the full range of conditions across the model domain is to use an additional module available for SnowModel to force model results to fit observed values of SWE. Unfortunately, the scale-mismatch between the point SWE measurements available from the model domain and the 28.5 m x 28.5 m pixels produced as model output prohibited a direct comparison between model output pixels and observed SWE. Comparison between modeled SWE and mean observed SWE for groups of observations within various gap fraction classes indicate that incorporating gap fraction information into the modeling process allows for a reasonable approximation of the differences between snow cover evolution under different gap fraction conditions. This implementation of the model does not, however, accurately simulate the difference between snow accumulation under dense and extremely dense coniferous forests (figure 13). In addition, both in situ SWE observations and MODIS-derived SCA maps indicate that this implementation of the model is prone to overestimating snow cover in areas where gap fraction is at or near 100%. Adding an additional model run with constant vegetation defined as rock (which would have a much lower snow holding capacity than grass, see Liston and

Elder, submitted) would result in decreased snow accumulation for exposed rocky areas, thus improving model results. Finally, the simulated distribution of snow cover in steep alpine terrain would probably have matched the observed distribution from late summer more closely if the model were able to account for redistribution of snow via avalanches and sloughing. Slopes near the crest of ridges in GNP are often steep enough to experience frequent avalanches and smaller sloughing events that move snow deposited in the lee of the ridge by wind further down slope.

The MODIS binary SCA product consistently maps more snow covered area than the fractional SCA product in Glacier National Park. This is partly because the fractional SCA product more accurately represents the patchy snow covers that exist at the highest elevations, where redistribution of snow cover by wind and sloughing/avalanching frequently results in snow free patches even in the middle of winter. We would also expect that the reduced SCA mapped by the fractional algorithm resulted partially from reduced SCA mapped in areas with dense coniferous forests. Our analysis indicated that this was sometimes, but not always the case.

5. Conclusions

Ecosystems where snow cover is present for a significant portion of the year are typically fairly dynamic, with processes such as forest succession, fire and other natural disturbances, as well as manipulation by humans resulting in both gradual and abrupt changes in vegetation type, structure, and density. These changes can

impact the snow hydrology of an area by changing snow accumulation and ablation patterns (e.g. Troendle and King, 1985). Spatially distributed snow models that account for the effects of vegetation on snow accumulation and ablation can help to predict the impact of known or potential landscape changes on snow hydrology at a variety of scales. This work evaluated one such model implemented with a simple parameterization approach designed to allow the model to use spatially distributed gap fraction information rather than simple land cover type. As is often the case for spatially distributed models, evaluating the model was hindered by the lack of in situ snow cover measurements throughout most of the model domain. Binary and fractional images of remotely sensed snow covered area indicated similar broad scale spatial patterns to those predicted by the snow evolution model. Unfortunately, these products could not be used to validate the model's ability to accurately simulate snow cover variability associated with vegetation variability because their accuracy was most likely also influenced by vegetation cover. This illustrates the need for a more solid understanding of how remotely sensed SCA is affected by overlying vegetation. The results presented here provide a preliminary indication of the effects of various vegetation densities on remotely sensed binary and fractional SCA, but further efforts that include a wider range of climate regimes and image acquisition dates as well as extensive in situ observations will be necessary to fully understand these relationships. This understanding would allow adjustments to be made to remotely sensed SCA products that would allow them to more accurately reflect SCA on the ground. These adjusted SCA products could then serve as one type of

validation for spatially distributed snow evolution models in areas of heterogeneous vegetation cover.

Acknowledgements

This work was supported primarily by NASA Grant NNG04GC52A. The authors wish to thank Jeri Lynn Ward of the Natural Resources Conservation Service Montana Snow Survey Office for assistance with acquiring SNOTEL data.

References

Adams, J.B., M.O. Smith, and P.E. Johnson. 1986. Spectral mixture modeling: a new analysis of rock and soil types at the Viking Lander 1 site. *Journal of Geophysical Research* **91**(B8): 8098-8112.

Berry, G.J. and R.L. Rothwell. 1992. Snow ablation in small forest openings in southwest Alberta. *Canadian Journal of Forest Research* **22**: 1326-1331.

Chavez, P.S., Jr., 1988. An improved dark-object subtraction technique for atmospheric scattering correction of multispectral data. *Remote Sensing of Environment*, 24, pp. 459-479.

Chavez, P.S., Jr., 1989. Radiometric calibration of Landsat Thematic Mapper

multispectral images. *Photogrammetric Engineering and Remote Sensing*, 55, pp. 1285-1294.

Chavez, P.S. Jr., 1996, Image-based atmospheric corrections - revisited and revised. *Photogrammetric Engineering and Remote Sensing,* 62, pp. 1025-1036

Cline, D.W., R.C. Bales, and J. Dozier. 1998. Estimating the spatial distribution of snow in mountain basins using remote sensing and energy balance modeling. *Water Resources Research* **34**(5):1275-1285.

Davis, R.E., J.P. Hardy, W. Ni, C. Woodcock, J.C. McKenzie, R. Jordan, and X. Li. 1997. Variation of snow cover ablation in the boreal forest: a sensitivity study on the effects of conifer canopy. *Journal of Geophysical Research* **102**(D24): 29,389-29,395.

Elder, K., W. Rosenthal, and R.E. Davis. 1998. Estimating the spatial distribution of snow water equivalence in a montane watershed. *Hydrological Processes* **12**:1793-1808.

Frazer, G.W., C.D. Canham, and K.P. Lertzman. 1999. Gap Light Analyzer (GLA), Version 2.0: Imaging software to extract canopy structure and gap light

transmission indices from true-colour fisheye photographs, users manual and program documentation. Copyright 1999: Simon Fraser University, Burnaby British Columbia, and the Institute of Ecosystem Studies, Millbrook, New York.

Gary, H.L., and C. Troendle. 1982. Snow accumulation and melt under various stand densities in lodgepole pine in Wyoming and Colorado. USDA Forest Service Rocky Mountain Forest and Range Experiment Station, Research Note RM-417.

Golding, D.L., and R.H. Swanson. 1986. Snow distribution patterns in clearings and adjacent forest. *Water Resources Research* **22**: 1931-1940.

Hardy, J.P., R.E. Davis, R. Jordan, X. Li, C. Woodcock, W. Ni, and J.C. McKenzie. 1997. Snow ablation modeling at the stand scale in a boreal jack pine forest. *Journal of Geophysical Research* **102**: 29,397-29,405.

Hardy, J.P., R. Melloh, P. Robinson, and R. Jordan. 2000. Incorporating effects of forest litter in a snow process model. *Hydrological Processes* **14**: 3227-3237.

Hardy, J.P., R. Melloh, G. Koenig, D. Marks, and A.Winstral. Pomeroy, J.W., Link, T. 2004. Solar radiation transmission through conifer canopies. *Agricultural and Forest Meteorology* **126**: 257-270.

Hedstrom, N.R. and J.W. Pomeroy. 1998. Measurements and modelling of snow interception in the boreal forest. *Hydrological Processes* **12**: 1611-1625.

Hiemstra, C.A., G.E. Liston, and W.A. Reiners. 2002. Snow redistribution by wind and interactions with vegetation at upper treeline in the Medicine Bow Mountains, Wyoming, U.S.A. *Arctic, Antarctic, and Alpine Research* **34**: 262-273.

Klein, A. G., D. K. Hall, and G. A. Riggs, 1998. Improving snow cover mapping in forests through the use of a canopy reflectance model. *Hydrologic Processes,* **12,** 1723-1744.

Koivusalo, H., and T. Kokkonen. 2002. Snow processes in a forest clearing and in a coniferous forest. *Journal of Hydrology* **262**: 145-164.

Lundberg, A., N. Yuichiro, H. Thunehed, and S. Halldin. 2004. Snow accumulation in forests from ground and remote-sensing data. *Hydrological Processes* **18**:1941-1955.

Link, T.E., D. Marks, and J.P. Hardy. 2004. A deterministic method to characterize canopy radiative transfer properties. *Hydrological Processes* **18**:3583-3594.

Link, T.E., and D. Marks. 1999. Point simulation of seasonal snow cover dynamics beneath boreal forest canopies. *Journal of Geophysical Research* **104**: 27,841-27,857.

Liston, L.E. and K. Elder. In review. A distributed snow-evolution modeling system (SnowModel).

Marks, D., J. Kimball, D. Tingey, and T. Link. 1998. The sensitivity of snowmelt processes to climate conditions and forest cover during rain-on-snow: a case study of the 1996 Pacific Northwest flood. *Hydrological Processes* **12**: 1569-1587.

Marks, D., and A. Winstral. 2001. Comparison of snow deposition, the snow cover energy balance, and snowmelt at two sites in a semiarid mountain basin. *Journal of Hydrometeorology* **2**(3): 213-227.

Marks, D., A. Winstral, and M. Seyfried. 2002. Simulation of terrain and forest shelter effects on patterns of snow deposition, snowmelt, and runoff over a semi-arid mountain catchment. *Hydrological Processes*, **16:**3605-3626.

Melloh, R., J.P. Hardy, R.N. Bailey, and T.J. Hall. 2002. An efficient snow albedo model for the open and sub-canopy. *Hydrological Processes* **16**: 3571-3584.

Metsamaki, S.J., S.T. Anttila, H.J. Markus, and J.M. Vepsalainen. 2005. A feasible method for fractional snow cover mapping in boreal zone based on a reflectance model. *Remote Sensing of Environment* **95**:77-95.

Painter, T.H., J. Dozier, D.A. Roberts, R.E. Davis, and R.O. Green. 2003. Retrieval of subpixel snow-covered area and grain size from imaging spectrometer data. *Remote Sensing of Environment* **85:**64-77.

Price, A.G. 1988. Prediction of snowmelt rates in a deciduous forest. *Journal of Hydrology* **101:** 145-157.

Selkowitz, D., A.W. Nolin, and D. Fagre. In review. Variable snow cover accumulation associated with vegetation type and density in Glacier National Park, Montana, USA.

Storck, P., D.P. Lettenmaier, and S.M. Bolton. 2003. Measurement of snow interception and canopy effects on snow accumulation and melt in a mountainous maritime climate, Oregon, United States. *Water Resources Research* **38**(11): 1223.

Vikhamar, D., and R. Solberg. 2003. Snow mapping in forests by constrained linear spectral unmixing of MODIS data. *Remote Sensing of Environment* **88:**309-323.

List of tables

List of figures

Table 1. Weather station data used for driving SnowModel. (H represents hourly measurements, D represents daily measurements).

Station	Air Temp	Relative Humidity	Wind Speed	Wind Direction	Precipitation
Saint Mary RAWS	H	H			
Sun Point USGS	H	H	H	H	
Many Glacier SNOTEL					D
Flattop Mountain SNOTEL					D

Table 2. Equations for weighting conifer, grass, and wind model runs based on gap fraction (g is gap fraction)

Gap Fraction Range	**Conifer Weight**	**Grass Weight**	**Wind Weight**
< 15%	1	0	0
15-60%	-0.022 g + 1.333	0.0222 g - 0.333	0
60-100%	0	-0.025 g + 2.5	0.025 g - 1.5

Table 3. Coefficents of determination (r^2) and significance (p) for relationships between gap fraction and vegetation fractions derived from linear spectral unmixing.

	Conifer	**Deciduous**	**Grassland**	**Burned**
r^2	0.688	0.020	0.667	0.311
p	0.00000	0.3700733	0.00000	0.00010

Table 4. Comparison of observed and modeled snow covered area for the model domain on August 10, 2004.

	snow free area (%)	snow covered area (%)
observed	97.2	96.9
modeled	2.8	3.1

Table 5. Potential errors and estimated magnitude and direction.

Process Affected	Error	Direction of Effect	Magnitude of Effect	Comments
gap fraction mapping	variable illumination conditions	both	up to 5% gap fraction	more significant for dense forest transects where range of gap fraction values is smaller
gap fraction mapping	leveling errors	negative (gap fraction underestimated)	up to 1% gap fraction	
gap fraction mapping	lack of distinction between topographic features and canopy	negative (gap fraction underestimated)	up to 5% gap fraction	less significant for dense forests
gap fraction mapping	mixed pixels (e.g. vegetation and rock)	both	up to 50% gap fraction for less than 1% of pixels	only affects pixels near treeline
gap fraction mapping	point spread function for Landsat pixels	both	up to 50% gap fraction for less than 1% of pixels	only affects pixels located at forest-meadow edge
gap fraction mapping	landscape changes after image acquisition (e.g. fires)	mostly negative (gap fraction underestimated)	up to 65% gap fraction for up to 10% of pixels	potentially affected pixels easily identified using latest fire GIS data
snow evolution modeling	input weather station data not representative of west-east precipitation gradient	mostly positive (SWE overestimated)	up to 400% overestimation of peak SWE for up to 30% of landscape	
snow evolution modeling	redistribution of snow via avalanches or sloughing	both	up to 10000% of peak SWE for up to 0.5% of landscape, up to 200% of peak SWE for up to 5% of the landscape	(overestimation of SWE on steep slopes near ridge crests, underestimation of SWE farther downslope)

Process Affected	Error	Direction of Effect	Magnitude of Effect	Comments
snow covered area (SCA) mapping	influence of vegetation canopy on mapped SCA	negative (SCA underestimated)	up to 60%	more significant for densely forested areas and for fractional product, see discussion for details
snow covered area mapping (SCA)	point spread function for MODIS imagery	both	up to 5% of total SCA	

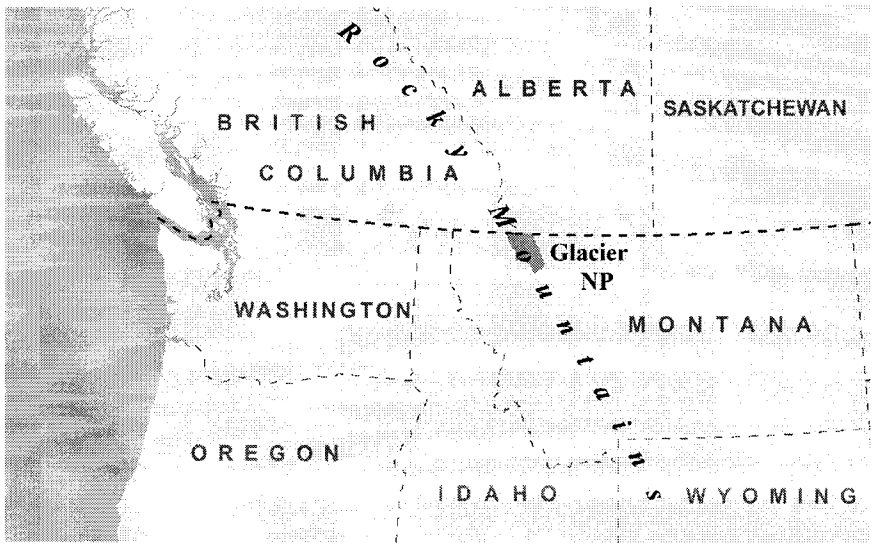

Figure 1. Glacier National park locator map.

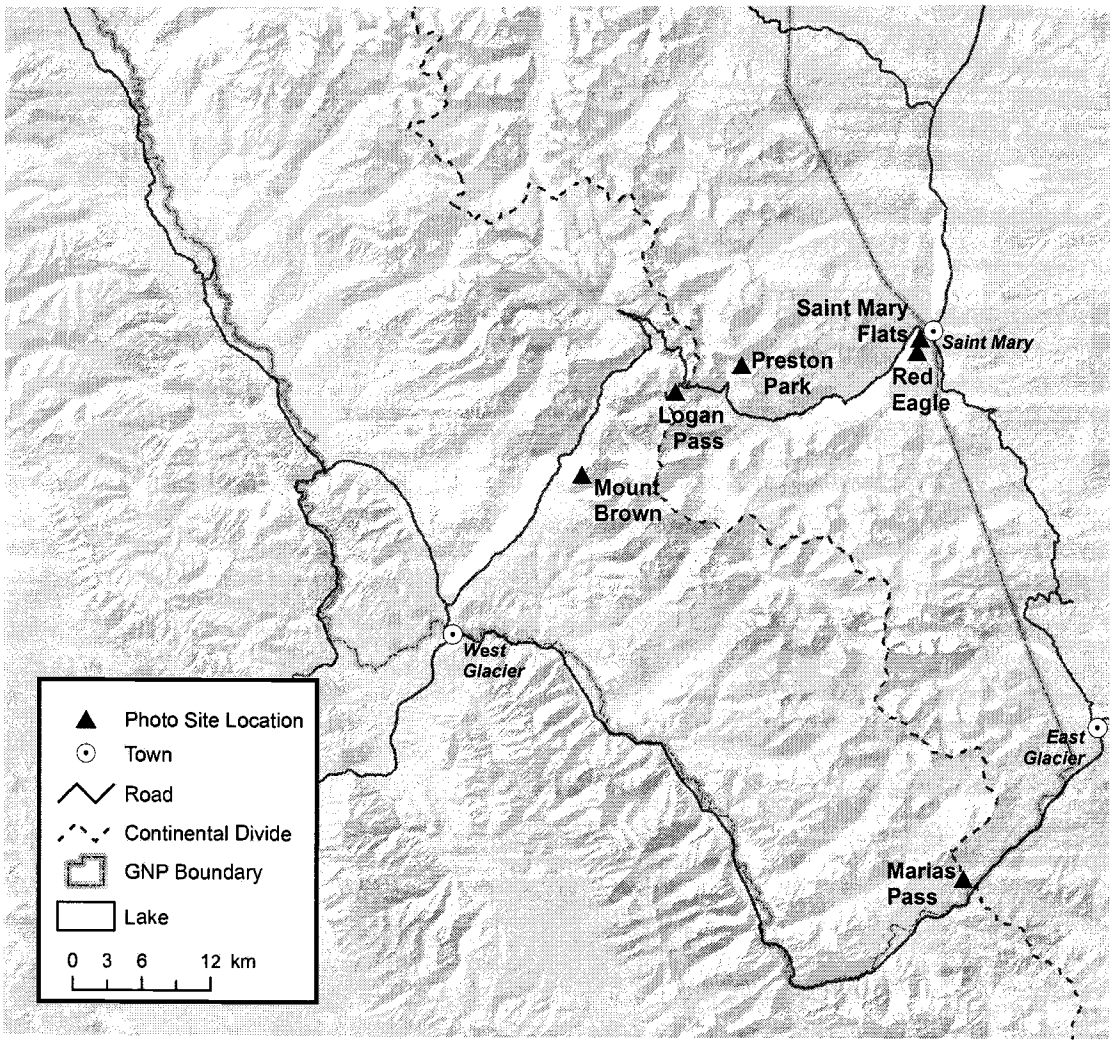

Figure 2. Hemispherical photograph point sampling locations in Glacier National Park.

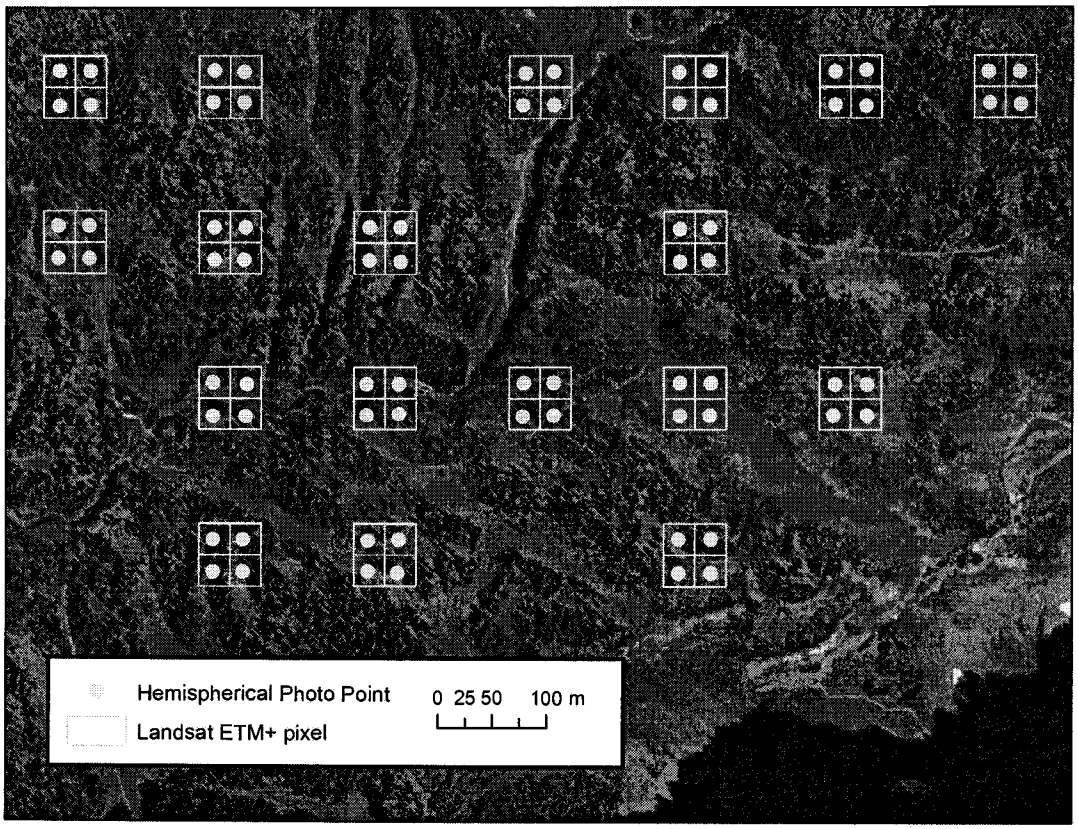

Figure 3. Example spatial arrangement of hemispherical photograph points in relation to Landsat ETM+ pixels.

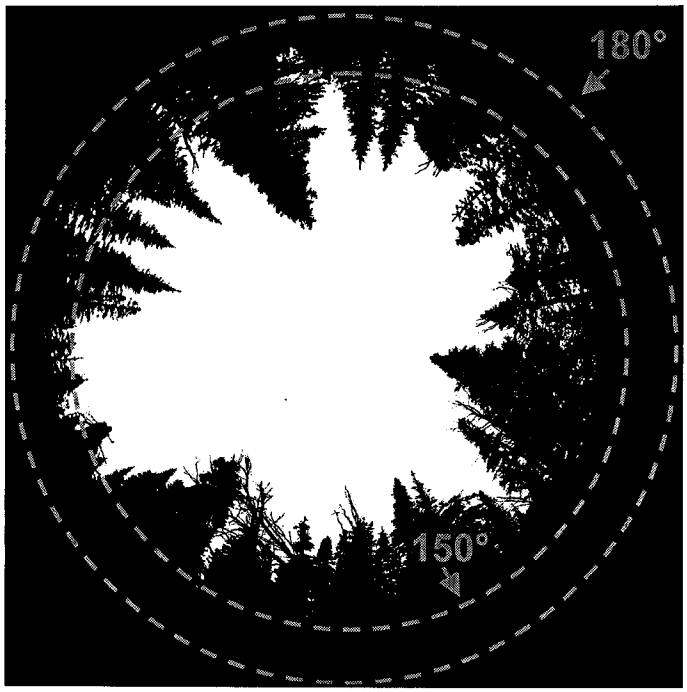

Figure 4. Hemispherical digital photograph with 150° and 180° field of view cones labeled. A threshold has been applied so that gap fraction appears as white and canopy is black.

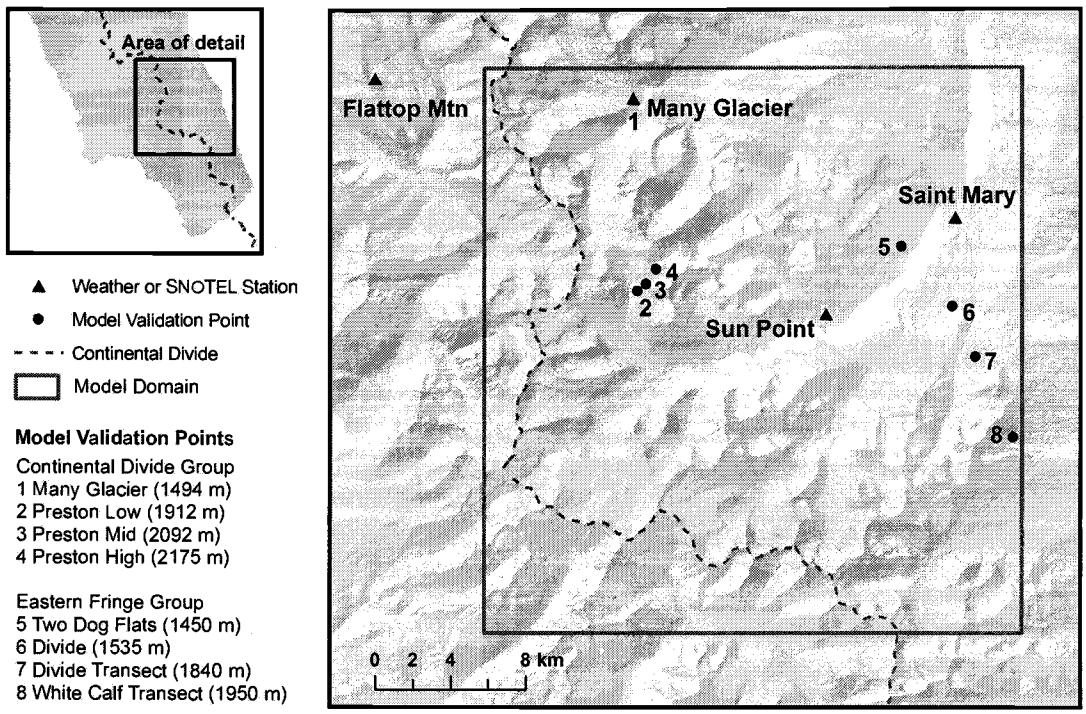

Figure 5. Model domain map with weather stations and snow survey points used for assessment of model results.

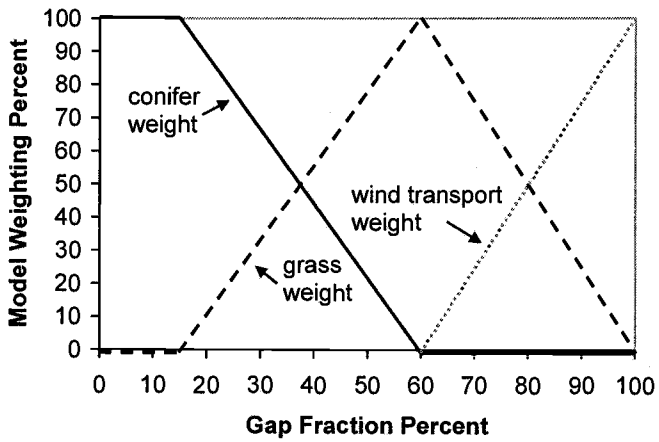

Figure 6. Parameterization scheme for weighting SnowModel output results from conifer, grass and wind model runs based on gap fraction percent.

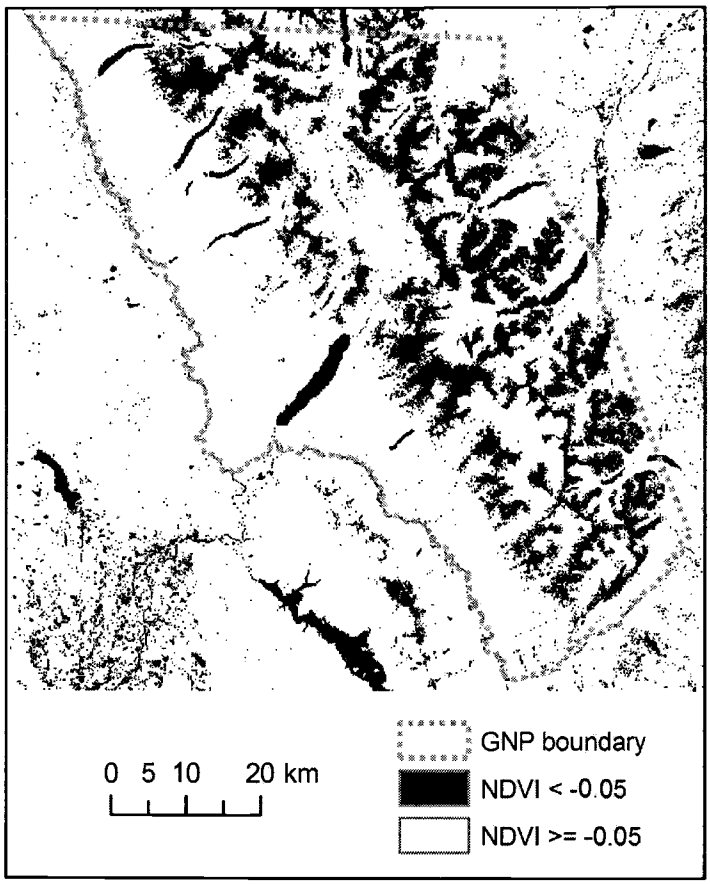

Figure 7. NDVI mask image of Glacier National Park area.

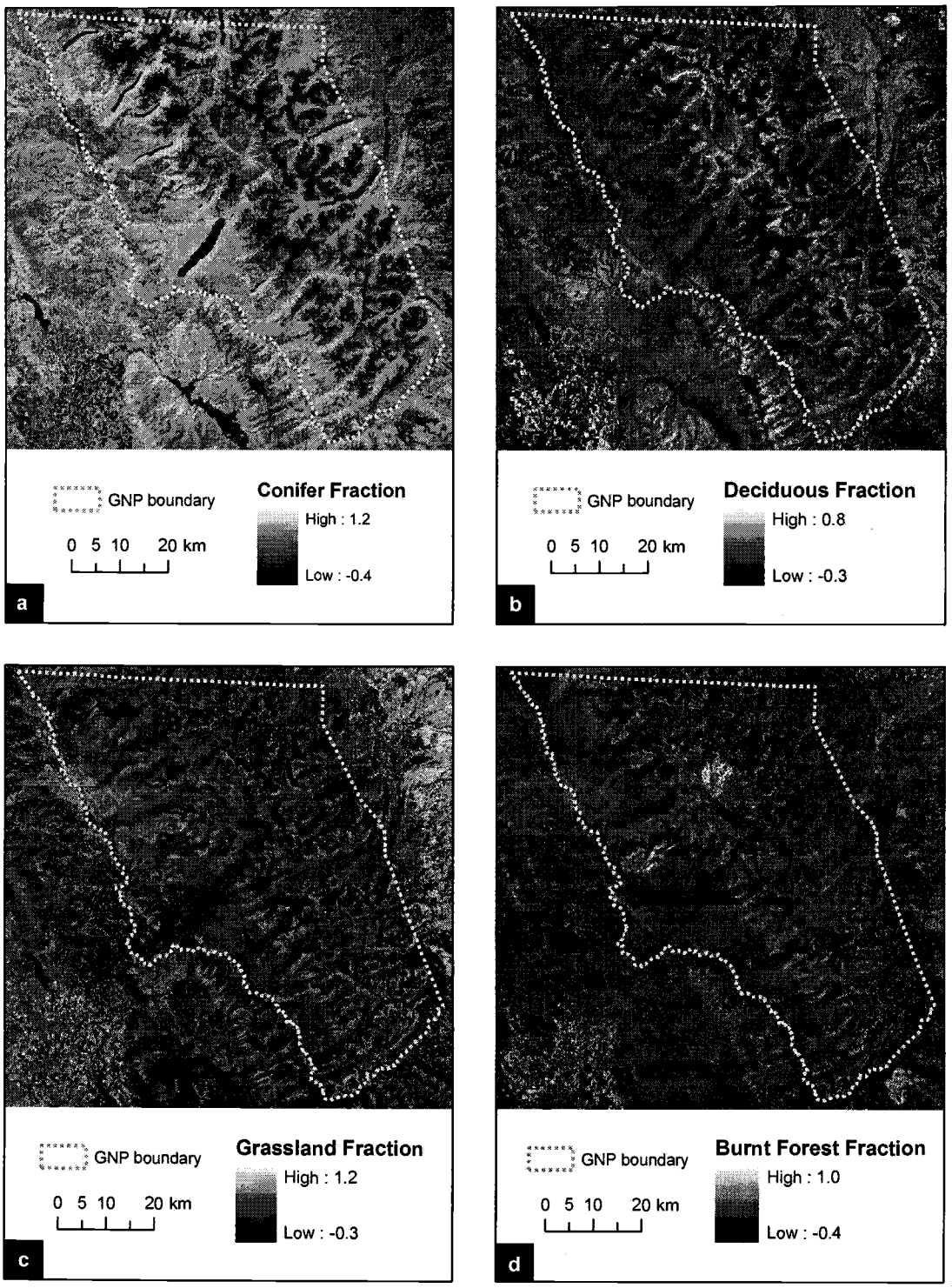

Figure 8. Vegetation type component images derived from linear spectral unmixing of Landsat ETM+ image.

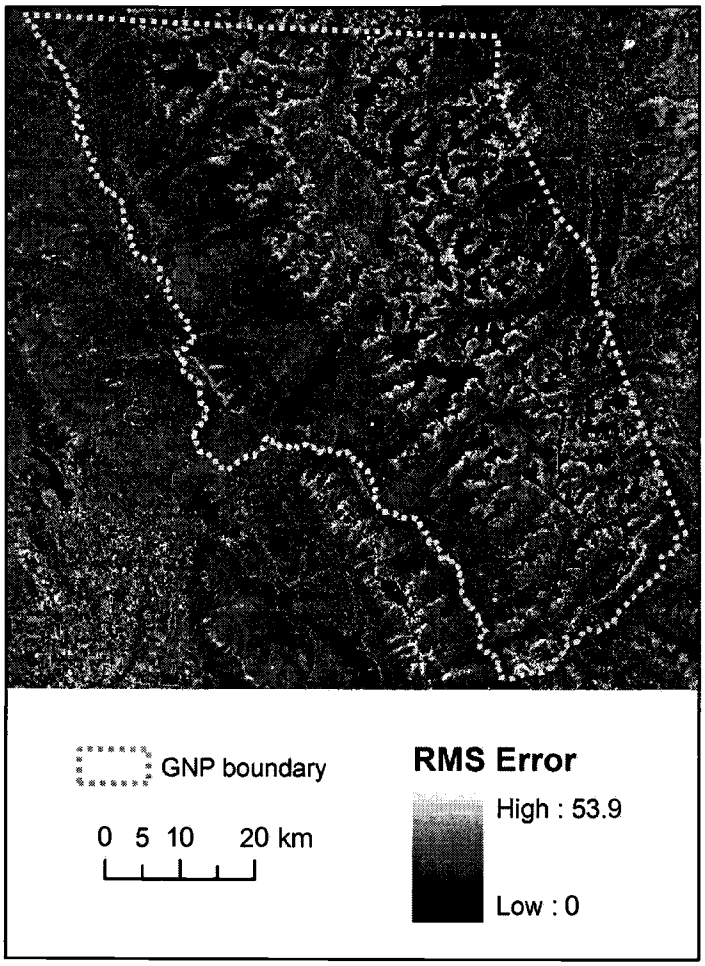

Figure 9. RMS error image for the linear spectral unmixing process.

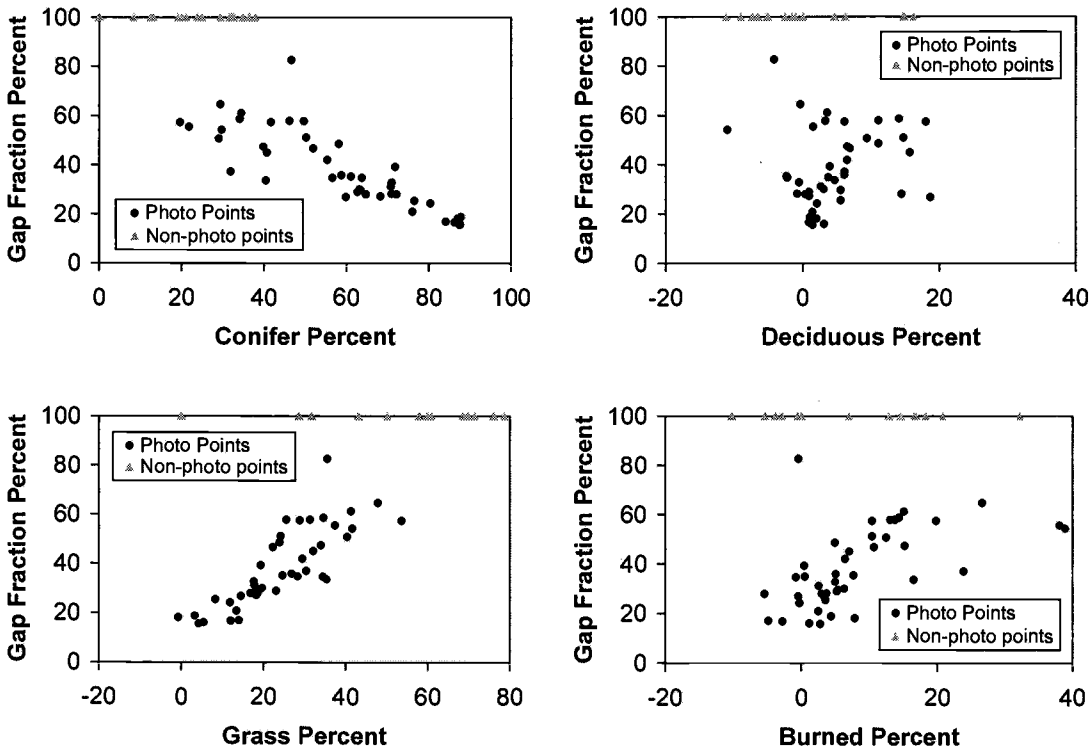

Figure 10. Scatter plots of in situ gap fraction measurements vs vegetation component scores for co-located Landsat ETM+ pixels.

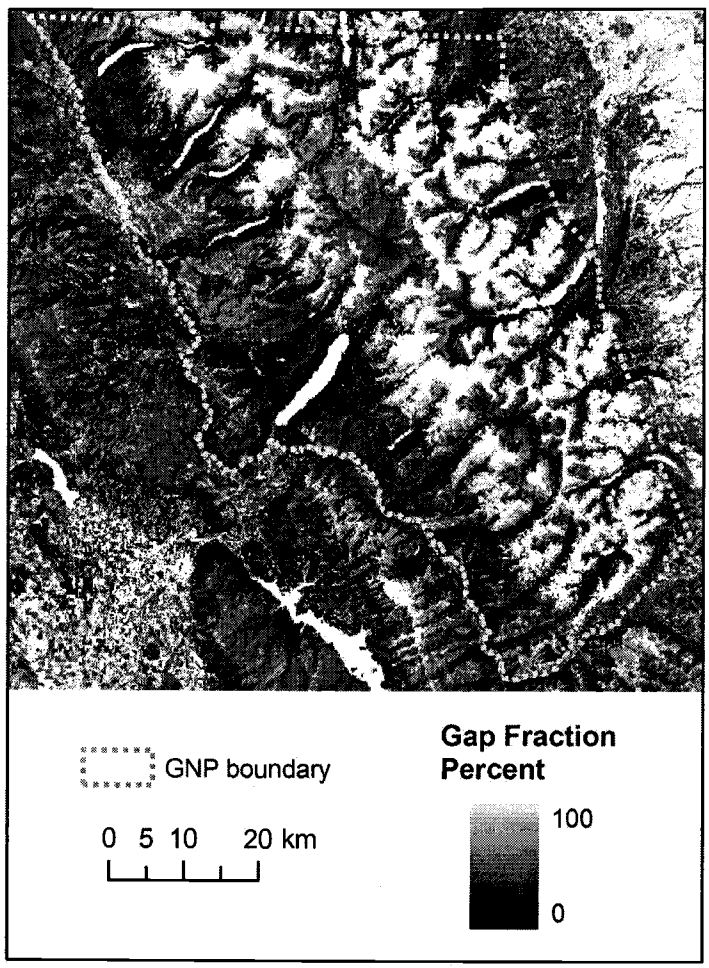

Figure 11. Gap fraction image for Glacier National Park.

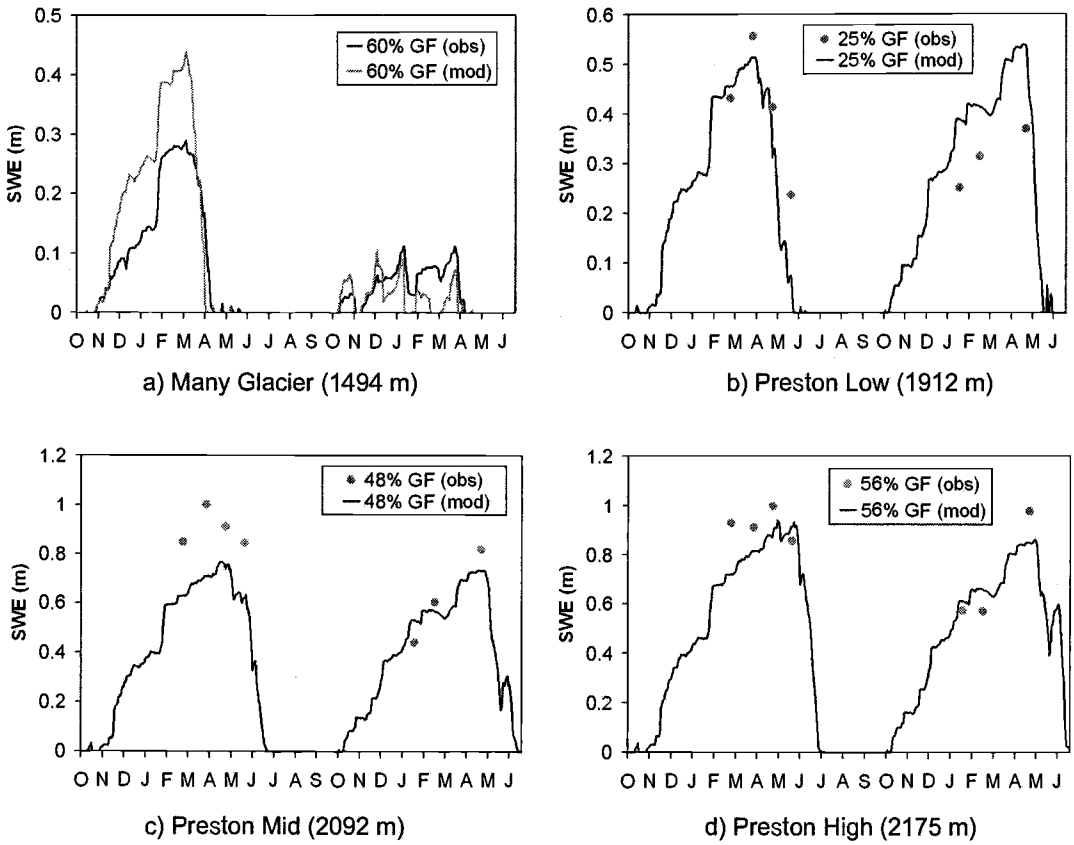

Figure 12. Comparison of modeled and measured SWE for SNOTEL and snow survey points near the Continental Divide.

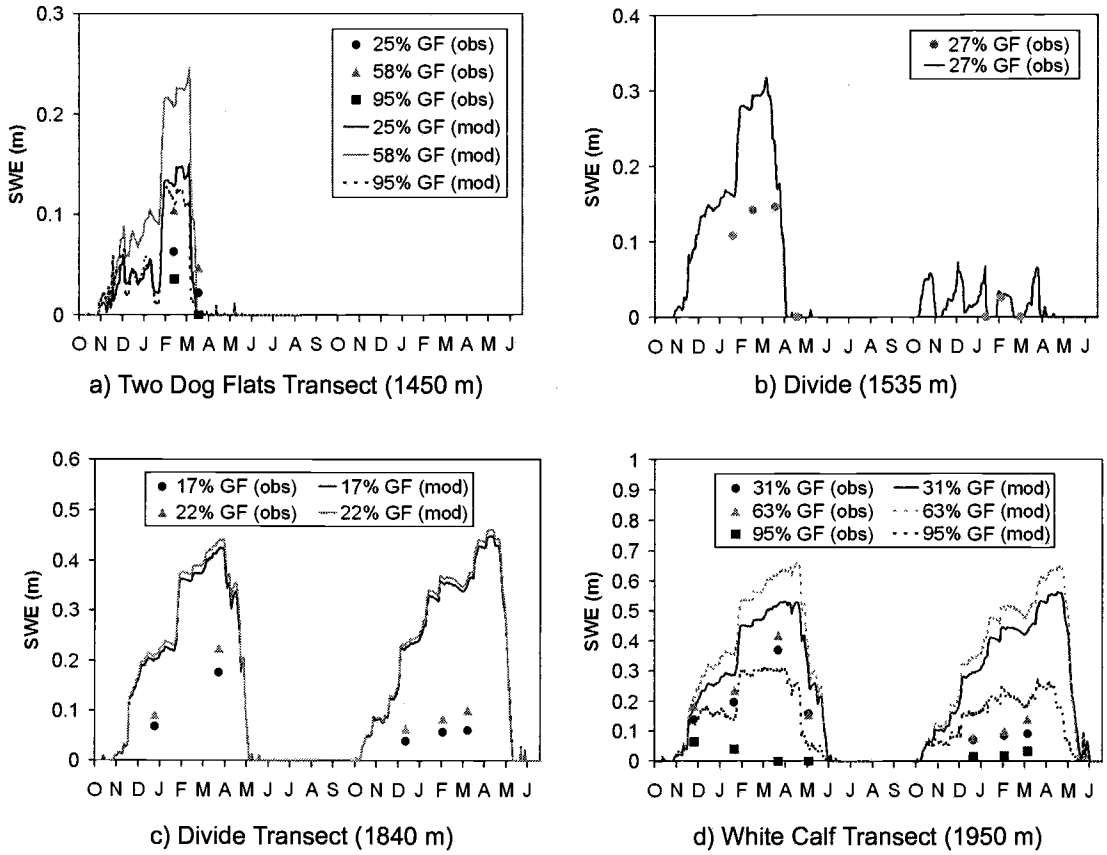

Figure 13. Comparison of modeled and measured SWE for snow survey points near along the eastern edge of Glacier National Park.

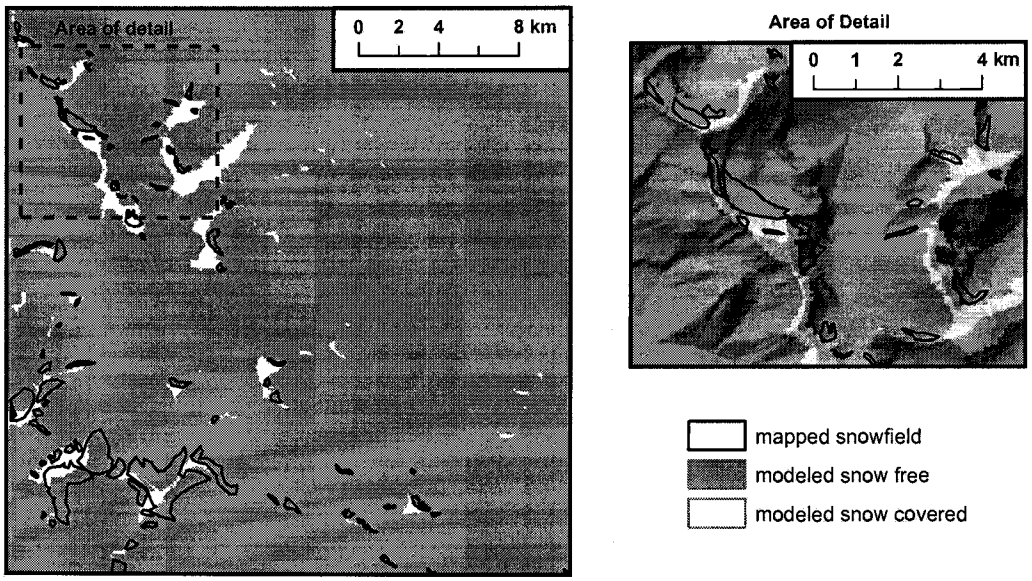

Figure 14. Modeled and observed snow cover for August 10, 2004.

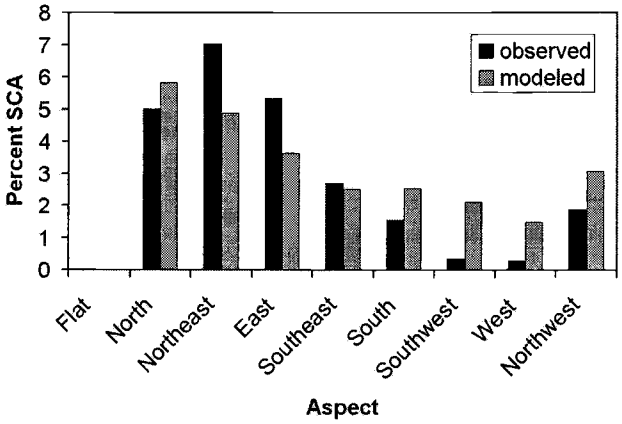

Figure 15. Comparison of percent SCA by aspect for modeled and observed snow cover on August 10, 2004.

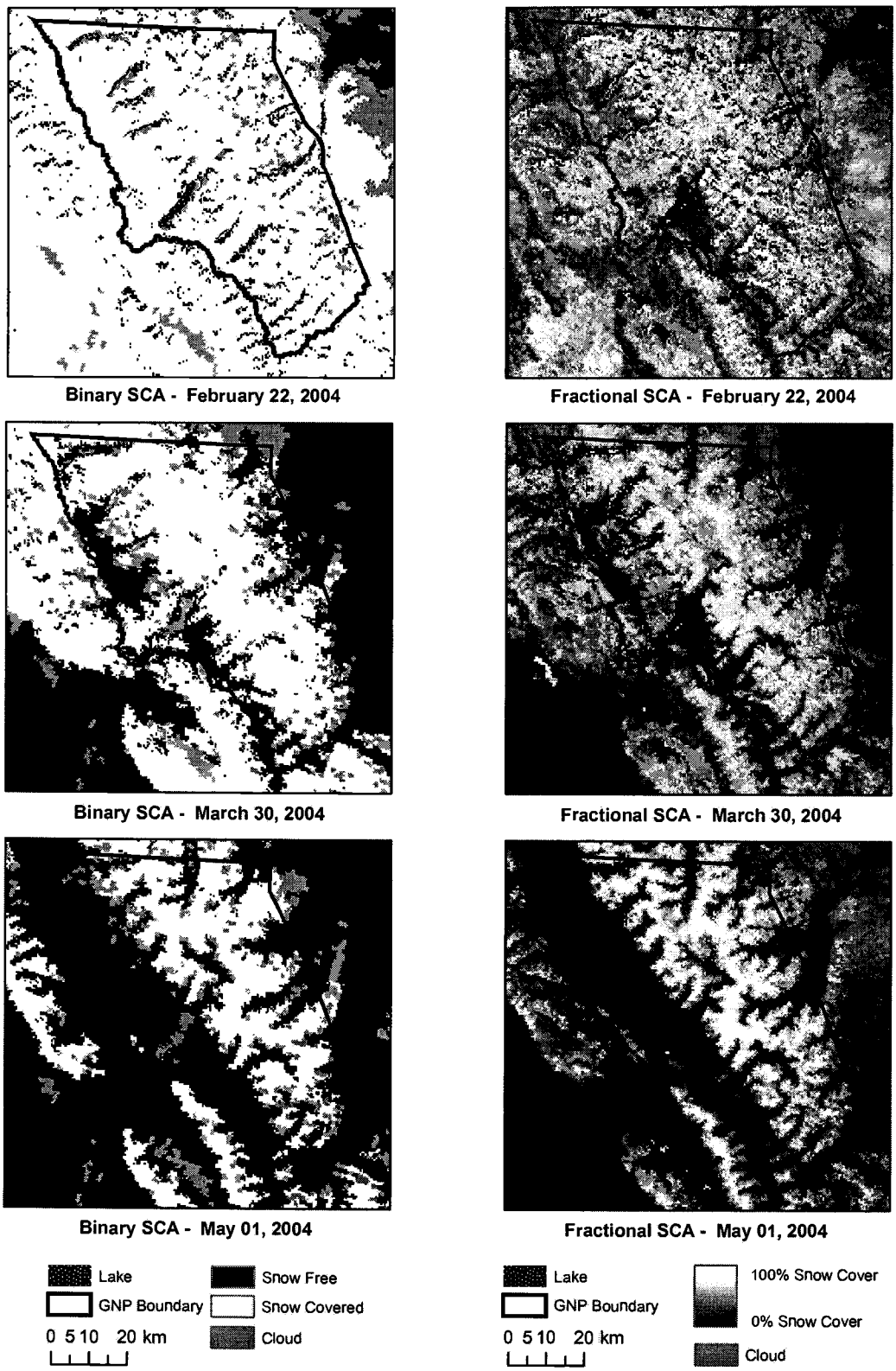

Figure 16. Binary and fractional MODIS-derived SCA for three dates.

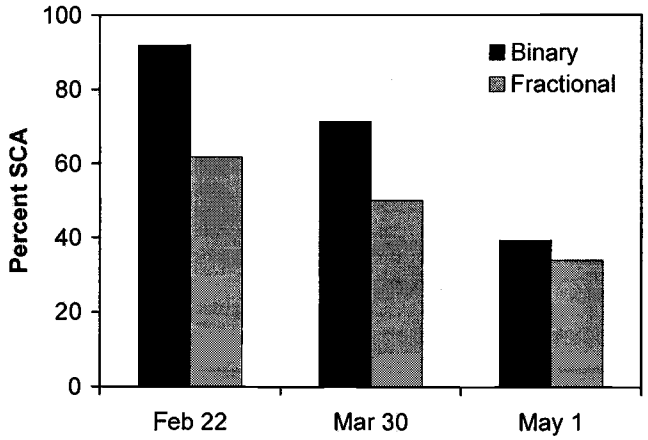

Figure 17. Comparison of percent of total area mapped as snow covered for binary and fractional MODIS-derived SCA products for three dates.

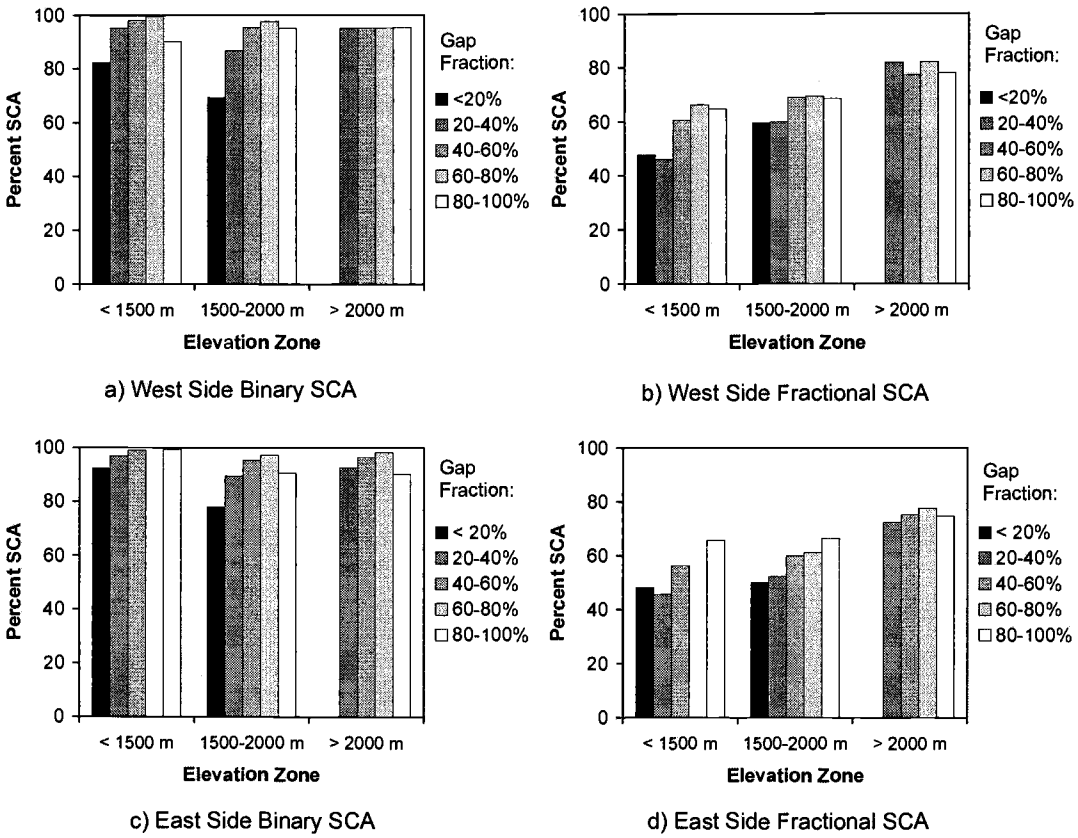

Figure 18. Comparison of February 22, 2004 binary and fractional SCA grouped by relationship to the Continental Divide, elevation zone, and gap fraction class.

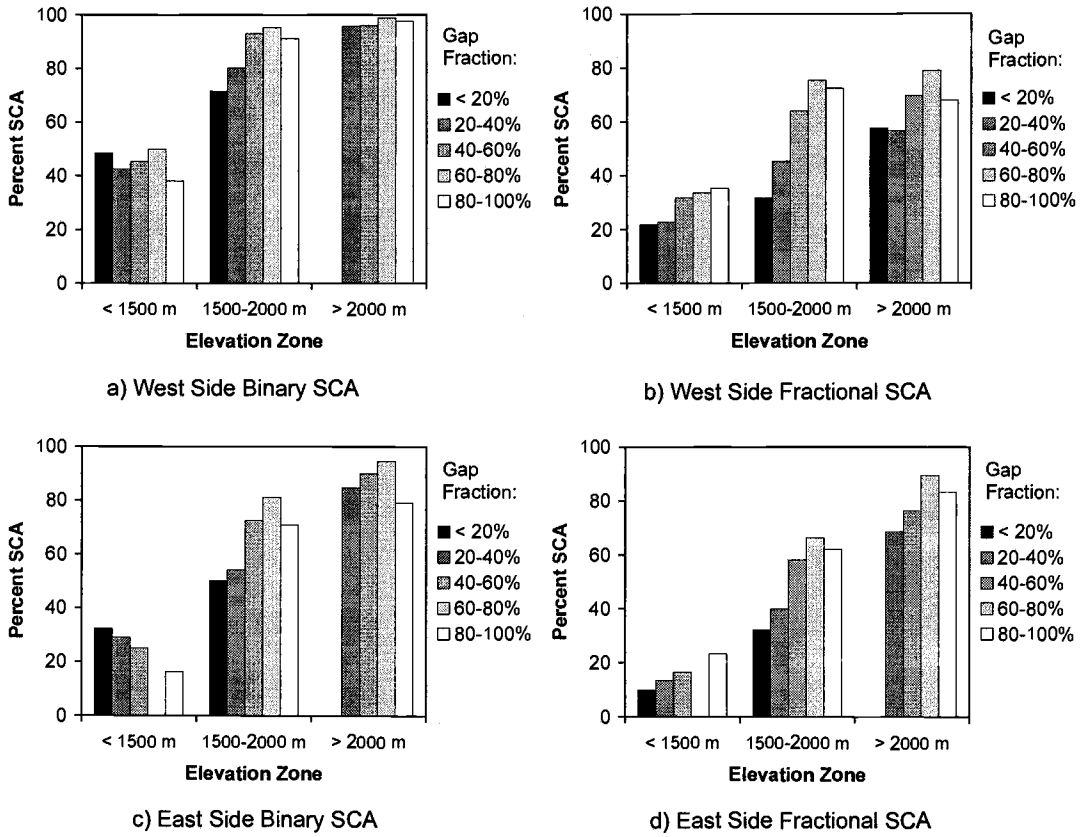

Figure 19. Comparison of March 30, 2004 binary and fractional SCA grouped by relationship to the Continental Divide, elevation zone, and gap fraction class.

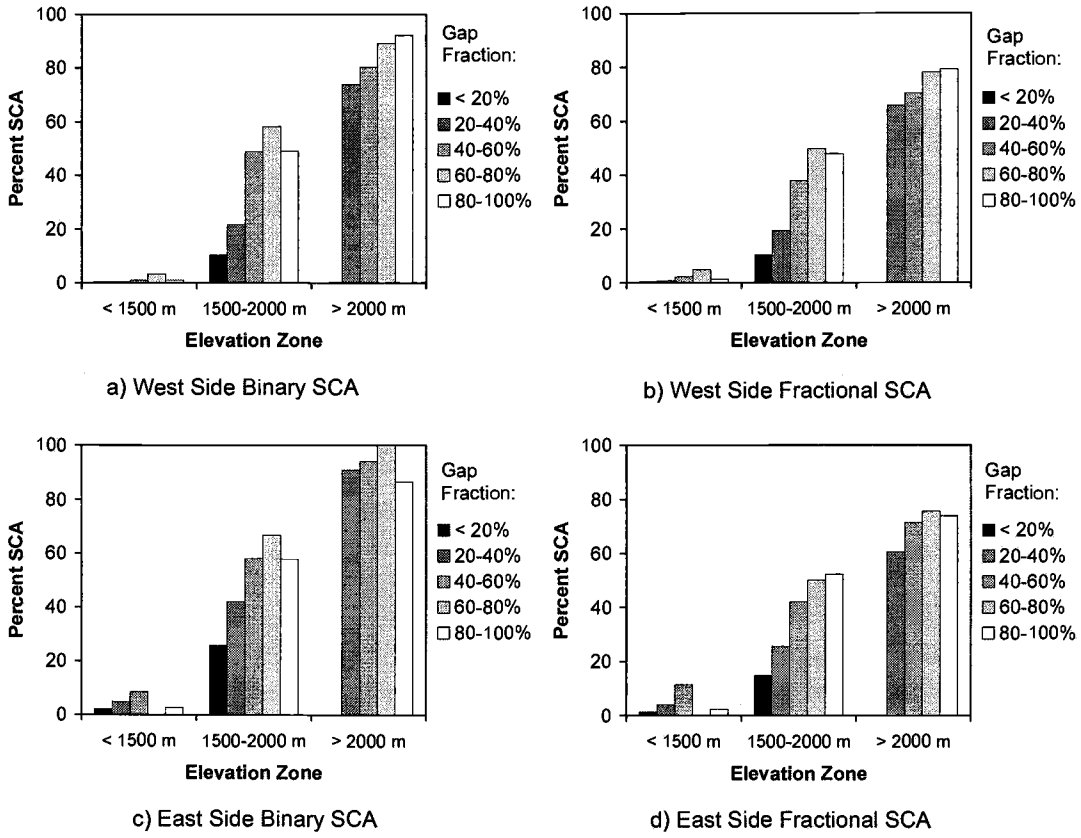

Figure 20. Comparison of May 1, 2004 binary and fractional SCA grouped by relationship to the Continental Divide, elevation zone, and gap fraction class.

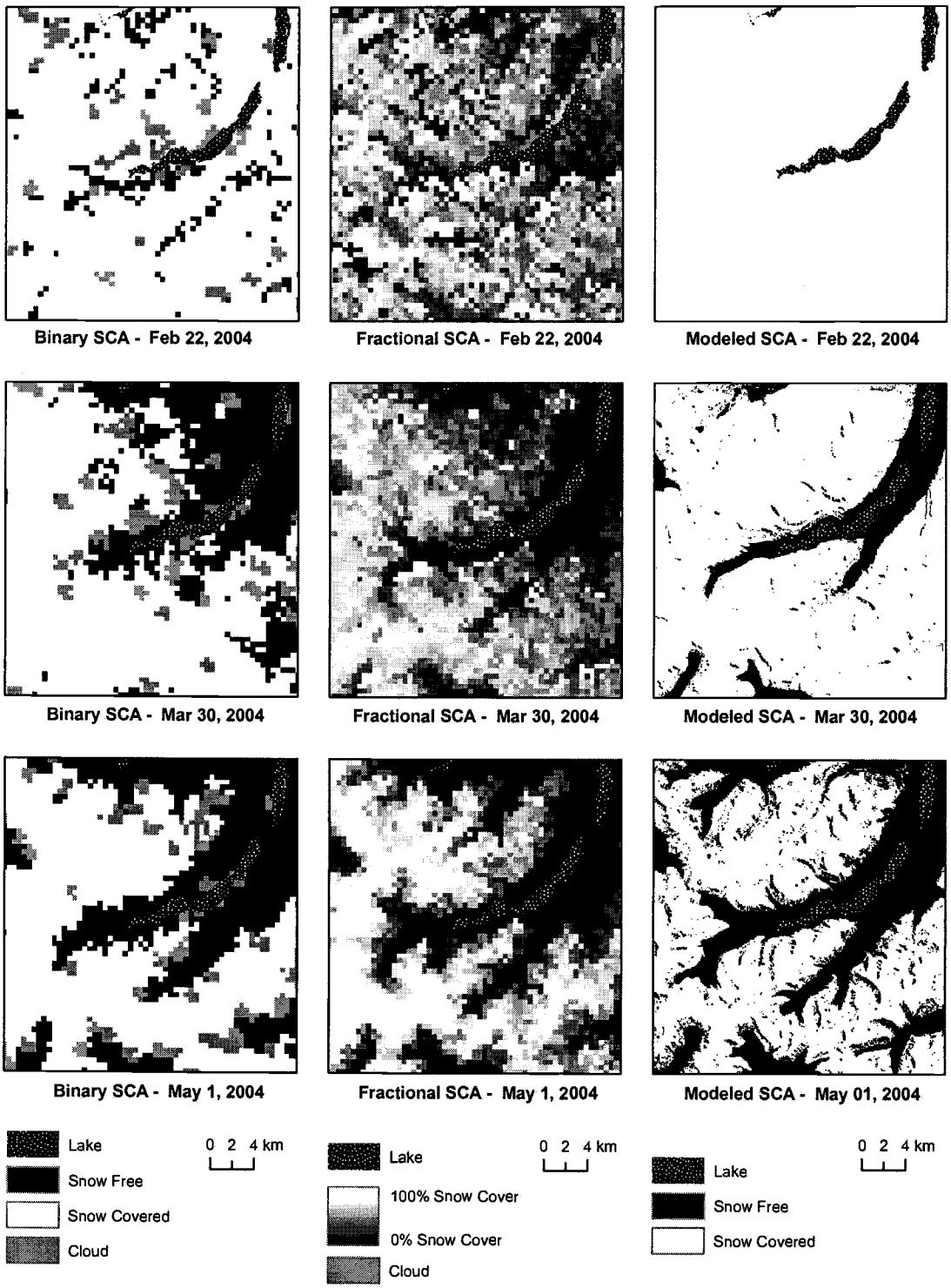

Figure 21. Comparison of MODIS-derived binary SCA, MODIS-derived fractional SCA, and modeled SCA for three dates.

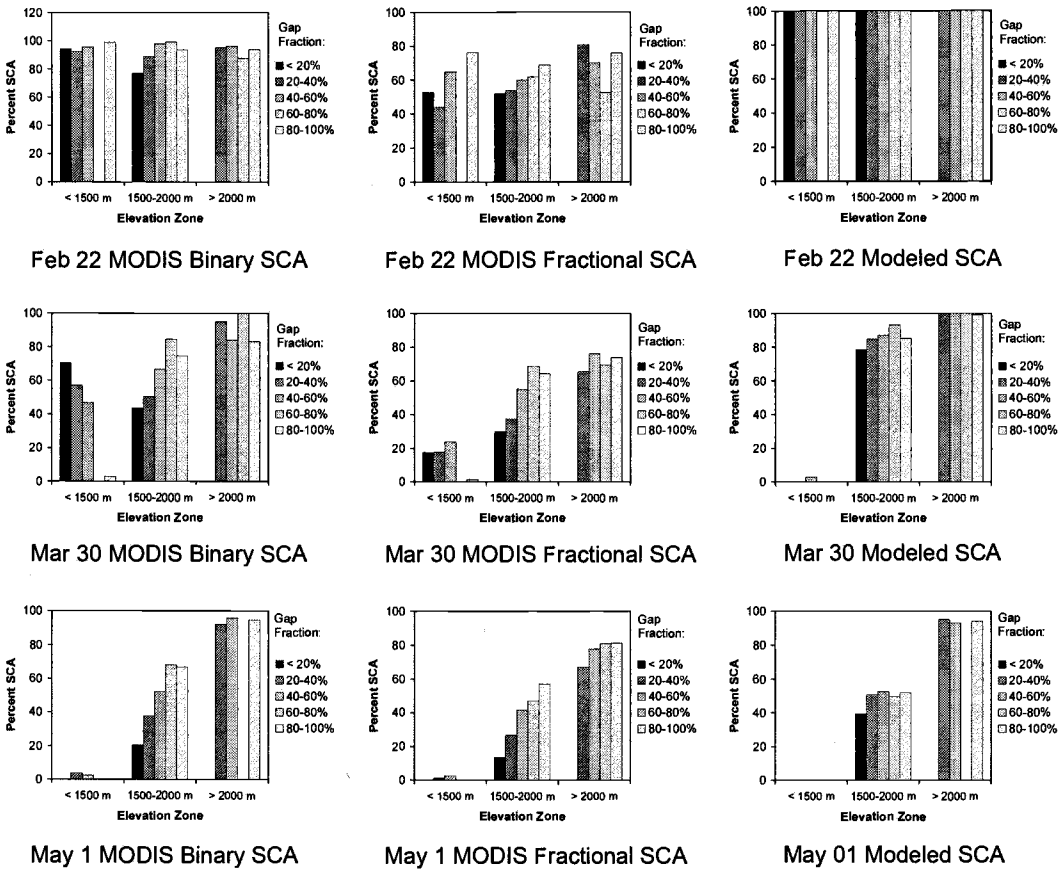

Figure 22. Comparison of MODIS-derived binary SCA, MODIS-derived fractional SCA and modeled SCA grouped by relationship to the Continental Divide, elevation zone, and gap fraction class.

CHAPTER 4: CONCLUSIONS

Understanding the complex relationships between vegetation, snow cover, and remotely sensed snow covered area is an important goal. Understanding these relationships will allow for significant improvements in modeling and remote sensing of snow cover in areas with spatially heterogeneous vegetation distributions, as well as improved simulations of potential changes in snow hydrology associated with landscape changes caused by fire, climatic fluctuation, or human manipulation.

The research presented in this thesis adds further support to the body of literature linking vegetation type or density patterns with snow evolution patterns. Unlike the majority of previous studies on vegetation-snow interactions, the research presented here attempted to describe, quantify, and model vegetation-snow relationships across a wide range of vegetation types and canopy densities, from open grassland to dense coniferous forest. In situ measurements of gap fraction and snow cover (depth or water equivalent) indicated that subtle differences in gap fraction can significantly impact snow accumulation, particularly when gap fraction is above 80% or below 30%. This is an important conclusion, as most modeling approaches that attempt to account for the influence of a vegetation canopy on snow evolution processes simply designate a point or grid cell as forested or open. The implementation of SnowModel described in Chapter 3 used a weighting scheme in order to incorporate spatially distributed quantitative estimates of vegetation density, rather than a limited set of land cover types. Though the modeled results were not particularly impressive when compared to in situ snow measurements, this

implementation of the model did appear to reproduce some of the observed differences between snow cover under different vegetation densities. A more conclusive assessment of the utility of this modeling approach would require snow depth or SWE measurements collected at a scale similar to the model scale, as well as meteorological station data collected in close proximity to the snow measurements.

Obtaining sufficient in situ measurements to effectively assess output from a spatially distributed snow evolution model is extremely difficult, especially for large areas with complex topography. An alternative solution for model assessment and validation is to use remotely sensed snow covered area. In areas of heterogeneous vegetation cover, however, this is not yet a reasonable option because the remotely sensed estimates of snow covered area depend not only on actual snow covered area, but also on the type and density of vegetation present in the area. Chapter 3 provides suggestive, but inconclusive evidence of the effect of various gap fraction densities on remotely sensed snow covered area. For both binary and fractional snow covered area products, snow covered area typically increased as gap fraction increased. Though this may have, to some extent, reflected actual patterns of snow distribution on the ground, this pattern was probably at least partially due to the misclassification of forested snow covered ground as snow free. Further research into the effect of canopy gap fraction on remotely sensed SCA at different times of the year and across a range of climate conditions is necessary and could form the basis for algorithms used to adjust remotely sensed SCA for the effects of vegetation canopies.

BIBLIOGRAPHY

Adams, J.B., M.O. Smith, and P.E. Johnson. 1986. Spectral mixture modeling: a new analysis of rock and soil types at the Viking Lander 1 site. *Journal of Geophysical Research* **91**(B8): 8098-8112.

Berry, G.J. and Rothwell, R.L. 1992. Snow ablation in small forest openings in southwest Alberta. *Canadian Journal of Forest Research* **22**: 1326-1331.

Bloschl, G. 1999. Scaling issues in snow hydrology. *Hydrological Processes* **13**: 2149-2175.

Chavez, P.S., Jr., 1988. An improved dark-object subtraction technique for atmospheric scattering correction of multispectral data. *Remote Sensing of Environment*, 24, pp. 459-479.

Chavez, P.S., Jr., 1989. Radiometric calibration of Landsat Thematic Mapper multispectral images. *Photogrammetric Engineering and Remote Sensing*, 55, pp. 1285-1294.

Chavez, P.S. Jr., 1996. Image-based atmospheric corrections – revisited and revised. *Photogrammetric Engineering and Remote Sensing*, 62, pp. 1025-1036.

Cline, D.W., R.C. Bales, and J. Dozier. 1998. Estimating the spatial distribution of snow in mountain basins using remote sensing and energy balance modeling. *Water Resources Research* **34**(5):1275-1285.

Daly, C., W. P. Gibson, G.H. Taylor, G. L. Johnson, P. Pasteris. 2002. A knowledge-based approach to the statistical mapping of climate. Climate Research, 22: 99-113.

Davis, R.E., Hardy, J.P., Ni, W., Woodcock, C., McKenzie, J.C., Jordan, R., and Li, X. 1997. Variation of snow cover ablation in the boreal forest: a sensitivity study on the effects of conifer canopy. *Journal of Geophysical Research* **102**(D24): 29,389-29,395.

Elder, K., W. Rosenthal, and R.E. Davis. 1998. Estimating the spatial distribution of snow water equivalence in a montane watershed. *Hydrological Processes* **12**:1793-1808.

Frazer, G.W., Canham, C.D., and Lertzman, K.P. 1999. Gap Light Analyzer (GLA), Version 2.0: Imaging software to extract canopy structure and gap light transmission indices from true-colour fisheye photographs, users manual and program documentation. Copyright 1999: Simon Fraser University,

Burnaby British Columbia, and the Institute of Ecosystem Studies, Millbrook, New York.

Frazer, G.W., Fournier, R.A., Trofymow, J.A., Hall, R.J. 2001. A comparison of digital and film fisheye photography for analysis of forest canopy structure and gap light transmission. *Agricultural and Forest Meteorology* **109**: 249-263.

Gary, H.L., Troendle, C. 1982. Snow accumulation and melt under various stand densities in lodgepole pine in Wyoming and Colorado. USDA Forest Service Rocky Mountain Forest and Range Experiment Station, Research Note RM-417.

Golding, D.L., Swanson, R.H. 1986. Snow distribution patterns in clearings and adjacent forest. *Water Resources Research* **22**: 1931-1940.

Hardy, J.P., Davis, R.E., Jordan, R., Li, X., Woodcokc, C., Ni, W., McKenzie, J.C. 1997. Snow ablation modeling at the stand scale in a boreal jack pine forest. *Journal of Geophysical Research* **102**: 29,397-29,405.

Hardy, J.P., Melloh, R., Robinson, P., Jordan, R. 2000. Incorporating effects of forest litter in a snow process model. *Hydrological Processes* **14**: 3227-3237.

Hardy, J.P., Melloh, R., Koenig, G., Marks, D., Winstral, A., Pomeroy, J.W., Link, T. 2004. Solar radiation transmission through conifer canopies. *Agricultural and Forest Meteorology* **126**: 257-270.

Hedstrom, N.R. and Pomeroy, J.W. 1998. Measurements and modelling of snow interception in the boreal forest. *Hydrological Processes* **12**: 1611-1625.

Hiemstra, C.A., Liston G.E., Reiners, W.A. 2002. Snow redistribution by wind and interactions with vegetation at upper treeline in the Medicine Bow Mountains, Wyoming, U.S.A. *Arctic, Antarctic, and Alpine Research* **34**: 262-273.

Koivusalo, H., Kokkonen, T. 2002. Snow processes in a forest clearing and in a coniferous forest. *Journal of Hydrology* **262**: 145-164.

Klein, A. G., D. K. Hall, and G. A. Riggs, 1998. Improving snow cover mapping in forests through the use of a canopy reflectance model. *Hydrologic Processes,* **12,** 1723-1744.

Link, T.E., Marks., D. 1999. Point simulation of seasonal snow cover dynamics beneath boreal forest canopies. *Journal of Geophysical Research* **104**: 27,841-27,857.

Link, T.E., Marks, D., Hardy, J.P. 2004. A deterministic method to characterize canopy radiative transfer properties. *Hydrological Processes* **18**:3583-3594.

Liston, L.E. and K. Elder. In review. A distributed snow-evolution modeling system (SnowModel).

Lundberg, A., and Koivusalo, H. 2003. Estimating winter evaporation in boreal forests with operational snow course data. *Hydrological Processes* **17**: 1479-1493.

Lundberg, A., Yuichiro, N., Thunehed, H., Halldin, S. 2004. Snow accumulation in forests from ground and remote-sensing data. *Hydrological Processes* **18**:1941-1955.

Marks, D. 1988. Climate, energy exchange, and snowmelt in Emerald Lake Watershed, Sierra Nevada. PhD Dissertation, Remote Sensing Hydrology, University of California, Santa Barbara. 149 pages.

Marks, D., Kimball, J., Tingey, D., Link, T. 1998. The sensitivity of snowmelt processes to climate conditions and forest cover during rain-on-snow: a case study of the 1996 Pacific Northwest flood. *Hydrological Processes* **12**: 1569-1587.

Marks, D., Winstral, T. 2001. Comparison of snow deposition, the snow cover energy balance, and snowmelt at two sites in a semiarid mountain basin. *Journal of Hydrometeorology* **2**(3): 213-227.

Marks, D., A. Winstral, and M. Seyfried. 2002. Simulation of terrain and forest shelter effects on patterns of snow deposition, snowmelt, and runoff over a semi-arid mountain catchment. *Hydrological Processes*, **16:**3605-3626.

Melloh, R., Hardy, J.P., Bailey, R.N., Hall, T.J. 2002. An efficient snow albedo model for the open and sub-canopy. *Hydrological Processes* **16**: 3571-3584.

Metsamaki, S.J., S.T. Anttila, H.J. Markus, and J.M. Vepsalainen. 2005. A feasible method for fractional snow cover mapping in boreal zone based on a reflectance model. *Remote Sensing of Environment* **95**:77-95.

Nolin, A.W., J. Dozier, and L.A.K. Mertes. 1993. Mapping alpine snow using a spectral mixture modeling technique. Annals of Glaciology, 17: 121-124.

Painter, T.H., J. Dozier, D.A. Roberts, R.E. Davis, and R.O. Green. 2003. Retrieval of subpixel snow-covered area and grain size from imaging spectrometer data. *Remote Sensing of Environment* **85:**64-77.

Pomeroy, J. W., Gray, D.M., Hedstrom, N.R., Janowicz, J.R., 2002. Prediction of seasonal snow accumulation in cold climate forests. *Hydrological Processes*, **16:** 3543-3558.

Price, A.G. 1988. Prediction of snowmelt rates in a deciduous forest. *Journal of Hydrology* **101:** 145-157.

Satterlund, D.R., Haupt, H.F. 1967. Snow catch by conifer crowns. *Water Resources Research* **3**(4): 1035-1039.

Satterlund, D.R., Haupt, H.F. 1970. The disposition of snow caught by conifer crowns. *Water Resources Research* **6**(2): 649-652.

Selkowitz, D., A.W. Nolin, and D. Fagre. In review. Variable snow cover accumulation associated with vegetation type and density in Glacier National Park, Montana, USA.

Shook, K., Gray, D.M. 1996. Small-scale spatial structure of shallow snow covers. *Hydrological Processes* **10:** 1283-1292.

Storck, P., Lettenmaier, D.P., and Bolton, S.M. 2003. Measurement of snow interception and canopy effects on snow accumulation and melt in a mountainous maritime climate, Oregon, United States. *Water Resources Research* **38**(11): 1223.

Vikhamar, D., and R. Solberg. 2003. Snow mapping in forests by constrained linear spectral unmixing of MODIS data. *Remote Sensing of Environment* **88:**309-323.